Cosmic Ray Showers

at Large

Zenith Angles

A thesis submitted to the
University of Durham for the
degree of Doctor of Philosophy

by

M. J. L. Turner B.Sc.

August, 1969.

Abstract

A large vertical array of muon detectors, of sensitive area 34 square metres, has been constructed and used to determine the frequency of observation of groups of coincident muons in E.A.S. as a function of the zenith angle and of the number of muons in the group.

These observations are compared with the results of theoretical predictions, based on the E.A.S. model of De Beer et al. (1966), and a composite sea-level electron size spectrum based on the results of many workers. Two alternative predictions have been made, one based on a model of the primary spectrum in which the primary flux suffers rigidity modulation at $\sim 10^{15}$ eV, the other on a model in which the heavy primaries fragment above a critical energy ($\sim 10^{15}$ eV) and the primary flux consists solely of protons.

The experimental observations are sensitive to the mean transverse momentum and the results suggest that this remains nearly constant at 0.4 GeV/c over the range of interaction energy 200 - 2000 GeV.

The results also suggest that the primary spectrum model containing a pure proton flux above $\sim 10^{15}$ eV is to be prefered, thus there is no evidence from this work for an increasing primary mass above $\sim 10^{15}$ eV as would have been expected from the rigidity modulation hypothesis.

Preface

The work reported in this thesis was carried out under the supervision of Dr. M. G. Thompson while the author was employed as Research Assistant in the Department of Physics.

The thesis describes observations of muons in E.A.S. at a variety of angles to the zenith, and calculations required to relate these to a measurement of the mass composition of primary cosmic rays in the energy region 10^{14} - 10^{17} eV.

The calculations described were the responsibility of the author as was the construction and operation of the apparatus, the collection and analysis of the data, and the deductions made on the primary mass composition.

Preliminary measurements with the apparatus have been published by Alexander et al. (1968), and the work reported in this thesis was published by De Beer et al. 1969, and Rogers et al. 1969. Other publications related to this work are Alexander et al. 1970, and Thompson et al. 1970 (Proceedings of the 11th International Conference on Cosmic Rays, Budapest). In all the publications mentioned the author is co-author.

Contents

CHAPTER 1

1.1 The Primary Cosmic Rays and their Astrophysics.

The emphasis of studies of the cosmic radiation has been changing over the last few years from the study of the nuclear interactions and decay products in the atmosphere, to an intensified search for knowledge of the primary cosmic rays, their nature and origin. This has come about both from the increasing use of accelerating machines to study nuclear physics, these being much more efficient producers of particles of up to a few tens of GeV. than cosmic rays, and from the current upsurge in Astronomy. It has been realised both by cosmic ray physicists and astronomers that cosmic rays play a much bigger part in the structure and functioning of the Universe than had been thought hitherto.

The primary cosmic rays are known to consist mainly of atomic nuclei with relativistic velocities permeating space in the environment of the earth. There are now known to be in addition smaller intensities of gamma-rays, x-rays and electrons in certain energy regions.

A striking feature of the primary cosmic rays is their energy spectrum. The intensity above a given energy falls continuously as the energy increases. A lower energy limit is defined by the geomagnetic latitude at a few Gev, where

the intensity approaches 3000 particles crossing one square metre, per second, per steradian. An upper energy limit has not yet been reached experimentally, measurements being extended to nearly 10^{20} eV with no sign of a cut-off. The intensity here is about 10^{-16} particles per square metre, per second, per steradian.

Because of the rapidly falling energy spectrum, direct studies of the primaries are only possible at present below 10^{12} eV. Here individual particles can be detected and their mass and energy determined. The results of such measurements give a composition, above a constant energy per nucleon, of 94% protons, 5.5% Helium, and 0.5% of heavier nuclei (up to Iron). It has recently been reported by Fowler et al. (1968) that there also exist nuclei heavier than iron up to and including Uranium.

The energy spectrum of the primaries is now known to have a certain amount of structure. The integral exponent remains constant at -1.6 out to about 10^{15} eV, where it increases to -2.1. This continues to at least 10^{18} eV where the exponent decreases to about -1.6 and continues so up to the limits of measurement. The composition in the whole region above 10^{14} eV is uncertain, because only indirect measurements can be used.

The arrival directions of the primaries can be measured at all energies and within experimental errors they appear to

be isotropic. These errors are very small at low energies and increase to about 10% at the highest energies. This fact has long been supposed to be due to magnetic fields in space which randomise the trajectories of the particles passing through them. Such fields of intensity 10^{-5} -10^{-6} gauss are known to exist within the Galactic plane, and would account for the observations on particles below about 10^{16} eV moving inside the Galaxy. The path length of intergalactic cosmic rays above this energy is so large that even with the smaller field intensity in intergalactic space, deflections will be large below 10^{21} eV. (Greisen, 1966a).

The composition by mass of the primaries is rather different from the known abundance of elements in the Universe. In particular there are more heavy nuclei, and also more nuclei of the L group (Lithium, Berylium). The former excess points to an origin of cosmic rays in old stars which have large fractions of heavy nuclei. The excess of L-nuclei is supposed to be due to fragmentation of the heavy nuclei in penetrating some 4 - 10 gm cm^{-2} of Galactic matter on their way to the Earth.

The origin of cosmic rays is still very much a mystery. The total energy contained in the cosmic radiation falling on the earth is of the same order as that in the electromagnetic radiation from the stars and so the sources of cosmic rays need to have a very large energy output. Because of this some

workers have suggested that the cosmic radiation is not Universal but is produced within the galaxy and trapped there by the action of magnetic fields. Even so, energy channelled into cosmic rays must be of the order of 10^{49} -10^{51} ergs (Ginsburg and Syrovatsky 1964). Energies of this order are known to be released in supernovae, and it has been supposed that these may be the source of cosmic rays. However the means of acceleration of the cosmic rays up to the very high energies observed can only be guessed at.

At present theories of origin are either hierachial (Morrison, 1961), where cosmic rays in different energy bands come from different groups of sources, or single source, in which the whole of the energy spectrum comes from a single type of source (G & S). Here we neglect particles of solar origin. In the first type, acceleration of low energy cosmic rays, (10 to 100 GeV), is supposed to occur in stars larger than the sun, those of moderate energies in supernovae and those of highest energies in certain types of radio-galaxies. In the second type acceleration is only supposed to occur in supernovae. Two mechanisms are favoured at present. In the first (G & S) acceleration takes place in the region of turbulent gas and magnetic fields surrounding a supernova by either the Fermi or statistical mechanism, where collisions between cosmic rays, and randomly moving magnetic fields result in an energy gain by the former, or alternatively by the

interaction of charged particles with a slowly varing magnetic field, (Betatron acceleration).

In the second mechanism the relativistic shockwave produced when a star in a pre-supernova state collapses, accelerates a small part of the outer shell of the star to relativistic energies (Colgate & White, 1965). At present there is no way of determing which if either of these theories is correct.

1.2 The Secondary Cosmic Rays and High Energy Nuclear Interactions.

The presence of the atmosphere, while hindering direct measurements on the primary cosmic rays, has two beneficial effects. The cascade of nuclear interactions produced when an energetic primary strikes the atmosphere provides a rich source of nuclear processes at high energies while the widely spread electron-photon cascades produced give a large collection area for very high energy primaries which otherwise would never be observed due to their low intensity.

The primary particles interact on average every 80 g cm^{-2} of atmosphere traversed. The interaction produces positive, negative and neutral pions, together with some K mesons. The neutral pions immediately decay each producing a pair of gamma-rays forming the start of an electron-photon cascade. The charged pions decay into muons, and neutrinos or interact with further air nuclei producing further pions.

Thus at sea level the cosmic ray flux consists mainly of muons, electrons, γ-rays and neutrinos, with some neutrons, pions and a few surviving protons. The study of these is important both for the knowledge it brings of the interaction processes themselves, and for information on the primary particles which can be derived.

Sea level observations are made either on extensive air showers, or on single cosmic rays. The latter are directed to measuring the energy spectra of the various components, together with the nature of their interactions with matter. The cosmic radiation is still the only source of particles of energy >70 GeV and in the past many new particles have been discovered as a result of cosmic ray studies; however, this work is now in the main better done with accelerating machines. Two postulated particles are however being looked for in the cosmic radiation, these are the quark, a possible building block for sub-atomic particles, and the intermediate vector boson, which would show up as an apparent direct production of muons in nuclear interactions. Both of these have already been searched for and not found in machine studies so that the only possible test at present is in the cosmic radiation where energies are higher. So far they have not been observed.

1.3 Extensive Air Showers

When the energy of the cosmic ray particle is so high that the cascade of interactions produced extends down to sea-level then the result is an extensive air shower (E.A.S.). The most obvious characteristic of a shower is the simultaneous arrival of a large number of particles, mainly electrons, over a wide area. A series of detectors laid out over the area would detect E.A.S. as coincident signals from several of the detectors.

The development of such an event starts with the interaction of a primary and an air nucleus high in the atmosphere. The surviving nucleon, retaining about half its initial energy, together with some high energy pions carries on down through the atmosphere to interact again. On average about 13 of these interactions take place before the primary reaches sea level, each producing further pions many of which themselves interact to produce more.

Thus a cascade of hadrons develops in the atmosphere, the 'core' of the E.A.S. Around this core the promptly decaying neutral pions initiate an electromagnetic cascade into which the hadron cascade is continually pumping energy in the form of further neutral pions as the cascade passes deeper into the atmosphere. The charged pions which do not interact, decay to produce muons, many of which, because of

their inert behaviour travel on unchanged to sea level.

Thus at sea level the E.A.S. has three main components; at the centre the nuclear active core, surrounding this the electron photon shower, and intermingled with the electrons and extending to even greater distances, the muon component. Such a shower at sea level may contain many millions of particles spread over an area of a few square kilometres.

The main incentive to the study of E.A.S. is to enable the intensity of the primary particles to be found as a function of their energy and mass. In order to facilitate this, models of the development of E.A.S. have been derived by various workers to relate measurable parameters of the showers to the parameters of the primary particle. An E.A.S. at a given level of measurement may be characterised by several parameters: the total number of electrons, and their lateral distribution, the lateral distribution and total number of muons, the degree of development of the shower, and the lateral distribution and total number of hadrons in the core. These parameters are sensitive to varying extents to the nature and energy of the primary.

A parameter which has been used extensively in the past which is sensitive to the primary energy, is the total number of electrons, together with the lateral distribution. A complication is the wide fluctuation in number of electrons

from primaries of a given energy, which results from fluctuations in interaction points of the primary. To some extent this can be avoided by making measurements at the level of maximum development of the shower where these are less important, and in fact much data on the primary intensity at high energies has been derived in this way.

1.4 Derivation of the Primary Energy Spectrum.

In the energy region up to 10^{12} eV measurements can be made directly on the primary flux. This is done by means of detectors carried on balloons and satellites. The presence of the atmosphere hinders balloon observations both because of albedo, due to interactions occurring below the detector, and fragmentation of the heavier nuclei in the 4 gm cm^{-2} of air above the detector. In the main however satellite work is confined to energies in the region 1 - 10 GeV, so that elsewhere balloon data must be relied on. Both counter and emulsion techniques have been used, the former being less sensitive to albedo.

In the energy region between 10^{11} & 10^{14} eV, the primary spectrum has been extended by observations on the secondary particles (gamma-rays and muons), the former high in the atmosphere the latter below ground. Beyond 10^{14} eV the primary intensity is so small that only the enhanced collecting

area made possible by E.A.S. studies can enable the determination of the energy spectrum.

The detection and measurement of the electron component of E.A.S. has lead to the extension of the primary spectrum from the upper limit of direct measurements to a few times 10^{19} eV. Extensive air shower detecting arrays have been described by many workers over the years. Basically they consist of several large area particle detectors spread in a regular pattern over a fairly large area. The use of fast-timing techniques with scintillation counters enables the direction of the shower to be measured. The density of particles recorded at each detector enables the electron density distribution to be determined, and hence by integration the total number of particles in the shower.

The task of deriving the primary energy from the electron shower size is not straightforward depending as it does on an intimate knowledge of the development of the shower. A complete model of the development of an E.A.S. would give the relation between primary energy and shower size. Such a model has been developed by the author and his collegues and is described in detail later. However such a model is only susceptible to test in the region of overlap between direct measurement and E.A.S. measurement, where several factors make such a test difficult. The errors in direct

measurement are large, the detection of small E.A.S. is difficult owing to the small spread of the showers, and model calculations are in general most accurate in the high energy region where the number of particles is large. Thus only approximate tests can be made in the low energy region, supplimented where possible by indirect methods.

Thus one way of deriving the primary energy is to use the results given by an E.A.S. model at the level of development of the shower where it is measured. A further way is to attempt to perform measurements on the shower when it is at maximum development. This usually means working at mountain altitudes. At the same time, because the shower maximum moves downward with increasing energy, only a limited energy range can be used. Proof that the showers detected are at maximum development can be obtained by looking at the variation of size with zenith angle of showers of the same intensity (presumably of the same energy), i.e. by varying the thickness of atmosphere through which the shower passes. At maximum development fluctuations are least and also the size is insensitive to the variations of model parameters (except the energy), so that size is very nearly proportional to primary energy. The problem of absolute calibration still remains and here one has to rely on the results of a model calculation.

The integral primary spectrum shown in figure 1.1 has

Fig. 1.1

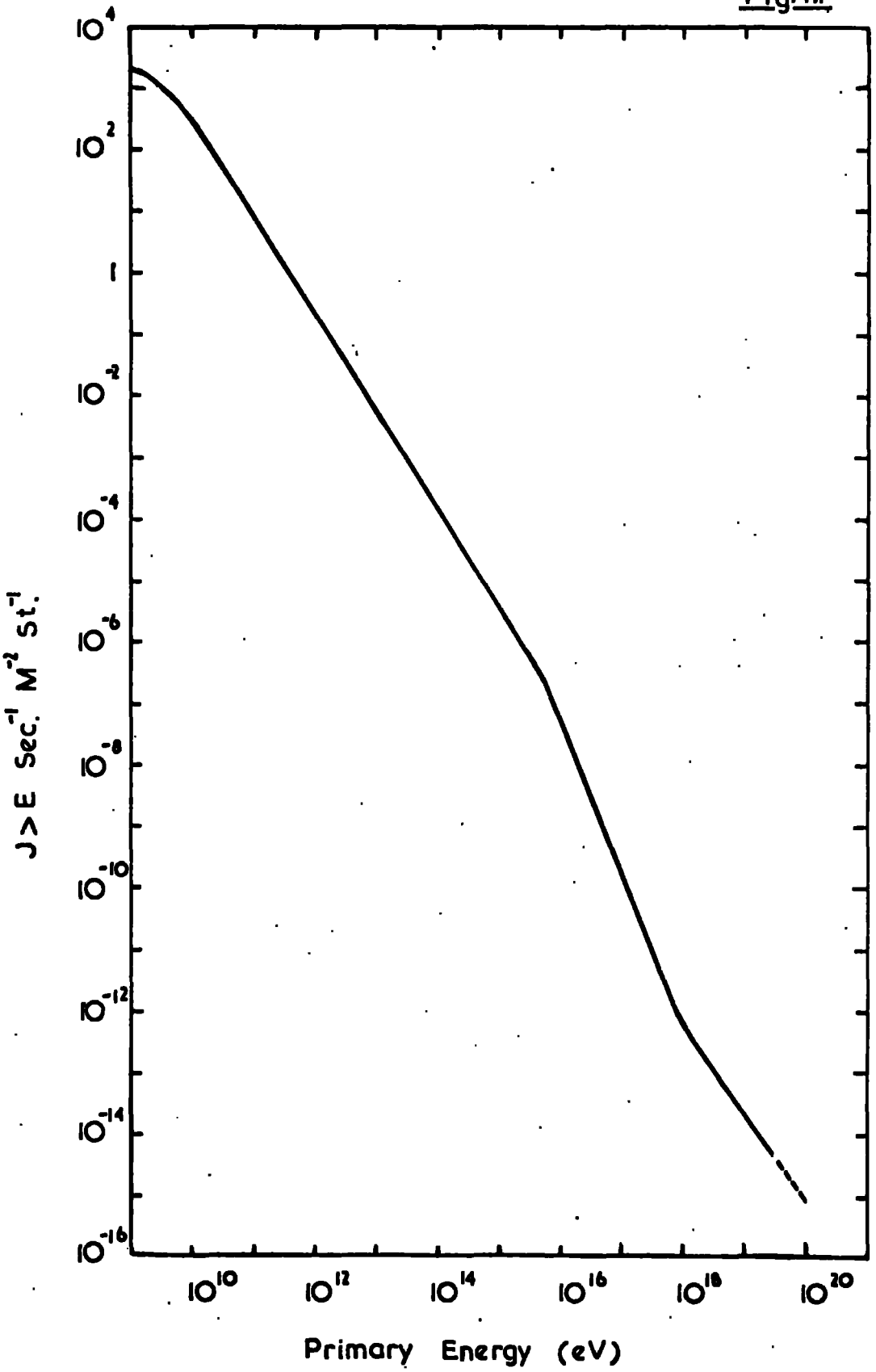

Integral Primary Energy spectrum (after Greisen 1966)

been derived from measurements of this type in the upper energy region, and from direct measurements below. At one time there was some doubt as to whether the so called 'kink' in the primary spectrum was genuine, or merely the result of a change in the nuclear interaction producing a change in the size spectrum. More recent work (Vernov, 1968, McCusker, 1968) has shown that the latter is unlikely.

It has been pointed out by Greisen (1966b) that if the recently discovered microwave radiation, equivalent to a black-body temperature of $3^{o}K$, permeates the whole of space, then a cut off in the primary energy spectrum may be expected between 10^{19} - 10^{20} eV due to photo-pion production by blue-shifted microwave photons. Present evidence (Linsley & Scarsi 1962) is against this, however a definite result must await more precise data.

1.5 Composition in the E.A.S. Region.

So far attention has only been paid to the energy spectrum of the primaries. The mass spectrum has been mentioned in the introduction where reference was made to direct measurements in the low energy region. Here provided sufficient data can be obtained the composition of the primaries can be easily determined.

In the E.A.S. region however it is extremely difficult to extract information on the composition of the primaries.

A detailed discussion of the various indirect methods used to infer the composition is given in chapter 2. Here it is sufficient to say that up to the present work there was some slight evidence in favour of an increasing fraction of heavy primaries beyond about 10^{15} eV (Bray et al. 1965) up to which energy the composition seemed 'normal'. Beyond 10^{17} eV Linsley & Scarsi (1962) have put forward some evidence that the primary flux is pure and probably protonic.

1.6 Astrophysical Significance of the Composition at High Energies

The isotropy of the cosmic radiation and also the amount of energy carried therein has always been explained by assuming that there are magnetic fields in the galaxy which not only contain the cosmic rays created within the galaxy, but also alter the directions of the particles so much that any anisotropy is obscured. The magnetic field of the galaxy has been detected and measured by radio-astronomers and is known to have a strength of about 10^{-5} gauss. At present the field is known to be confined to the spiral arm but little is known of its direction or whether it is ordered or random.

An attractive hypothesis has been put forward by Linsley (1962) to explain the shape of the primary spectrum, and the above mentioned observations on composition in the E.A.S. region. This is partly based on an earlier paper by Peters (1961). It is assumed that below 10^{15} eV the primary spectrum is

characteristic of the Galaxy and that cosmic rays here are trapped by the magnetic field of the Galaxy. As the radius of curvature of the particle trajectories in the field approaches that of the field itself they will leak away from the Galaxy. Because, for a given magnetic rigidity, heavy nuclei will have a higher energy than protons and light nuclei, the latter will disappear earlier from the primary energy spectrum, causing it to steepen. Also the mean mass of the primaries will increase with energy as more of the lighter nuclei escape till eventually the intensity of Galactic cosmic rays, now almost entirely iron nuclei, falls below that of those from other galaxies. These may be expected to be protons as the amount of matter they have encountered should be sufficient to fragment all heavy nuclei.

Thus the supposed increase in mass above the kink, and also Linsley's observation of a pure protonic flux above 10^{17} eV are explained. A critical analysis of this hypothesis will appear in chapter 2. The purpose of the present work is to test this hypothesis by determining the mass composition above and below the kink to see if the data are consistent with the escape of cosmic rays from a magnetic field. The method relies on measurements made on the muon component of E.A.S. at large zenith angles together with measurements made on the sea-level electron component by other workers.

1.7 The Muon Component of E.A.S.

Because electrons constitute the great majority of particles

in an E.A.S. they have been studied extensively in the past. More recently the trend has been towards the study of the muon component because of the better quality of the information obtainable. However there are considerable experimental difficulties.

Because of the relativistic extension of their lifetime muons above a few GeV survive to sea-level. This results in the muon size at sea-level being much less sensitive to the points of interaction of the primary. Thus fluctuations in number are much smaller than in the case of electrons. In addition it has been shown by Orford & Turner (1968) that observations on energetic muons, far from the core, can lead to information from the first one or two interactions of the primary.

There have been experimental studies of muons in near vertical air showers. Mainly these have been attempts to measure the composition of the primaries by observing whether the width of the fluctuations in muon numbers for a constant electron number is large or small. Also Vernov et al. (1968) have attempted to measure the total number of muons in E.A.S.

A serious experimental problem is to exclude the electrons and photons in the shower and only observe the muons. Because muon numbers are small much bigger detectors are needed and these have to be heavily shielded. The result is that only crude measurements on muon size are possible at present.

The root of the present interest in muon showers is the positive correlation between number of muons at sea-level for a given energy and primary mass. This arises because the probability of pion decay rather than interaction decreases with energy. Muons are thus more favourably produced by primaries of lower nucleon energies i.e. heavy primaries. Thus a study of the muon intensity in an air shower could in principle lead to measurements of the primary mass.

1.8 Muon Showers at Large Zenith Angles.

Much of the experimental difficulty of studying the muon component can be removed by detecting muons in E.A.S. making large angles with the vertical. The atmospheric attenuation of the electron component is large away from the zenith. At moderate zenith angles where there are still some electrons present, a relatively small thickness of absorber placed vertically on one side of the detector has a sufficient thickness along the particle trajectories to absorb them. Thus exculsion of the electron component is much simpler than in the case of a horizontal detector. For this reason the present experiment is directed towards the horizon. Two other experiments have been done at large zenith angles by Sekido et al. (1965) and Parker (1967). These experiments are described fully later and comparisons between them and the present work given. However in the case of the present

work there was available a comprehensive series of E.A.S. model calculations carried out by the authors colleagues at Durham since 1966; De Beer et al. (1966, 1967, 1969). These calculations gave the numbers of muons and electrons at sea-level, together with the muon lateral distribution for a variety of zenith angles from the vertical to 84^{o}. From these using a simple model of the nature of an E.A.S. produced by a heavy primary it has been possible to calculate predicted intensities of the muon component for different primary compositions and test these experimentally.

A further advantage of these model calculations was that they enabled the muon density spectrum to be calculated. This is much simpler to measure experimentally than the size spectrum because it needs only one set of detectors.

The present work describes the experimental study of primary mass in the region 10^{14} - 10^{17} eV by measurements on the muon density spectrum. The measurements are compared with theoretical predictions based on two primary spectrum models, one containing a rigidity modulated mass increase above 10^{15} eV, the other a pure proton flux above 10^{15} eV. The theoretical predictions are made solely from the sea-level electron size spectrum as derived from the results of many workers, and the E.A.S. model calculations of De Beer et al. (1966, 1967, 1969). Thus internal consistency is achieved.

In chapter 2 a survey of previous mass composition

measurements is made. A description of the apparatus and details of data collection are given in chapters 3 and 4. The theoretical analysis and comparison of theory and experiment appear in chapters 5 and 6, while comparison with the results of other workers is made in chapter 7. Conclusions as to the mass composition of the primary cosmic rays are drawn in chapter 8 and a possible new model of the primary flux is proposed.

Appendix 1 gives details of experimental measurements on electron showers at large zenith angles, and comparison is made with theoretical calculations based on their production by electromagnetic interactions of single muons. Appendix 2 gives details of the pressure coefficient of the muon showers, observed in the main experiment, together with their distribution in siderial time, also estimates are made of the mean energy of muons in the events observed and comparison is made with theoretical predictions.

CHAPTER 2

The Mass Composition of the Primary Cosmic Rays.

2.1 Experiments Near the Top of the Atmosphere.

Direct measurements on the primaries have been made by many workers using balloon borne apparatus. Both nuclear emulsion and counter techniques have been used. The main problems in this work are the corrections due to albedo and to fragmentation of nuclei in the few gm cm^{-2} of matter above the apparatus.

Albedo, since it consists mainly of singly charged particles, is most important for proton measurements, and comprises two components: the splash albedo, and the geomagnetic albedo. The former is contamination due to upward moving products of primaries interacting in the atmosphere below the detector, the latter consists of those splash albedo particles, trapped in the geomagnetic field which reappear moving downwards. The use of Cerenkov detectors reduces the effect of splash albedo, and the effect of geomagnetic albedo can be allowed for knowing the intensity of the splash albedo.

Because the interaction lengths of heavy nuclei are short, there is an appreciable chance of an interaction in the air above the apparatus. This has the effect of increasing the observed flux of lighter nuclei at the expense of the heavy

nuclei. Extensive work has been done (Waddington, 1960a) to measure the fragmentation probabilities of heavy nuclei thus to enable the extrapolation of the observed flux to that at the top of the atmosphere.

Helium nuclei are a special case because the incident flux of these is much greater than the spurious flux due either to albedo or fragmentation. Thus measurements of the helium intensity are the most precise.

Figure 2.1 shows the intensity of the various primary components as measured by many workers. Below 10 GeV there is a wealth of data. The measurements of Ormes and Webber (1968) are shown for all the mass components together with the values of the intensity above 2.6 GeV/nucleon quoted by Waddington (1960). It is seen that there is agreement between these values.

The energy spectra are derived either directly (Ormes & Webber) or by combining measurements made at different geomagnetic latitudes and cut-off rigidities (Waddington, 1960).

Above 10 GeV the flux is already falling rapidly and most authorities agree that the spectra of all components (except possibly the L-nuclei) are approaching an exponent of -1.6 (integral).

Emulsion measurements made by Anand et al. (1968) on the helium component out to 16 GeV/nucleon are shown, also those of Koshiba et al. (1968) on all heavy primaries ($Z \geqslant 6$)

Fig. 2.1.

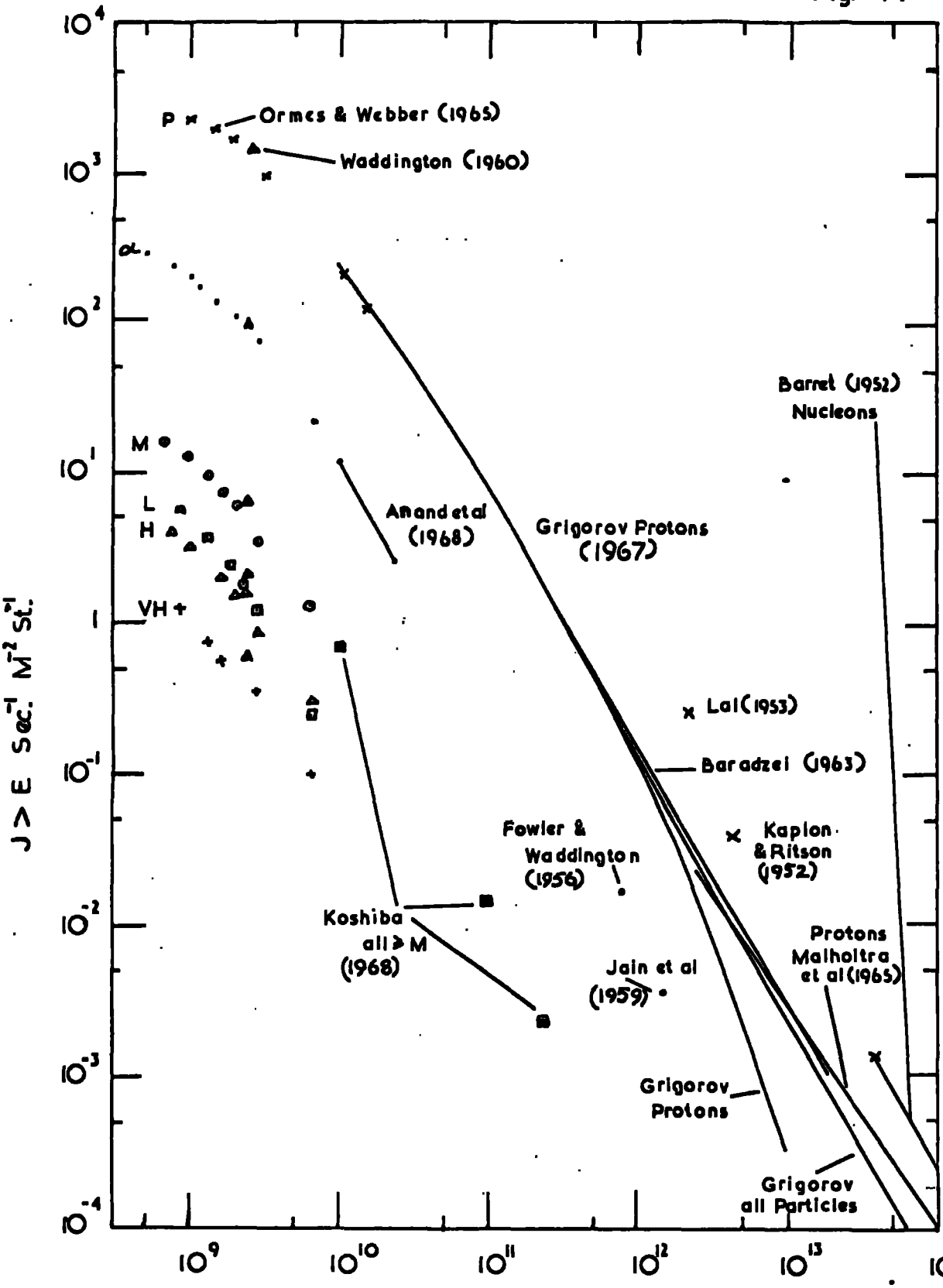

Direct Measurements of the Mass Composition of the primaries.

out to 240 GeV per nucleon. Measurements of the integral intensity of Helium nuclei above 800 GeV per nucleon by Fowler and Waddington (1956), are shown together with those of Jain et al. (1959) above 1500 GeV per nucleon. These measurements are really the last direct atmospheric measurements on the primaries and consist of a few events only.

Beyond 10^{12} eV we only have isolated observations of nuclei. The Sydney 20 litre emulsion stack detected 112 particles of energy $> 10^{12}$ eV of which 52 were protons, 18 were Helium nuclei and 42 were heavy nuclei. The Brawley & Bristol stacks detected 1 proton and 1 oxygen nucleus of $2\ 10^{14}$ eV and one calcium nucleus of $4\ 10^{14}$ eV (quoted by McCusker, 1968) Malholtra et al. (1965) observed 46 events above $2\ 10^{11}$ eV of which 34 were protons, 3 were neutrons, 6 were Helium nuclei and 3 heavy nuclei.

The values of Lal (1953) and Kaplon and Ritson (1952) for the proton flux between 10^{12} & 10^{13} eV are given although some doubt has been cast on these measurements because of their disagreement with later work. Kaplon and Ritson used a technique where the electromagnetic shower produced by the particle could be observed in the stack and so its energy determined. The charge was determined from the track of the incident particle, 8 protons were observed and 2 Helium nuclei at an energy above $4.5\ 10^{12}$ eV.

Thus direct atmospheric measurements of the primary flux

are far from comprehensive above 10 GeV and in many cases only indications of the presence of various components are available. Below 10 GeV however the intensity is such that accurate measurements can be made and some confidence is possible in the results presented in figure 2.1.

2.2 Low Energy Satellite Measurements.

The advent of earth satellites has made it possible to measure the flux of cosmic rays well beyond the earths' atmosphere. However at present although problems of background are eliminated, only counter techniques can be used and in some cases loss of data occurs due to telemetry faults. The data of Fan et al. (1968), are shown in fig. 2.1. These were obtained using solid state devices which measured energy loss and total residual energy thus identifying nuclei in the energy range 35-200 MeV/nucleon.

2.3 Satellite Measurements at High Energies.

Grigorov et al. (1967) have published results on the proton and all particle spectra from 10 GeV to approximately $5\ 10^{13}$ eV obtained from the satellites 'Proton I' and 'Proton II'. These contained proportional counters to measure charge and an ionization calorimeter to measure energy. The spectrum of protons was derived from those particles penetrating the whole detector, and that of all nuclei from the energy spectrum

in the calorimeter. Figure 2.1 shows that above 10^{12} eV the proton spectrum falls below the all particle spectrum and by 10^{13} eV is already a factor of 10 down.

If these measurements were substantiated it would imply that the mean mass of the primaries increases beyond 10^{12} eV. However there are grave doubts as to the validity of this work. Both satellites were known to 'tumble' and only approximate allowance could be made for the earths shadow. Also numerous corrections had to be made for malfunctioning of the apparatus and incomplete data transmission. Thus although this work would have ideally solved the problem of the composition up to 10^{14} eV some caution must be exercised in accepting the results.

2.4 γray Spectra in the Atmoshpere.

Because γ-rays high in the atmosphere have their origin in the π^0s produced in the interactions of the primary cosmic rays, a study of these may be expected to give some information on the primary spectrum.

The information gained is not so reliable as direct measurement as the γ-rays can only be related to the nucleons in the atmosphere and so the mass of the primary is obscured. It has been suggested by several workers Kidd (1963), Malholtra et al. (1966) Bowler et al. (1962) that the observed steepening of the γ-ray spectrum beyond about $2.5\,10^3$ GeV (γ ray energy) reflects a steepening of the primary nucleon

spectrum at $> 10^{12}$ eV. This could relate to a rigidity limit for the primary nuclei (Yash Pal & Tandon, 1966). It has also been related to an increase in the cross section, or inelasticity of the nuclear interaction. The data on this change in slope are however rather imprecise.

Baradzei et al. (1962) have quoted a spectrum of nucleons of energies 10^{11} to 10^{13} eV interacting in their apparatus producing γ rays. This spectrum is shown in figure 2.1. Malholtra et al. (1966) have also measured the nucleon component and, assuming the composition to be the same as at low energies, have quoted a proton spectrum from $2.6\ 10^{12}$ to $2.6\ 10^{14}$ eV.

These measurements can be used to extend the primary spectrum out to $3\ 10^{14}$ eV. However since they depend on the rather uncertain relation between γ-ray spectra and the primary spectrum there is some possibility of error. As mentioned above the information on composition is indirect and uncertain. The idea of a rigidity limit will be dealt with fully in a later section.

2.5 Muon Studies.

The points on the primary spectrum derived by Barrett et al. (1952) are shown in figure 2.1. These are based on measurements deep underground of the intensity of pairs, and single muons. Using simple assumptions as to the nature

of the primary interaction Barrett et al. were able to deduce the primary energy to which these measurements correspond. From comparisons between the energy derived from the muon data and the size of the accompanying electron shower at ground level Barrett et al. were able to deduce that the primaries at the two energies $4\ 10^{13}$ eV & $2\ 10^{15}$ eV are predominantly protons and Helium nuclei.

Again the measurements rely on a theory of nuclear interactions and to this extent must be regarded as subject to error.

2.6 Summary of Direct Measurements.

From the preceeding sections it can be seen that reliable measurements on the energy spectra of the various components extend up to 10^{10} eV. In order to make comparisons with E.A.S. data we need to extrapolate these measurements over many orders of magnitude taking as a guide the rather less direct measurements at higher energies.

At about 10^{10} eV the integral spectra of the various components seem to be approaching an exponent of -1.6. The points of Fowler & Waddington (1956) and Jain et al. (1959) confirm this for α particles out to 10^{12} eV and the spectrum of Koshiba et al. gives support as far as the heavier nuclei are concerned.

The energy spectra of Malholtra, and Baradzei together

with the observations of Lal, and Kaplon & Ritson are in agreement with the Proton I & II satellite measurements above 10^{12} eV on all nuclei. It may be permissible to disregard the Proton I & II measurements on the proton flux above 10^{12} eV.

Above this energy we have no energy spectra for different mass components only the isolated observations of heavy primaries already mentioned. It seems however that to assume that the composition once it has attained its asymptotic value at a few times 10^{10} eV remains constant up to at least 10^{14} eV is in no way against the experimental evidence presented so far.

2.7 Derivation of the Normal Composition

Figure 2.2 shows the best estimate of the primary spectrum assuming that the composition is constant above 10^{10} eV and using all direct measurements to give the best composition value and exponent in the region 10^{9} - 10^{14} eV. This spectrum is expressed as intensity above a constant energy per nucleon. The composition shown is the best estimate of the normal composition. This is to some extent uncertain as none of the direct comprehensive measurements extend sufficiently far to give the composition in the constant exponent region. It has been assumed that the composition does not change above 2.6 GeV following Waddington (1960).

Figure 2.2 Asymptotic values of the spectra of the primary nuclei as a function of nucleon energy. The 'normal' composition.

Fig. 2.2.

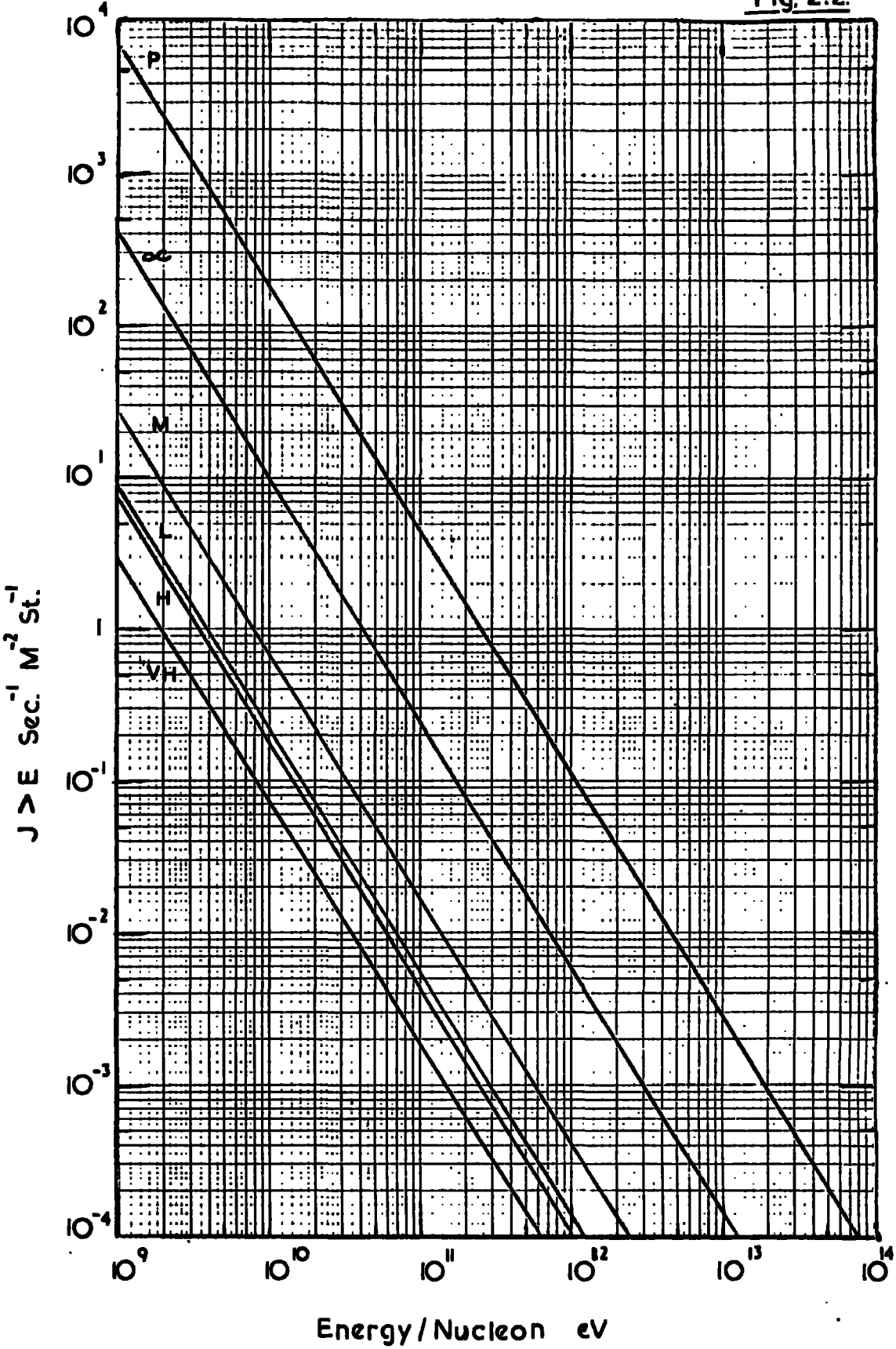
P
∝
M
L
H
VH
10^{4}
10^{3}
10^{2}
10^{1}
1
10^{-1}
10^{-2}
10^{-3}
10^{-4}
$J > E$ Sec.$^{-1}$ M^{-2} St.$^{-1}$
10^{9}
10^{10}
10^{11}
10^{12}
10^{13}
10^{14}
Energy / Nucleon eV

2.8 The Normal Composition as a Function of Primary Nucleus Energy.

Since in E.A.S. work the total energy of the primary is measured not the energy/nucleon it is necessary before proceeding, to derive the normal composition as a function of total nucleus energy. This means that the relative intensities of the heavy nuclei are enhanced compared to that of protons so that about half the nuclei above a given total energy are heavy and the mean mass of the primaries approaches 10.

The method of conversion to a spectrum of total nucleus energy is to shift each intensity greater than E eV/nucleon to an energy of A x E eV. This is repeated for each mass component. The result is shown in figure 2.3.

2.9 The Effect of a Rigidity Cut-Off in the Primary Energy Spectrum.

As mentioned in Chapter 1, the inflection in the primary energy spectrum between 10^{15} eV and 10^{18} eV has been explained by some workers as due to a rigidity cut off in the primary flux.

If this were so, the relative frequency of heavy nuclei in the primary flux would increase rather rapidly above a critical energy (assumed to be close to 10^{15} eV). Thus it is permissible to regard evidence for such a cut off (see below) as evidence on the primary mass composition above this

Fig. 2.3.

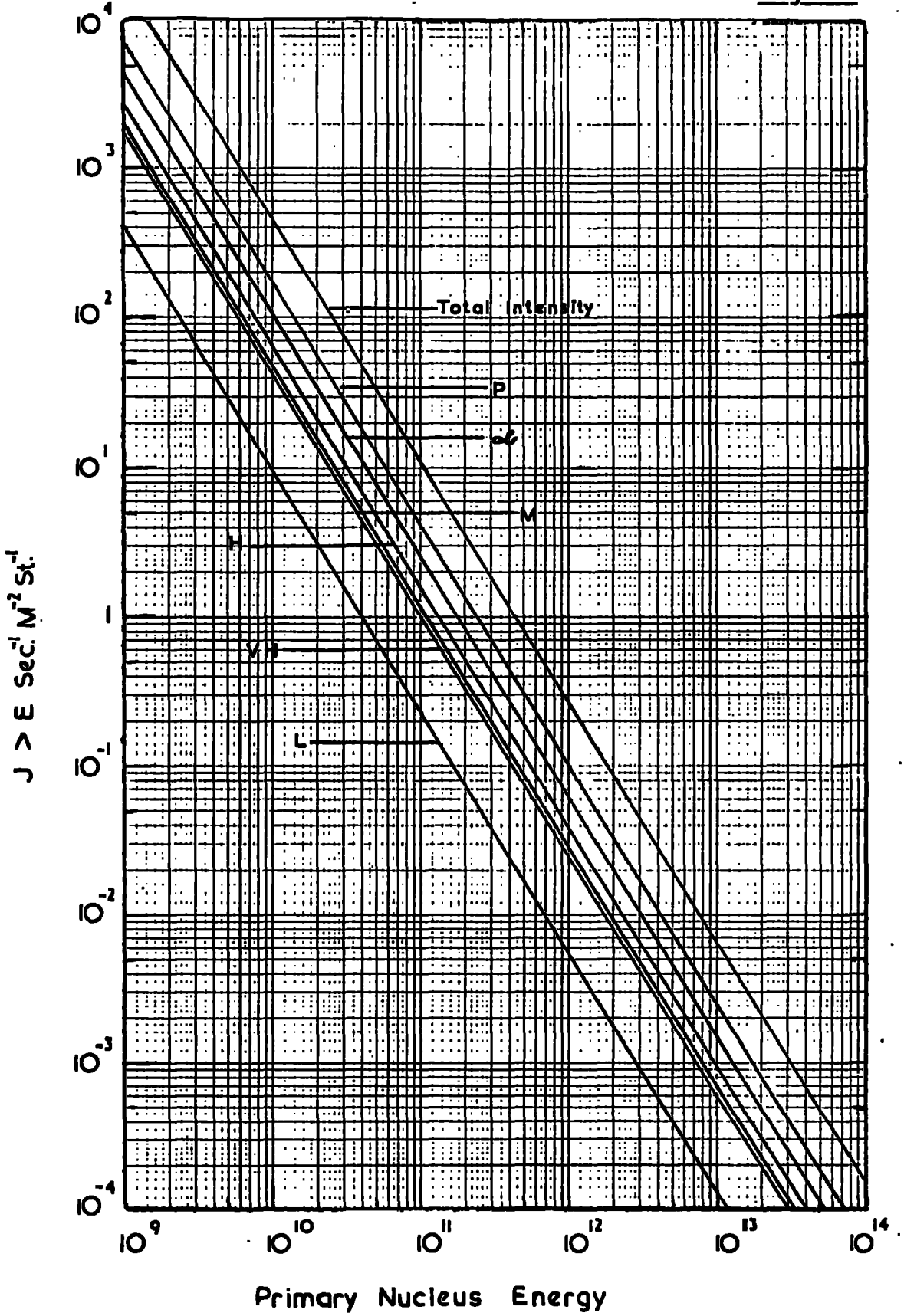

The normal composition as a function of primary nucleus energy

energy.

Peters (1961) has made several predictions which if verified may be taken as evidence for a rigidity cut off and hence for an increase in the mean mass of the primaries above 10^{15} eV. The existence of a limiting magnetic rigidity is equivalent to a limit to the primary nucleon energy. Thus any evidence for this may be taken as evidence for a rigidity limit and hence for a change in primary composition. These predictions are:

1. Measured parameters which depend only on the energy per nucleon of the primary should above a critical energy become constant.

2. Parameters which depend (for a given energy per nucleon) on the total energy of the primary, become proportional to the mass of the primary.

Examples of Parameters of the first type are: the energy spectra of atmospheric gamma rays and nuclear active particles. Parameters of the second type are: Shower size, and number of muons in the shower. The density spectrum of electrons in E.A.S. is a special case. If the individual cascades in an E.A.S. due to the separate nucleons in the primary merge at the point of measurement, then the density is of type 2. If however the cascades are distinguishable then the density is of type 1.

The following sections deal first with evidence from

E.A.S. studies which bears directly on the mass of the primary, and then with evidence for a limiting energy per nucleon.

2.10 Fluctuations in Electron Size.

It has recently been pointed out (De Beer et al. 1968) that fluctuations in electron numbers in E.A.S. have far reaching effects on the interpretation of E.A.S. measurements. An example of such an effect is the difference between the electron size calculated for a fixed primary energy and that resulting from the steep primary spectrum combined with the effect of fluctuations. This can be as large as a factor of 4.

These authors find that fluctuations in size are mainly due to fluctuations in position of the first few interactions of the primary, subsiduary contributions come from fluctuations in inelasticity and possibly multiplicity. The width decreases both with primary energy and with increasing mass. The former is due to the fact that generally the maximum of the shower, for which fluctuations are smallest approaches nearer to the level of observation as the energy increases. The latter effect is due to the superposition of the several separate cascades reducing the effect of interaction point fluctuations, and is the basis on which deductions as to the primary mass may be made.

A datum is necessary against which to measure variations of electron shower size for a given primary energy. De Beer et al. (1968) give predictions both for the variation of electron size at a constant muon size and vice versa. The analysis is made for two alternative models of the primary spectrum, one protons only and one having an increasing proportion of heavy nuclei above 10^{15} eV. Adcock et al. (1968) give a comparison of this theoretical work with available experimental data both for fixed muon size and fixed electron size. They conclude that at present no conclusions can be drawn due to the inaccuracy of the experimental data.

2.11 The Ratio of Muons to Electrons in E.A.S. as a Function of Electron Size.

If one assumes that an E.A.S. due to a heavy primary can be regarded as a superposition of the individual nucleon initiated cascades, then as primary mass increases the number of muons, at sea-level, in a shower of a given energy increases, while the number of electrons decreases. Thus a measurement of the ratio of muons to electrons can in principle give an estimate of the primary mass.

Because systematic errors are large a more sensitive indication may be obtained by studying the variation in this ratio with shower size and hence energy. If $N_\mu = K N_e^{\alpha}$ α is practically constant at 0.8 for all masses. However K varies with mass so that a change in composition should

result in an alteration in the apparent value of α . An increase in mean mass of the primaries will produce an increase of α whereas a decrease has the opposite effect. A region of the spectrum where the composition is not changing will cause α to return to its true value 0.8.

At present Adcock et al. (1968) find that no indication can be drawn due to insufficient data. Very recently however there has been some evidence (Maze, Private Communication) that the modulation effect has been observed to occur over a small range of shower sizes close to 10^{15} eV.

If substantiated this result would not be consistent with the Linsley (1962) picture. The energy range over which the modulation appears to take place is much too narrow. Chatterjee (1964), has presented a theory based on observations made of on E.A.S. at Ooty, which could possibly support the observations of Maze. It is suggested that at 10^{14} eV the primary spectrum suffers a very sharp rigidity cut off, at the same time at 10^{15} eV there is an influx of protons, from another source, of energy spectrum exponent -3.1 (differential). This explains Chatterjee's results and also the first kink in the primary spectrum at 10^{15} eV.

2.12 Multiple Cores

Experiments by Bray et al. (1965) on the lateral distribution of electrons close to the core of an E.A.S.

revealed that two types of shower were observed, those with a single steep core, and those which appeared to have several sub cores. The variation of frequency of the different types with electron size was of great interest. It showed that below a size corresponding to approximately 10^{15} eV single cored showers made up about 50% of all showers (i.e. the same proportion as protons in the primary flux). Beyond 10^{15} eV the fraction of single cored showers fell rapidly. The coincidence between this behaviour and the expected rigidity modulation of the primary spectrum lead Bray et al. to postulate that in some way proton initiated showers had single cores and heavy initiated showers, multiple cores.

In order to explain these results these workers commenced a series of E.A.S. model calculations in an attempt to predict this behaviour. It was found that only by assuming that the tranverse momentum of particles released in the nuclear interaction was large could these results be explained in terms of heavy primaries. More recently, Thielheim (1968) has also performed such calculations and concluded that data on the primary mass would be unobtainable in this way because sub-cores would only be separated by a few centimetres.

The experiment has also been done by other groups. Matano et al. (1968) found that two types existed, but found that only about 3% of the showers had multiple cores. This

result was important because spark chambers were used so that very good resolution was obtained. Bray et al. used 10 cm thick plastic scintillation counters and as a consequence the measurement of particle number was less direct.

An even more sophisticated experiment has recently been carried out by the Kiel Group, Bohm et al. (1968). They used neon flash tubes each of area a few cm^2 covering 32 square metres, to study core structure. They found that less than 0.5% of showers had multiple cores.

A recent paper by the Kiel group, (Samorski et al. 1969) contains a comprehensive analysis of the situation of multiple core studies. The conclusions they reach are as follows:

1. There is no experimental evidence for multiple cores requiring large transverse momenta.

2. Large background effects due to interactions of low energy hadrons, and poissonian fluctuations exist. These are not resolvable in apparatus as used by the Sydney group (Bray et al. 1965).

3. It is possible to predict the effect observed by Bray et al. simply from a consideration of the above factors.

Thus it would appear that there are now strong objections, both theoretical and experimental to the initial conclusions of Bray et al. and it would appear that no measure of the primary mass can be derived from studies of multiple cores.

2.13 The Muon Lateral Distribution at Large Distances from the Core.

Orford and Turver (1968) have suggested that the rather flat lateral distribution of muons (above 40 GeV), at large distances from the core, implies a height of origin of these particles corresponding to the region of the first few interactions of the primary. In order to explain the flux of these muons they find it necessary to postulate that the multiplicity of pions produced is proportional to the square root of the interaction energy, and that the mass of the primary particles is greater than 10. Thus these workers would not agree with the findings of Linsley and Scarsi (1962), and the BASJE Group (Toyoda et al. 1965) that at 10^{17} eV, (the energy at which Orford & Turver have worked), that the primaries are protons.

2.14 Density Spectrum Measurements.

Norman (1956) was first to point out that the electron density spectrum appeared to steepen at about 500 P/M^2. These measurements were repeated by Prescott (1956) and later at different altitudes above sea-level, Swinson & Prescott (1965). Further measurements at sea level (Reid et al. 1961, McCaughan et al, 1965a), pointed towards a cut off at 5000 P/M^2 at sea level.

Swinson & Prescott (1965) have interpreted the existence

of this cut off, and its movement towards higher densities, as the level of measurement rises, as evidence for a limit to the energy/nucleon of the primary spectrum. Their argument relies on the separate nature of the cascades due to the individual nucleons in a heavy primary induced E.A.S. As pointed out above it is now considered that these may not in fact be separable so that some other explanation may be necessary.

2.15 Gamma-Rays in the Atmosphere

The gamma-ray spectrum at high altitudes has already been mentioned as a way of measuring the primary energy/nucleon spectrum. Several workers e.g. (Malholtra et al. 1965) have observed an apparent steepening of the gamma ray spectrum at about $2\ 10^3$ GeV. This may be interpreted as an energy/nucleon cut off at $1.4\ 10^{13}$ eV. However some measurements (Baradzei et al. 1962) do not show a steepening and it may possibly be an experimental bias. Also such a cut off is much lower than the customary postulate of 10^{15} eV.

2.16 Summary of Mass Composition Measurements.

Below 10^{14} eV figure 2.1 shows a summary of the measurements discussed in the text. It would appear reasonable to assume that in this region the composition maintains its 'normal' value derived from direct measurements.

In the region of 10^{17} eV measurements by Linsley and by

the BASJE group support the idea that the primaries are protons. Orford & Turver would not support this, however the use of the $E^{\frac{1}{2}}$ multiplicity law is not necessarily justified, and some other explanation of this result may be possible.

It would appear that in view of the recent work of the Kiel group it is no longer possible to rely on the evidence of multiple cores implying an increasing mean mass above 10^{15} eV.

The hypothesis of a rigidity cut off in the primary spectrum has received support from several experiments. However there is a wide divergence of opinion as to where it occurs. Gamma-ray spectra suggest a rather low value at 10^{13} eV, while density spectrum measurements give a value closer to 10^{15} eV. The apparent steep fall in the proton spectrum observed by Grigorov et al. (1968), could also be interpreted as due to a rigidity cut off.

The study of fluctuations at present does not lead to any conclusions on the primary mass. However increased statistical accuracy in the future may lead to a definite conclusion.

The whole question of composition in the E.A.S. region turns on the reason for the change in exponent of the primary spectrum at 10^{15} eV. If this is due to a rigidity cut off then the mass of the primaries must increase. If not, then either the composition will remain constant, or will change,

approaching a pure proton flux. The former is not considered likely on astrophysical grounds. The latter could be due to a new source of cosmic rays appearing at about 10^{15} eV, the heavy primaries having dropped out of the spectrum. Recent data from the Haverah Park array extends the spectrum to beyond 10^{18} eV with no sign of a change in slope. It is hard to reconcile this with a rigidity cut off at 10^{15} eV, where it would be expected that the spectrum could continue at most to about 10^{17} eV.

Thus the overall composition picture is confused and little can be concluded with certainty. Indications of an increase in mean mass above 10^{15} eV are inconclusive, equal uncertainty attends the other possibility that the primaries are mainly protons above this energy.

CHAPTER 3

3.1 Introduction

The experimental problem is to build an apparatus which will measure the frequency of occurence of coincident groups of muons as a function of the zenith angle and number of muons in the group (multiplicity). As mentioned in the introduction both experimental and theoretical problems are fewer in the horizontal direction.

An earlier form of the apparatus is described in Alexander et al. (1968) where preliminary measurements were presented. It was obvious from this work that contamination of events by electrons was a problem. It proved to be true that the electron component of E.A.S. was largely filtered out by the atmosphere, however the production of electromagnetic showers by muons interacting in the lower atmosphere is sufficient to produce quite an intense electron component at large zenith angles. Details of measurements on this component are given in Appendix 1.

The experimental steps necessary to discriminate against the electron component were threefold. As reported in Alexander et al. the increase of absorber thickness from 1.5 to 4.5 radiation lengths, reduced the flux of electrons to a large extent. Also the reduction of the coincidence requirement from fourfold to twofold increased the detection probability

for muon showers. The final step, not reported in Alexander et al., was the design of two 'muon detectors' as triggering units, instead of the simple pair of counters used in Alexander et al. These gave unambiguous identification of muons as detailed below and enabled precise experimental measurements to be made.

Thus the final form of the apparatus had good spatial resolution over an area of 34 sq.metres, angular resolution over the same area of $\pm 10^{o}$ for individual tracks, and precise identification of the two triggering particles as muons by their penetration of 9 radiation lengths of absorber, and their parallelism to within 4^{o} as measured in the muon detectors. (Theoretical calculations lead to an average scattering angle of muons of approximately 3^{o} in E.A.S.). In addition the acceptance of the apparatus in terms of triggering probability and solid angle, could be calculated precisely. The use of detectors such as neon flash tubes and plastic scintillation counters, means that the efficiency of detection of particles is almost 100%.

There are as mentioned below gaps between the flash tube trays. In the final analysis these are not important as we are concerned only with the number of particles in a given sensitive area, and not with apparent densities, or variations of density. However there could in principle be some loss due to particles which trigger the telescopes (see below) and do not pass through the array trays. In the design of the

apparatus this number was made as small as possible by suitable positioning of the detectors. A further allowance was made in the data collection (section 4.1).

3.2 General description of the apparatus.

The arrangement of the multiple muon apparatus is shown in fig. 3.1. It consisted of a vertical stack of trays of Neon Flash Tubes, twelve in all, each containing four columns of 66 tubes. The trays were arranged in four columns of three so as to form a rectangular vertical plane, its normal directed 18° to the East of True North. The northern face of this array was shielded by 1.5 and in the final form, 4.5 radiation lengths of iron plates. The overall dimensions of the apparatus were 7.2M by 11.6M. The detecting elements were five scintillation counters each of area one square metre. Four of these were arranged to form two counter telescopes, one at each end of the flash tube array. The fifth was placed horizontally at the top of the array and served to reject near vertical showers. Each counter telescope contained further trays of flash tubes and a further layer of iron plate to help in the identification of muons.

The flash tube array was triggered whenever a coincidence between the two telescopes occurred without a coincident pulse from the fifth scintillator. The flash tubes were photographed by one camera via a system of mirrors. Thus it was possible to observe the tracks of particles in an air shower which

Figure 3.1 (a) Front and plan views of the apparatus.
T_1----T_{12} are 2.8 square metre trays of Neon flash tubes, S_1 - S_5 are 1 square metre plastic scintillation counters.

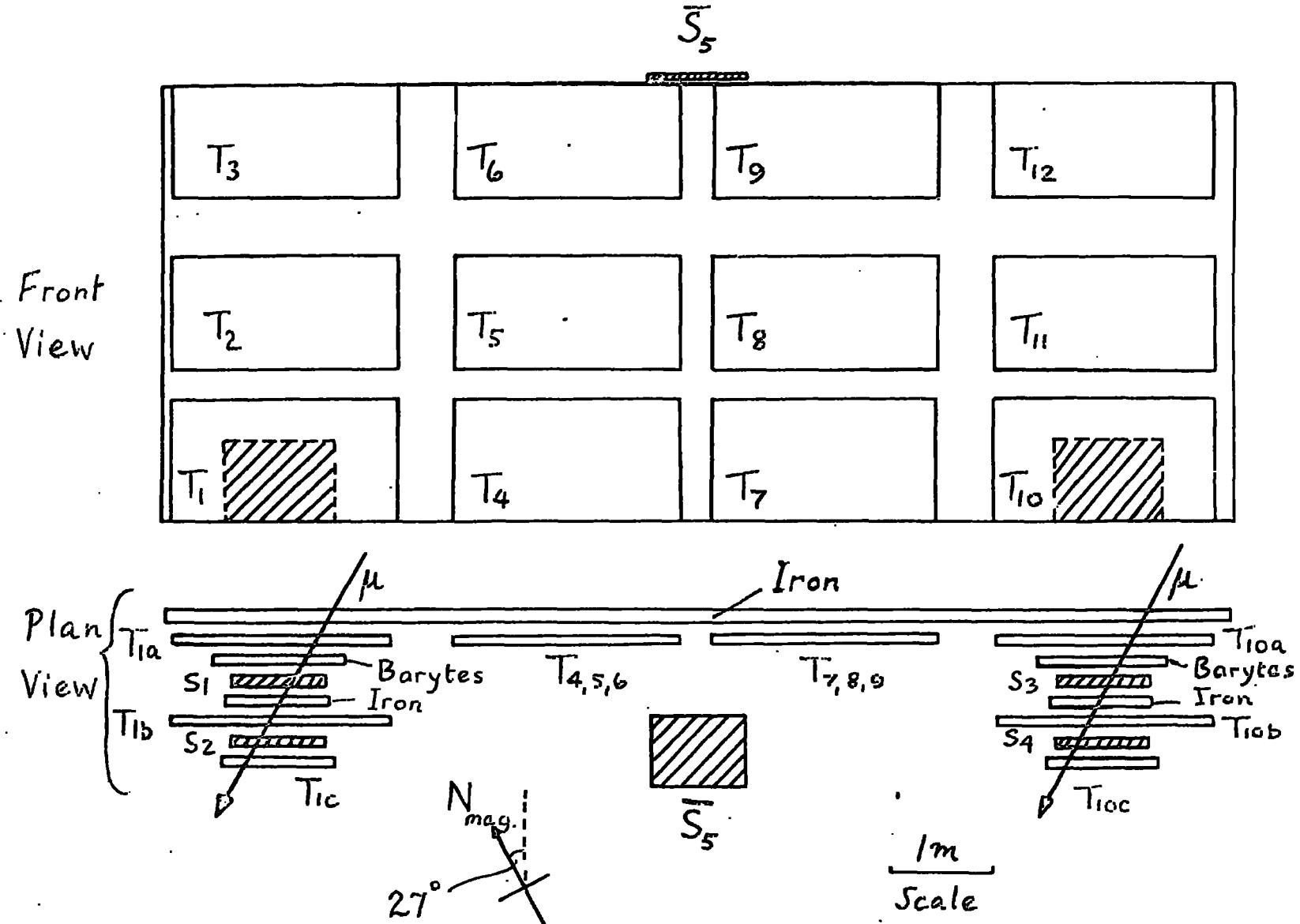
$\bar{S}_5$
T_3
T_6
T_9
T_{12}
Front View
T_2
T_5
T_8
T_{11}
T_1
T_4
T_7
T_{10}
Plan View
T_{1a}
T_{1b}
T_{1c}
μ
Iron
Barytes
S_1
S_2
$T_{4,5,6}$
$T_{7,8,9}$
T_{10a}
T_{10b}
T_{10c}
S_3
S_4
$N_{mag.}$
27°
1m
Scale

Fig. 3.1 (a).

Fig. 3.1.(b).

Detailed view of one of the muon detectors.

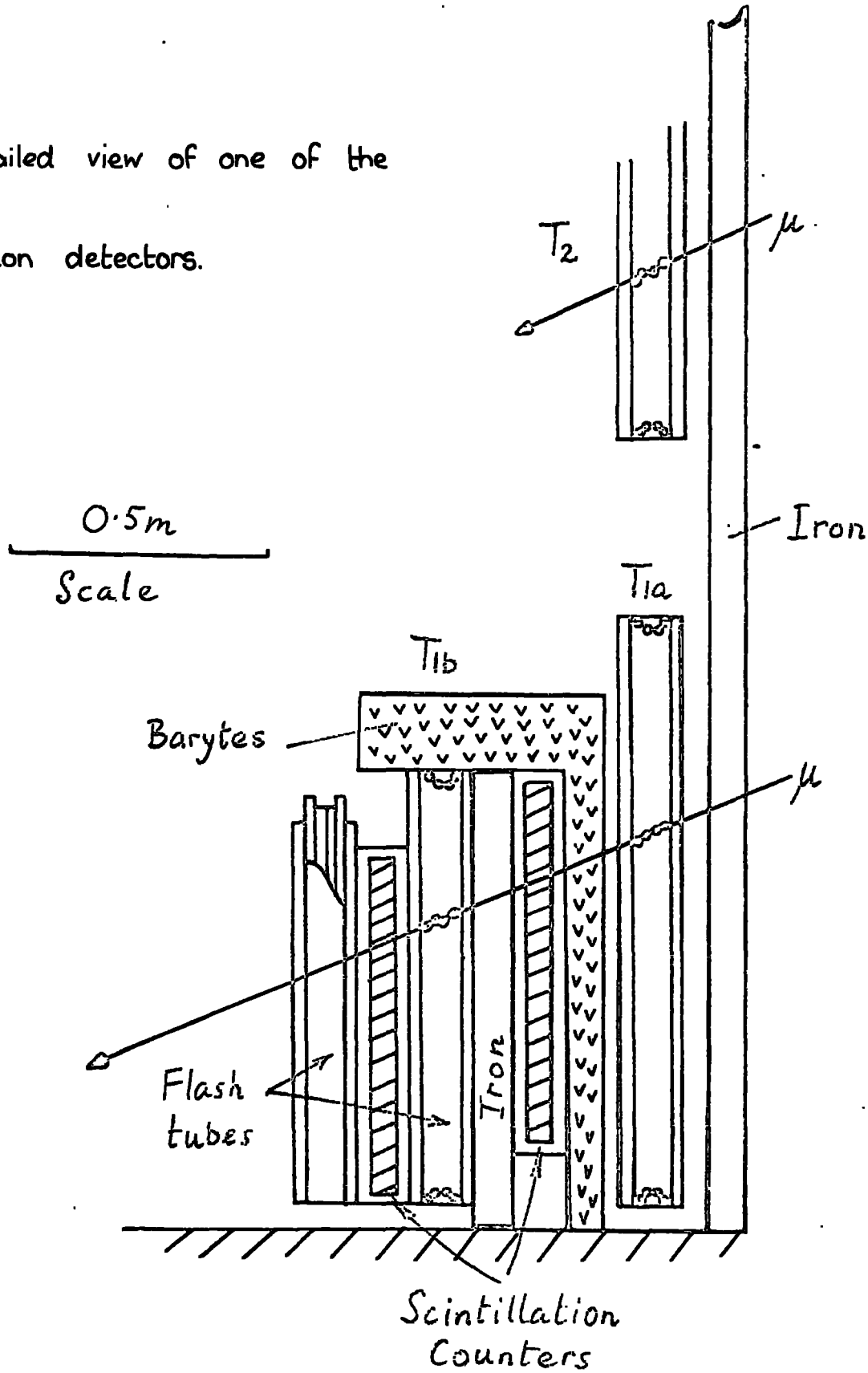

provided at least two penetrating particles, (one in each counter telescope), over a sensitive area of 34 square metres. The Neon flash tube array was capable of extremely good spatial resolution combined with moderate angular resolution. The additional flash tube trays in the counter telescopes improved the angular resolution for the triggering particles. A detailed description of the individual components of the system follows.

3.3 The Neon Flash Tubes:

This is a type of particle detector which has been in use at Durham for nearly a decade, and is now being used at other Universities in this country, and also in South Africa and India. It was first described by Conversi and Gozzini.(1956). Later much research on the practical application of the device was carried out by the Durham group, notably Coxell and Wolfendale (1960) leading to the present form of the Neon Flash tube.

The type used in this experiment consisted of a soda glass tube 1.5 cms. in internal diameter having a wall thickness of 1 mm. The tubes in the main array were 2.5M. in length and those in the telescopes were of two lengths 2M. and 1M. During construction one end of the tube has a flat window formed on it, the tube is then evacuated and filled with commercial grade Neon to approximately 60 cms. Hg. pressure and the other end is drawn out and sealed. The window end is then painted

white for about 30 cms. of its length and the other end black for the same length. When the tubes are packed into trays they are interleaved with black polyethylene film so that no tube wall is in optical contact with another. When a pulsed electric field of 4.5 K.V./cm., a few microseconds long is applied to a tube within a few microseconds of the passage of an ionizing particle through the tube a discharge takes place producing an intense flash of light which may be photographed through the window at the end. The light is sharply collimated along the axis of the tube and the purpose of the white paint at the window end is to broaden the angular distribution of the light so as to make photography of large numbers of tubes easier. The black paint and black polythene are to prevent the light escaping from the side of one tube setting off another. This mechanism is possibly the production of electrons from the glass wall as ultra-violet light cannot penetrate the glass and photo-ionization of Neon gas by Neon light is energetically impossible.

Certain tubes have the property of flashing whenever a pulse is applied independent of the passage of ionizing radiation. These 'flashers' form less than one per cent of any batch of tubes and may have irregularities on the glass surface which provide a source of ions. Once recognised these can be ignored in scanning of the film.

The tubes were mounted in trays consisting of 2.4M. x 1.2M. aluminium (16g) sheets mounted in an iron framework. The

outer pair of sheets were separated by 'Tufnol' spacers which had a central slot to take the third sheet. This was thus insulated from the frame and formed the high voltage electrode, the outer sheets forming the earthed electrodes. This arrangement besides being safe, reduces radiation of the applied pulse. Fig. 3.2 shows how the tubes were arranged in the trays in a close packed fashion with the polyethylene film interleaved. Each tray was constructed with lugs to lock it to the tray above and on the window end had supports for a mirror welded to top and bottom. The outer electrodes were earthed and the centre electrode was connected to a socket into which the cable carrying the high voltage pulse could be plugged. This cable which was coaxial had its outer sheath connected to the outer electrodes thus ensuring an efficient return for the pulse.

The iron girder framework which supported the apparatus can be seen in the photograph (fig. 3.3). The twelve trays were arranged in columns of three. The window ends faced each other looking into two gaps, one between the 1st and 2nd columns, and one between the 3rd and 4th. These gaps were left so that vertical mirrors could be placed in front of the windows at 45° to the plane of the trays to reflect the light from the tubes out perpendicular to the array. Horizontal gaps were also left between the rows of trays so that no flash tubes were placed where they could not be photographed because of the prescence of the supporting girders.

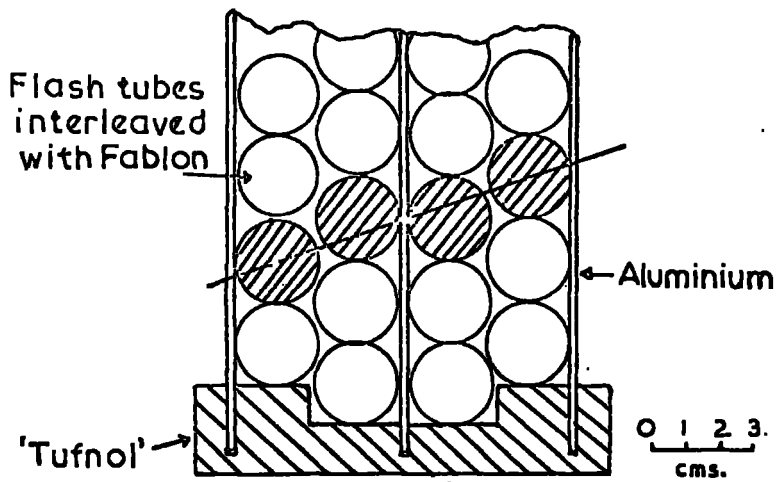

The construction of the flash-tube trays.

Figure 3.3 Photograph of the apparatus.

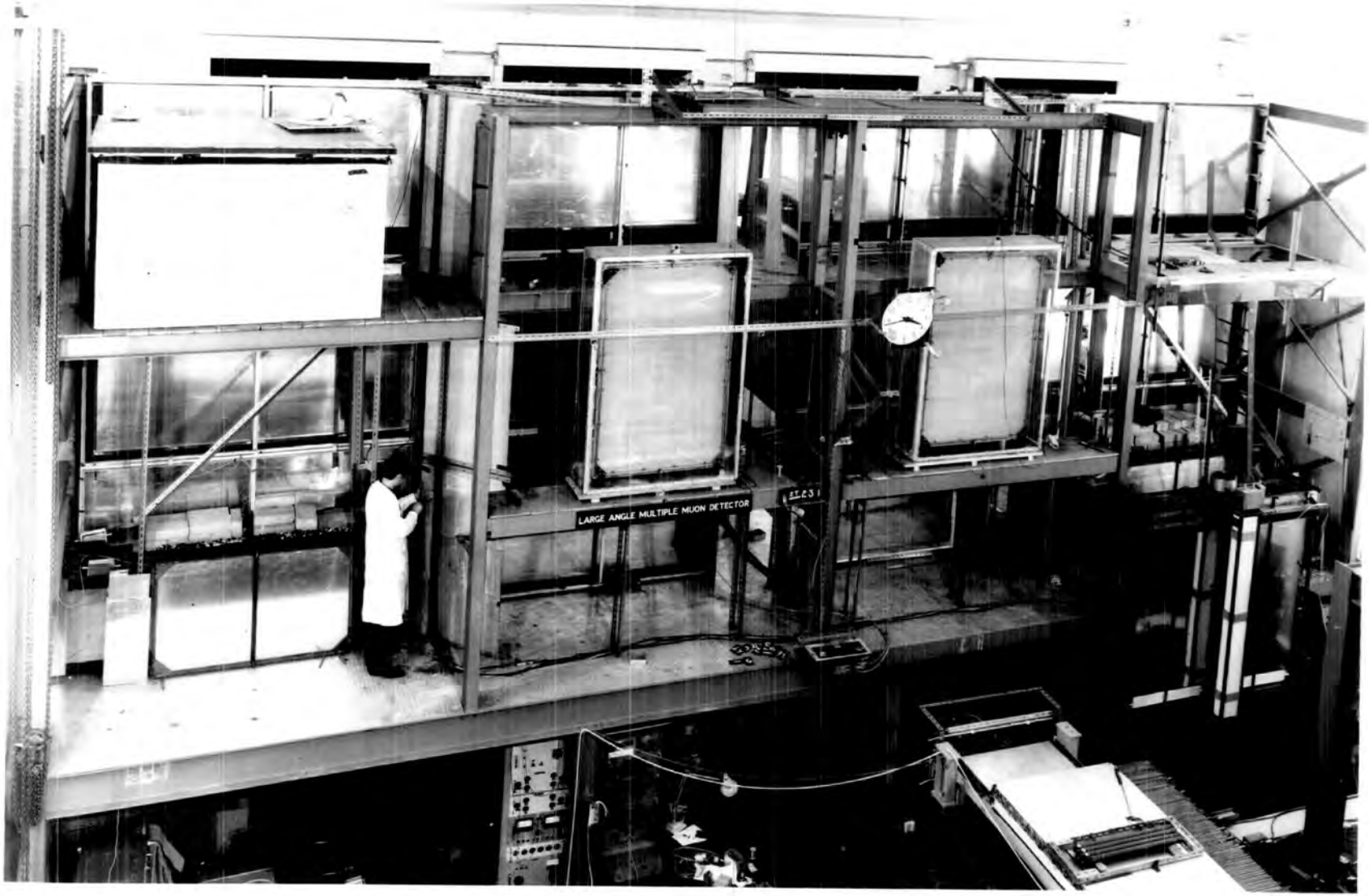
LARGE ANGLE MULTIPLE MUON DETECTOR

3.4 The Mirror System:

Opposite each vertical gap in the flash tube array were placed three 5ft. x 3ft. mirrors, one for each row of trays. These were angled at 45° to the normal to the array so as to reflect the light from the pair of tray-mirrors back, parallel to the tubes, towards the centre of the array. Here six similar mirrors were placed facing and parallel to the earlier mirrors so that the light from the vertical gaps on each side of the array was reflected out, perpendicular to the array, in two close parallel beams. On the opposite wall of the laboratory a large mirror (6ft. x 8ft.) was placed so as to reflect the two beams back towards the centre of the array. Here a narrow mirror was mounted on the centre girder at 45° to the horizontal to reflect the light vertically down. A platform was constructed level with the first floor of the array on which a camera was placed on a kinematic stand looking upwards into the narrow mirror. Thus the 3,300 flash tubes could be photographed by one camera. The system is shown in fig. 3.4.

The purpose of this rather complex system was to enable the optical path to be made large so that the camera could look almost axially down every flash tube. It has been mentioned that the light from the flash tubes is sharply collimated and if the axis of the camera were to be more than 10° from the axis of the tubes no light would be visible. Even with this path length (24M.) it was found necessary to

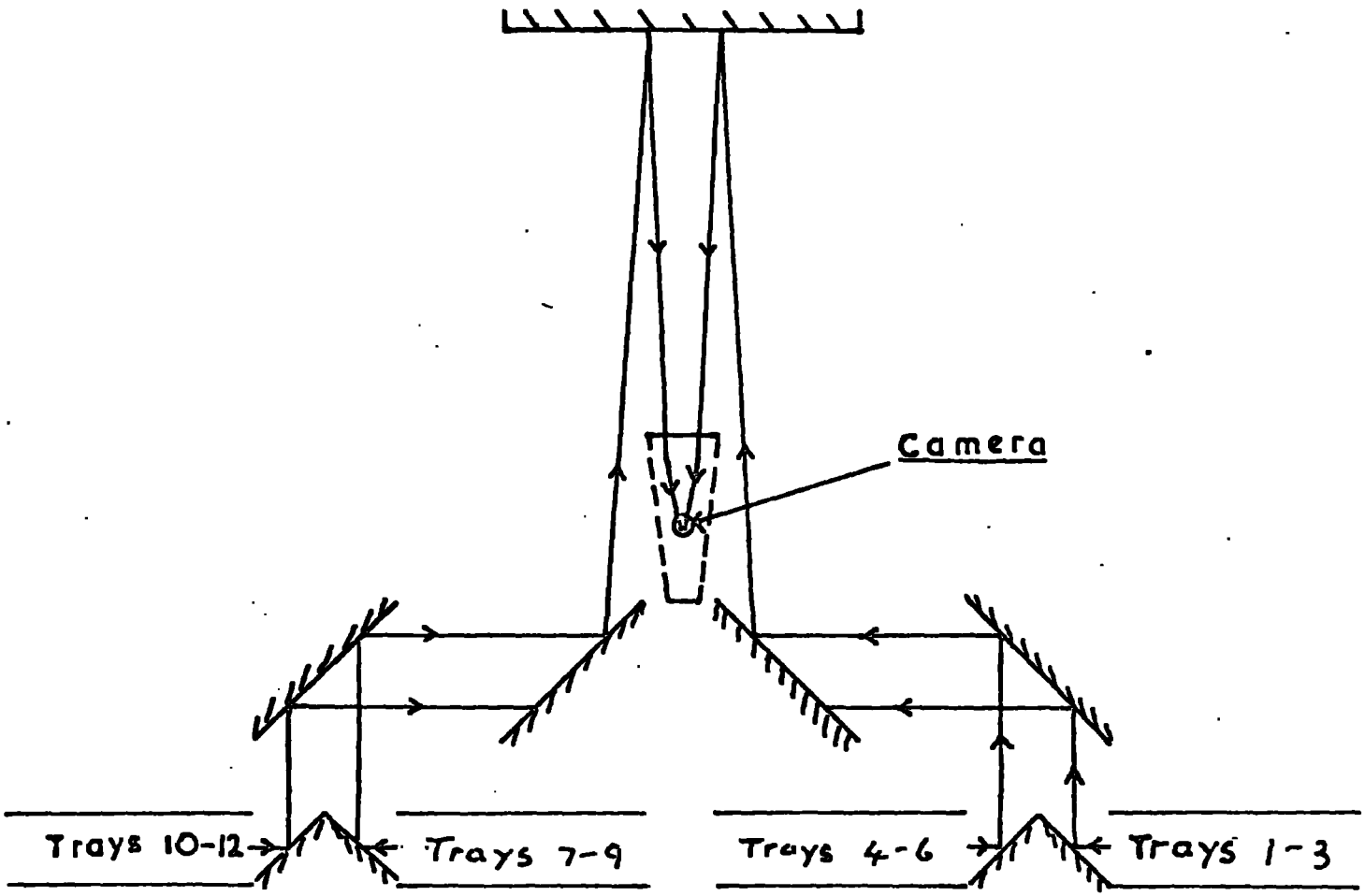

Fig. 3.4. The mirror system

tilt the mirror system of the top and bottom rows of trays so that the axis of the camera was more nearly parallel to that of the flash tubes.

The use of such a long optical path brought two further difficulties. The first was that at this distance the image of a single tube is almost a point. So that the tubes had to be operated at a higher potential than is normally used to increase their brightness. The second difficulty was caused by the type of mirror used; because of the high cost of such a large area of plate glass, thin silvered ordinary glass was used and in spite of careful selection of individual glass sheets, there was some distortion of the image. This was overcome in the scanning of the film by the scanner filling in the tubes which had flashed on a copy of a scale diagram of the window ends of the flash tube trays. In this way the human eye was used to take out the distortion produced by the mirrors. This was possible because the tracks of particles at any angle produce only a few, well recognizable patterns of flashed tubes which when transferred to the scale diagram regained their original configuration. The distortion was in general on a scale comparable with the size of a tray so that individual tracks were barely affected. Two fiducial lamps were mounted on each tray to assist in location of the image of the trays.

3.5 The Iron Shield:

The whole of the Northern face of the flash tube array was

shielded by iron plates, in preliminary experiments this was one inch thick (1.5 radiation lengths) and in the final form it was 3" thick (4.5 radiation lengths). The thickness of absorber along the path of the incident particles was 4.7 radiation lengths at a zenith angle of 75°, 5.2 at 60°, 6.4 at 45° and 9.0 at 30°. Thus the absorber thickness increased at the smaller zenith angles where the intensity of the electron component is higher.

3.6 The Detecting elements

These were five scintillation counters each of area 1 square metre. The counters were constructed out of aluminium alloy channel and were 8' x 2'6" x 3". A slab of Ncl02A plastic scintillator (133 cm. x 75 cm. x 5 cm.) was mounted in the frame so made. Light guides of 'Perspex' acrylic plastic in the form of a trapezoid were attached to the shorter ends of the scintillator with optical cement. The ends of the light guides tapered down to 2" x 2" so that a 2" diameter photomultiplier could be fixed on to each end with optical cement. Ashton et al. (1965) have shown that this design gives good efficiency and uniformity while being economical in photomultipliers. The Photomultipliers were shielded against magnetic fields by μ-metal cylinders, with outer iron cylinders. A dynode resistor chain (fig.3.5) was soldered on to the base into which a photomultiplier was plugged. An insulated wire carried the E.H.T. to the base from a Plessey type coaxial socket mounted in the frame. A single wire carried the pulses from the anode

Fig. 3.5.

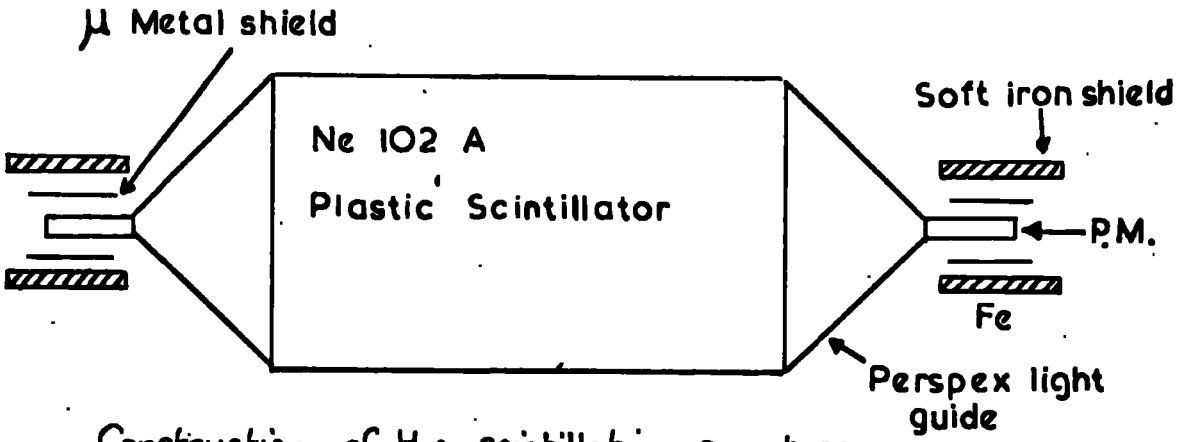

Construction of the scintillation counters

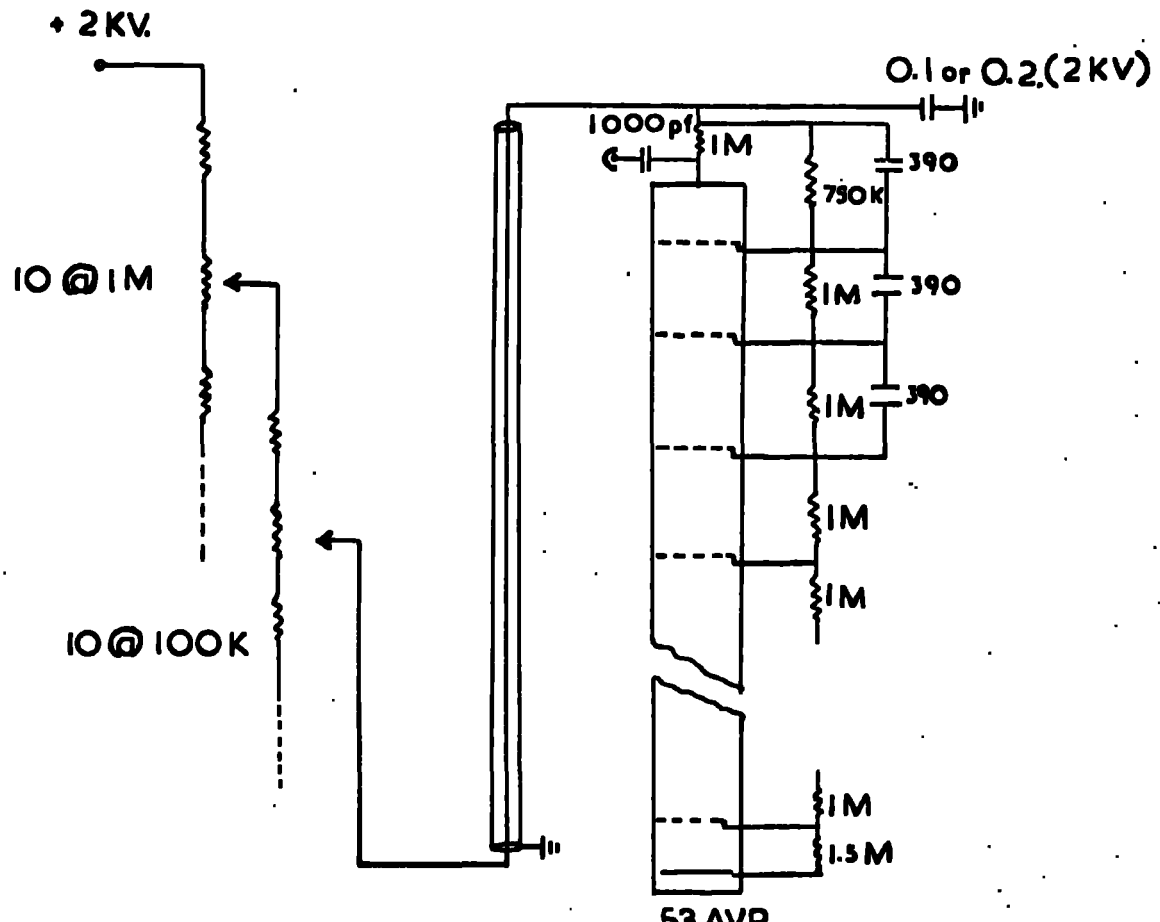

Gain control of the photomultipliers

which was positive with respect to earth via a condenser - to the outside of the counter. The open faces of the counter were covered by aluminium sheet screwed down and light sealed with black adhesive tape.

The EHT to each individual photomultiplier was separately controlled by a switched resistance chain in the control room from whence it was carried by coaxial cables to the counters.

The photomultiplier pulses on exit from the light tight box were fed to a 3 transistor head amplifier, one at each end of the counter. The pulses were then fed into an adding circuit followed by an inverter amplifier. From here the pulses followed two paths, one after a further emitter follower lead via a cable to the control room, the other entered a fast discriminator (tunnel diode) and the discriminator pulses after differentiation were also fed oncable to the control room. The circuitry described here was mounted on each individual counter inside a metal gauze box. Thus each counter had five cables associated with it all being lead to the control room. These were; two EHT leads (one for each photomultiplier); two pulse leads (the discriminator pulse and the added pulse), and one power cable for the electronics.

The discriminators had a fixed level and in order to alter the level of discrimination the E.H.T. delivered to each photomultiplier was varied, thus varying the gain. Initially the counters were adjusted by using a small scintillator telescope to select cosmic ray particles passing through the

centres of the counters. The pulse from the telescope was used to gate the input to a 400 channel pulse height analysis (P.H.A.) By unplugging each end of the counter in turn the distribution of pulse heights from each end of the counter could be observed and the gain adjusted till the peaks were at the same channel on the P.H.A. In this way the two ends of the counter are balanced. The pulses were then allowed to add as in normal operation of the counter and the total distribution observed. Then the P.H.A. was gated on the discriminator pulses from the counter and the position on the distribution where the discriminator operated could be seen. The gain of both ends was then readjusted so that the whole of the pulse height distribution due to particles appeared above the discrimination level. This of course allowed some of the noise through the discriminator but the coincidence arrangement effectively curtailed any possible ill effects due to this.

Thus each counter was set so as to be virtually 100% efficient for cosmic ray particles passing through it. The counters had lifting lugs screwed into the frames so that they could be moved with ease.

3.7 The Muon telescopes.

Figure 3.1 (b) shows the design of the two detecting elements. These were formed out of four of the scintillation counters.

Each pair of counters formed a telescope which was placed

on the south side of the flash tube stack, separated from the trays by a layer of barytes concrete. The axes of the telescopes passed through trays 1 & 10 in the main stack. The northern counters in each telescope were raised 15 cm. with respect to the southern ones in order to bias the system towards particles from the North. Between the counters forming an individual telescope was a layer of 4.5 radiation lengths of iron and a tray of flash tubes, both being extended over the whole sensitive area. On the south side of each telescope a tray of vertical flash tubes was positioned to give an estimate of the azimuth of the triggering particles. It was possible by suitable positioning of additional mirrors to enable all these trays of flash tubes to be seen in the main mirror system. However the thickness of glass and number of reflections involved for the azimuth trays (nine in all), made it rather difficult to gain precise information from them, and in particular it was not possible to get a track visible in this tray for every particle passing through the scintillators. However for the horizontal trays this was no problem and accurate information on the zenith angle of the particles passing through the telescopes could be obtained. This information was derived using the tray in the main stack (1 or 10) together with the telescope trays. Each tube in the two trays (the main tray and the telescope tray) was numbered and could be individually identified on the photograph by means of its relationship to the fiducials. This was

ensured by examining many photographs of events and tracing the position on the film of the flashed tubes. In this way it was possible to build up a picture of the whole tray as it appeared on the film and compare this with the actual positions of the tubes. With the aid of this tracing it was possible to draw on to a scale diagram of the tubes an exact picture of the track. Thus by using the two trays it was possible to measure the zenith angle of the track to a high degree of accuracy.

3.8 The Coincidence and Pulsing Systems:

The discriminator pulses from the counters on reaching the control room were fed to individual blocking oscillators which produced square pulses. These were added and fed to a variable discriminator. In this way the discriminator could be set to operate when from 2 to 6 pulses were added at the same time. A vetoe gate was operated by the anti coincidence counter. Two output pulses were available from this coincidence unit. In the final form the coincidence was four-fold plus an anti-coincidence pulse.

The pulse from the coincidence unit was fed to a cycling system which consisted of a paralysis gate to stop following pulses from triggering the system before the event had been recorded, an amplifier to provide a pulse to trigger the flash tube pulsing system, and a series of cams driving micro switches

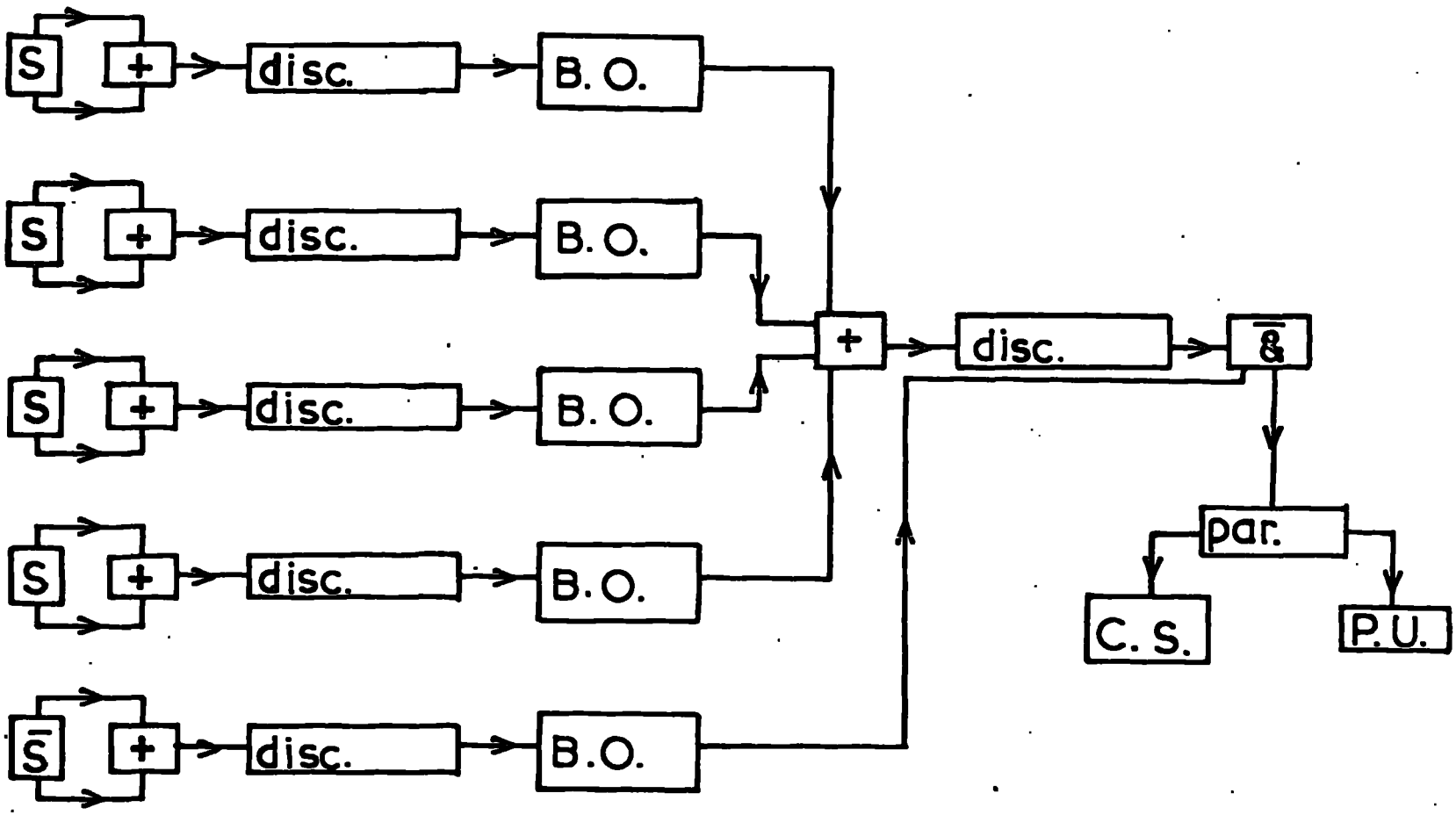

Fig. 3.6. Block diagram of the logic system

Fig. 3.7

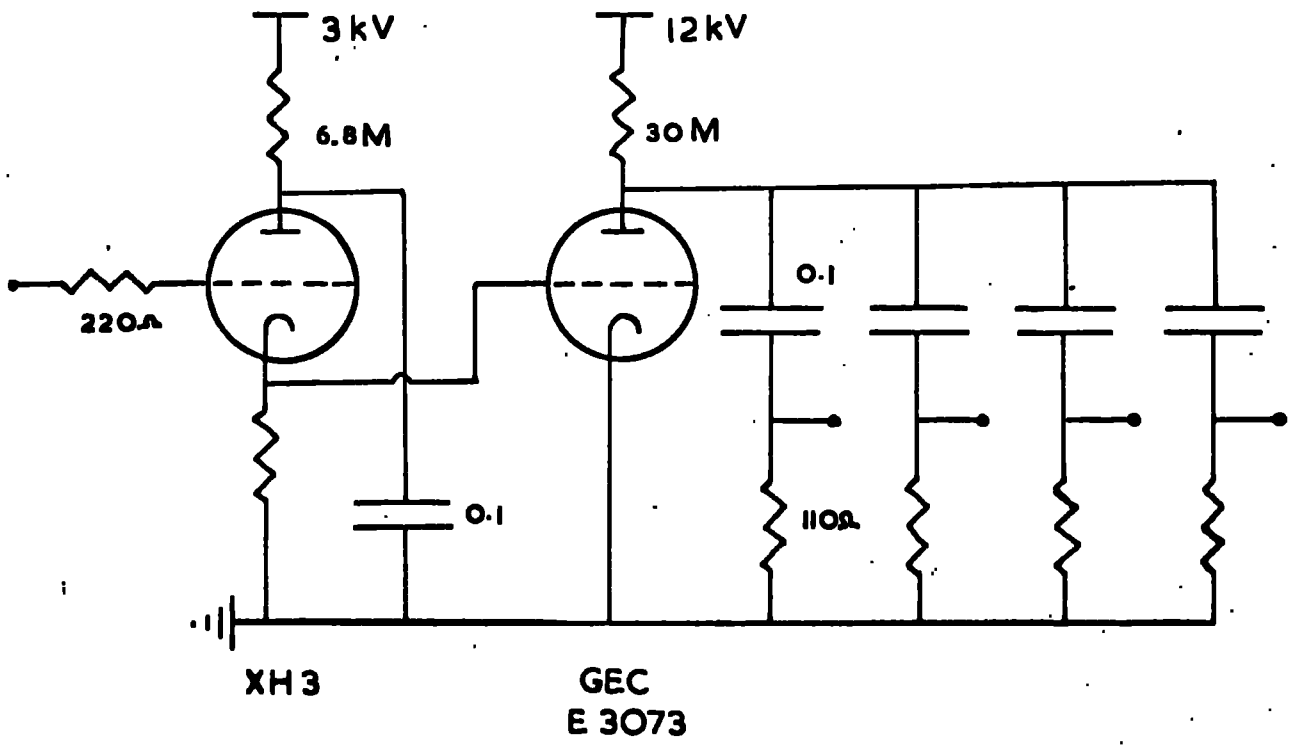

The Flash-tube pulsing system

which gave the sequence of controls to record the event. The input pulse set the paralysis gate, started the cams rotating, and triggered the pulsing unit. The cams then lit the fiducials for a set time, illuminated the clock, wound on the camera, reset the paralysis and finally switched themselves off. Rheostats on the apparatus enabled the many fiducial lamps and clock illuminating lamps to be adjusted in intensity.

The amplifier providing the trigger to the pulsing unit was made of a single high voltage transistor. This was because an inevitable pulse of about 50 volts was fed back down the line when the pulsing unit fired. The final stage of the pulsing unit was a 'surge diverter' (a cold cathode gas filled discharge device G.E.C. E.3073). This discharged a bank of 6, 0.1 micro-farad condensers through 100 ohm. resistor chains. The pulse from the chains was fed via coaxial cable to each flash tube tray, one condenser feeding a group of three trays.

The surge diverter was triggered by several devices during the running of the apparatus. The greater part of the time it was triggered by an XH3 Hydrogen thyratron triggered in turn by a pentode amplifier. The final stages of the work were completed using a television line transformer, as a pulse transformer and triggering this with a thyristor discharging a small condenser charged to 200 V.

Both systems enabled an R.C. pulse of peak voltage 14 Kv to be applied to the trays within about 4 microseconds of the

coincidence. The pulse had a typical decay time of 30 microseconds. This was found to produce efficient bright tubes. The condensers were charged at the rate of 1 mA during the major part of the run and at 5 mA in the later stages. This charging rate was of little consequence as the event rate was low, about 2/hour.

3.9 Operational details

During the main run the details of operation were as follows. The apparatus could only be run at night except at week-ends and holidays due to other work being done during the day. In the evening the laboratory was first darkened and the camera wound on a few frames. The first event started the cycling system and flashed the tubes which were recorded on the film. The cycling system illuminated the fiducials and the clock and a board containing details of the run. Thus the time and date of the event were recorded on the film to within a few seconds. Finally the film was wound on a few frames before switching on the lights. Such items of information as the starting and stopping times, the atmospheric pressure, the rate of events and the number assigned to the film were recorded in a log-book so that everything relating to that particular run was available at a later date. The camera was then removed and the film developed and stored until it could be scanned. The film used was Ilford FP3 as this gave better definition of the flash tube images than HPS despite

the greater sensitivity of the latter, because the images were so small.

In this way the apparatus was operated for approximately a year in the final run. Some runs were missed because of apparatus breakdowns and others had to be discarded due to errors of other types. The final data is made up entirely of runs in which the efficiency of the apparatus was known to be a maximum.

Thus we have a record of events where two or more penetrating particles trigger the telescopes as a function of the parameters that can be read from the film. These were the number and type of accompanying particles, the projected zenith angle and in many cases the azimuth angle of the event.

CHAPTER 4

Collection and Analysis of the Experimental Data.

4.1 Details of the Operation of the Apparatus.

The apparatus described in the previous chapter was operated for approximately a year in the Sir James Knott Laboratory at Durham. The data in the present work was collected during a sensitive time of 2218 hours. Over 5000 triggers occurred in this time and approximately 800 events were finally selected for analysis.

The running of the apparatus was limited to night time and week-ends because a camera with an open shutter was used and the laboratory could only be darkened at these times. A log-book was kept in which the date, starting and finishing times, atmospheric pressure, and number of triggers was recorded, together with the number assigned to the run. The number also appeared on each frame of the film. Details of any failure of the apparatus, or interruption in the run were also recorded.

Each film record was removed from the camera at the end of the run, developed, and checked for malfunctioning of the equipment. Films for which there was doubt as to the continuous efficiency of the apparatus during the run were discarded. In this way a permanent record was obtained of

each event which was detected during efficient operation of the apparatus. The time at which each event occurred was recorded automatically on the film as detailed in the previous chapter. The number on the film enabled it to be correlated with the log-book data at a later date.

4.2 Checks on the Efficiency of the Apparatus.

During the initial setting up of the apparatus certain measurements were made on the efficiency of the various components. Other checks were made before and after each run, and at periodic intervals during the experiment.

4.2. 1 The Flash Tubes.

The efficiency of the flash tubes was measured during the setting up procedure by selecting single particles passing through the trays with a small scintillator telescope. The theoretical layer efficiency of these tubes is 88%, this arises due to the finite thickness of the glass walls. Measured values of the efficiency gave a mean of 86%. Because there are four layers of tubes, and a track is recognised if two layers flash, the overall efficiency is higher than this, the chance of a muon penetrating a tray, and not being recognised, being less than 3%.

The delay between detection of a shower and the pulse being applied to the flash tubes was never greater than 4 micro-seconds. Thus inefficiency due to recombination

was minimal.

4.2. 2 The Scintillation Counters.

The previous chapter describes the initial setting up of the counters. A regular check was made by displaying the pulse height spectrum on the P.H.A. and making any necessary adjustments to keep the gain of the photomultipliers constant.

A separate check was made on the telescope counters by recording the rate of passage of single muons through each telescope. This rate (22 sec^{-1}) remained remarkably constant, any deviations being directly attributable to a failure of one of the counters. Thus a daily check could be made, simply by recording this rate for each telescope.

An absolute check on the efficiency was made by triggering the apparatus on these single muons and recording the angular distribution. This was found to agree with that calculated both in terms of shape and intensity.

4.3 Efficiency of Data Collection.

Since in this work it is intended to make absolute comparisons with theory it is necessary to ensure that no genuine events are lost due to inefficiency in the apparatus or in data collection.

The absolute rates measured depend on a knowledge of the

sensitive time of the apparatus. Because the time at which each event occurs is recorded on the film errors in estimating the sensitive time should be small.

In order to minimise the possibility that genuine events were rejected in the initial scanning of the film every effort was made to assign a physical explanation to each event on the film. In this way the only criterion for not selecting an event from the film was that it had some physical explanation other than that of being a muon shower. All events selected were carefully recorded in entirety on scale drawings. All data presented in this work were scanned from the film, and finally selected by the author.

In the final selection of events (see below, sections 4 & 5) certain 'out of geometry' events have been included. The majority of these are due to one of the triggering particles missing one of the flash tube trays, thus the condition of parallelism (see below) could not be tested. Inevitably a small fraction of these events will be spurious due to the detection of unassociated muons, or energetic electrons. Thus there is a small over-estimate in the number of muons showers recorded. The fraction of 'out of geometry' events does not exceed 5% and the fraction of these which are of spurious origin must be much smaller.

In the counting of the number of muons accompanying the triggering pair two effects can possibly cause an overestimate

of the number. The first of these is the 10% probability that a muon leaving the iron shield will have an accompanying knock-on electron. The second effect is that one trigger in four is expected to have a non-coincident muon track somewhere in the apparatus. It is clear that the probability of either of these effects producing a track within $\pm 10^{o}$ of the trajectories of the triggering muons is very small.

In view of the above it is considered that the collection of data as detailed below is an efficient process and that no serious errors in absolute rates can arise from this source.

4.4 The Initial Selection of Events from the Film Records.

In order to examine the film and select events it was projected at a magnification of 30× on to a horizontal table. A chart on which fiducial points were marked was used to align the image using the fiducial lights on the flash tube trays. Figure 4.1 shows two film records of muon showers.

The events on the film comprised, in addition to muon showers from the North, similar showers from the South, unassociated muon pairs and electron showers from North and South. The total rate was 2.5/hour, the rate of acceptable events was 0.5/hour. Acceptable events were defined under the following criterion:

At least one particle from the North in each telescope,

Figure 4.1 Film record of muon showers.

(a) Shows a group of 10 muons

(b) a pair of muons

each such particle showing one or both of the following characteristics: being parallel to the other, or penetrating the telescope without being scattered or absorbed.

Each event so selected was then copied on to two scale diagrams. One being of the flash tubes in the telescopes and one of those in the main array. The degree of precision of the former is high as mentioned in Chapter 3, that of the latter is not so important as only approximate information as to the angle and position of each additional track is required. The telescope flash tubes were identified individually, wheras only the pattern and approximate position of the flashed tubes in the main array were recorded. Also recorded on the scale drawings were the date and time at which the event occurred, together with the film number and the serial number of the event on the film. In this way a complete record of each selected event was obtained. As mentioned in section 4.3 also included in the initial selection were out of geometry events.

4.5 Final Selection of Muon Events.

The projected zenith angle of each telescope track could be measured from the scale drawings to within $\pm \frac{1}{2}^{o}$. The distribution of divergent angles between the tracks in each telescope is shown in figure 4.2. This is sharply peaked, the tail being due to unassociated single muons which leaked

Fig. 4.2.

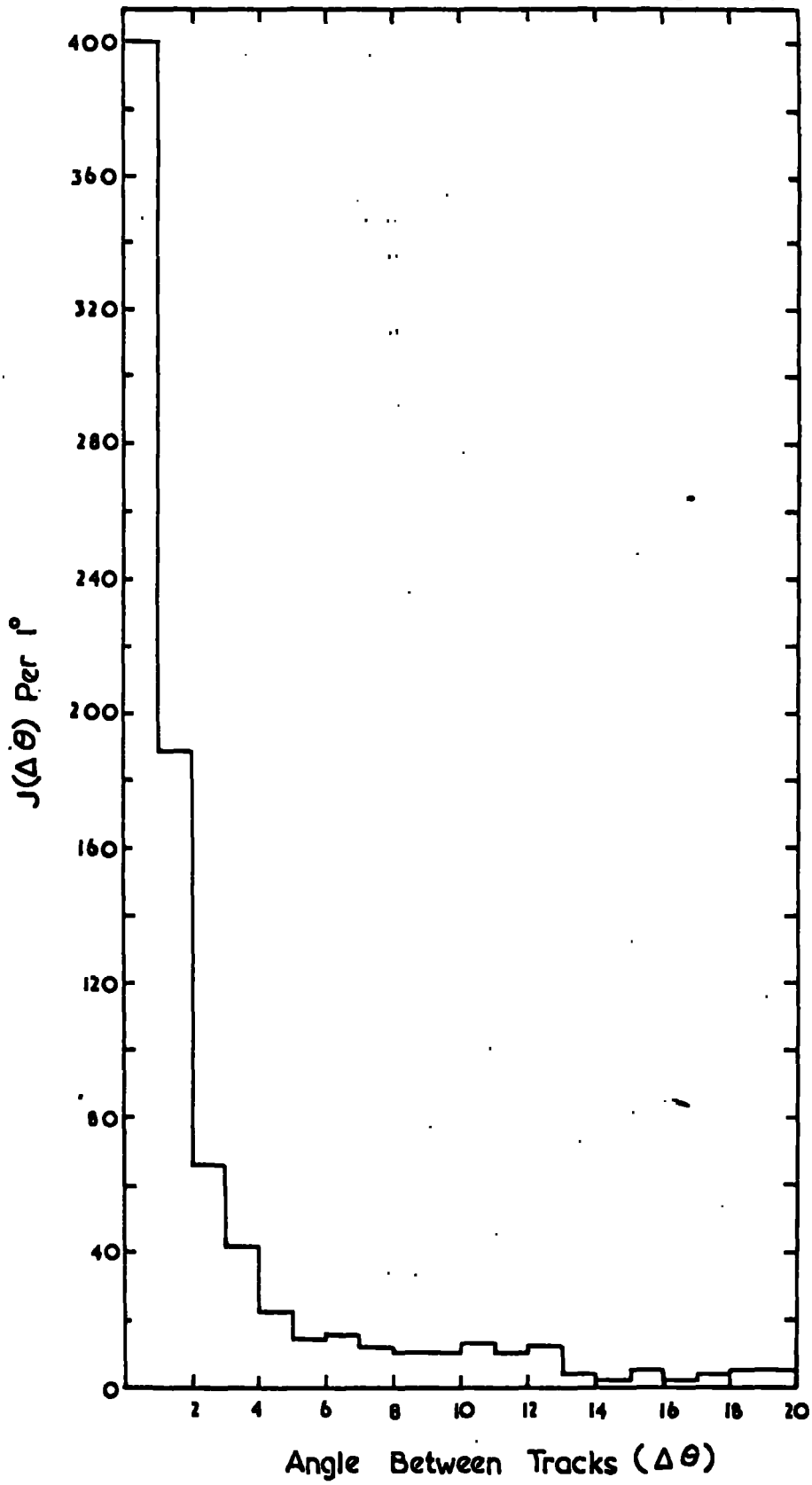

The distribution of projected angles between muons in E.A.S.

through the coincidence system.

The final selection was made by rejecting those events in which the angle between the telescope tracks was greater than 4^{o}. Thus the selected events were triggered by muon pairs of known zenith angle, parallel to within 4^{o}. The few out of geometry events were also included provided that the zenith angle of one of the triggering tracks was known precisely, and that there was no evidence that the other was not a muon, parallel to the first. (The angular resolution of a single flash tube tray varies from $\pm 5^{o}$ to $\pm 15^{o}$ depending on the zenith angle).

4.6 Distribution of the Events with Respect to Projected Zenith Angle.

It has already been mentioned that the expected average scattering angle of muons in E.A.S. is of the order of 3^{o}. Inspection of figure 4.2 shows that the root mean square angle is closer to 1^{o}. Thus it would appear justifiable to regard the mean projected zenith angle of the pair of triggering muons as a good measure of the angle made by the shower axis to the vertical. The events were therefore divided into 12 groups, according to angle, each group being 5^{o} wide. In this way adequate statistical accuracy was obtained for the number in each group. This angular distribution is given in Chapter 6 (figure 6.8) where comparison is made with theoretical predictions.

4.7 Analysis of the Data in Terms of Multiplicity

In the angular distribution all events selected were included. The majority consisted of pairs of muons only, one in each telescope. The events in each angular cell were inspected, and the number of muons in the main array determined, this number, plus the triggering muons is termed the multiplicity of the event.

In determining the multiplicity of the event, tracks in the main array, which were not parallel to the triggering tracks were not included. These were due either to knock-on electrons, or unassociated single muons. The angular resolution was 10^{o} for these tracks so in a few events spurious tracks will have been included which appear parallel to the others.

The events in each angular cell were then grouped in terms of multiplicity. In order to make the best statistical use of the data the cell width was doubled successively to cope with the steeply falling multiplicity spectrum.

Table 4.1 shows the data grouped both by angle and multiplicity as detailed above. A typical multiplicity spectrum appears in Chapter 6. (figure 6.10) where comparison is made with theory.

Table 4.1

Basic Data.

Multiplicity	No. of events per 5° range of zenith centred about angle stated												Total
	30°	35°	40°	45°	50°	55°	60°	65°	70°	75°	80°	85°	
2	42	60	103	79	87	68	50	34	20	4	1	4	552
3.4	15	20	40	46	29	14	14	9	5	2	-	-	194
5-8	2	4	8	10	12	11	8	8	2	1	-	-	66
9-16	2	4	5	7	5	4	2	1	-	-	-	-	30
17-32	-	-	-	2	2	3	1	-	1	-	-	-	9
33-64	-	-	1	-	-	-	1	-	-	-	-	-	2

4.8 Discussion.

The experimental object was to determine the absolute rate of groups of muons, triggering the apparatus, as a function of their zenith angle, and multiplicity. The determination of the sensitive time has already been mentioned. The calculations of the aperture and triggering probability of the apparatus are given in Chapter 6. The remaining problem is identification of the particles detected as muons.

The selection criterion (section 4.4) is based on the ability of muons to penetrate large thicknesses of absorber, and on the expected small angular deviation of muons in an E.A.S. The identification of the triggering particles as muons is certain for several reasons. The amount of absorber through which they must pass to trigger the apparatus is at least 9 radiation lengths, this alone is sufficient to identify them. The distribution of angles between the tracks is sharply peaked and typical of E.A.S. muons, and (see appendix 2) the mean energies of the particles detected have been measured by observing the frequency of production of small electron showers in the iron. These mean energies are in relative agreement with the assumption that the particles are muons in E.A.S. This last test applies also to the tracks observed in the main array.

The condition of parallelism cannot be applied to the accompanying particles in the main array because of the

relatively poor angular resolution. However, the thickness of absorber ranges from 4.5 radiation lengths at 90^{o} to 9 at 30^{o} and the scattering of electrons in this thickness of absorber is sufficient to identify them. Thus the identification of the particles detected as muons is ensured.

CHAPTER 5

Theoretical Analysis of Expected Density Spectra

5.1 Introduction

In order to use the experimental data obtained as described in Chapters 3 and 4 to enable an estimate of the primary mass composition to be made, it is necessary to make theoretical predictions based on different models of the mass composition, and compare these with experiment. It is the purpose of this chapter to describe the derivation of muon density spectra at various zenith angles for two models of the primary composition. The comparison of these density spectra with experimental results is described in Chapter 6.

The two composition models are derived in such a way that when predictions are made of the sea-level electron size spectrum, using the E.A.S. model calculations of De Beer et al. (1966), both give results in very close agreement with experimental measurements. These two models are then used to predict the muon density spectrum at various zenith angles, again making use of the E.A.S. model of De Beer et al. In this way internal consistency is achieved. This method minimises the effect of uncertainty in the parameters of the E.A.S. model, which are impossible to check in the

region of energy where they are used.

5.2 The E.A.S. Model of De Beer et al. (1966)

The starting point of these calculations has been the results of the E.A.S. model calculations of De Beer et al. (1966, 1968). These were carried out by the author's colleagues during the time when the apparatus was under construction and data being collected. The assumed parameters of the E.A.S. model are listed below.

1. The nucleons have a mean free path in the atmosphere of 80 gm cm^{-2}, they lose on average half their initial energy in each interaction with an air nucleus.

2. The secondary particles are assumed to be pions, equal numbers of positive, negative, and neutral pions are produced. Their energy distribution is as given by Cocconi, Koester and Perkins (1961) (The 'CKP' relation).

3. The number of pions produced in each interaction is given by $n = 2.7 \times E^{\frac{1}{4}}$ where E is in GeV and the inelasticity is 0.5. For other values of the inelasticity (K), (as in pion-nucleon interactions) the relation is $n = 2.7 \times 2^{\frac{1}{4}} \times (K\,E)^{\frac{1}{4}}$.

4. The mean transverse momentum (P_t) is assumed to be independent of energy and equal to 0.4 GeV/c. The distribution

of transverse momentum is also taken from the work of Cocconi, Koester and Perkins (1961).

5. The interaction length of pions is assumed to be 120 gm cm^{-2}. Their interactions are catastrophic, and the energy and transverse momentum distributions of the pions produced follow the CKP relations.

6. Fluctuations in the inelasticity of the nucleon interaction are included, as well as those in interaction points of the primary.

Calculations were also done for different models of the nuclear interaction, in particular a model with a rapidly rising multiplicity law ($\propto E^{\frac{1}{2}}$) was used.

The method of calculation employed the Monte-Carlo method to produce the interaction points of the primary, as well as the energy released in each interaction. For each cascade so produced the magnitudes, at sea-level, of the total number of electrons, and the total number and lateral distribution of muons of energies 1, 3, 10, 30 and 100 GeV were calculated. The effects of ionization loss, and μ - e decay were included. This treatment should be valid for muons down to 1 GeV.

The above method was used for calculations in the vertical and at 30^{o}. A numerical method, which employed

fixed interaction points was tested in the vertical and used for muon calculations at large zenith angles. It was found that the width of fluctuations in muon number is very small so that the neglect of variations in interaction point is not important. At large zenith angles where the number of interactions is larger, this neglect is even less important. However it was found that there were relatively large fluctuations in the lateral distribution of muons. As will appear in section 5.8 the muon density spectrum is not very sensitive to the extremities of the lateral distribution but only to the middle region between 50 and 150 metres from the core. Thus fluctuations in shape will have only a small effect on the density spectrum. Abrosimov (private communication) has shown experimentally that fluctuations in lateral distribution are small in the middle distance region.

The results of these calculations are shown in figures (5.1, 5.2, 5.3). Figure 5.1 shows the numbers of muons and electrons produced at sea level by primary protons as a function of energy, at a zenith angle of 30° (the mean angle of observation for many vertical E.A.S. arrays. Figure 5.2 shows the results from De Beer et al. (1966) with the muon number corrected by later more precise calculations. It also shows the muon number from primary protons as a function of energy for zenith angles 60°, 75°, 84°.

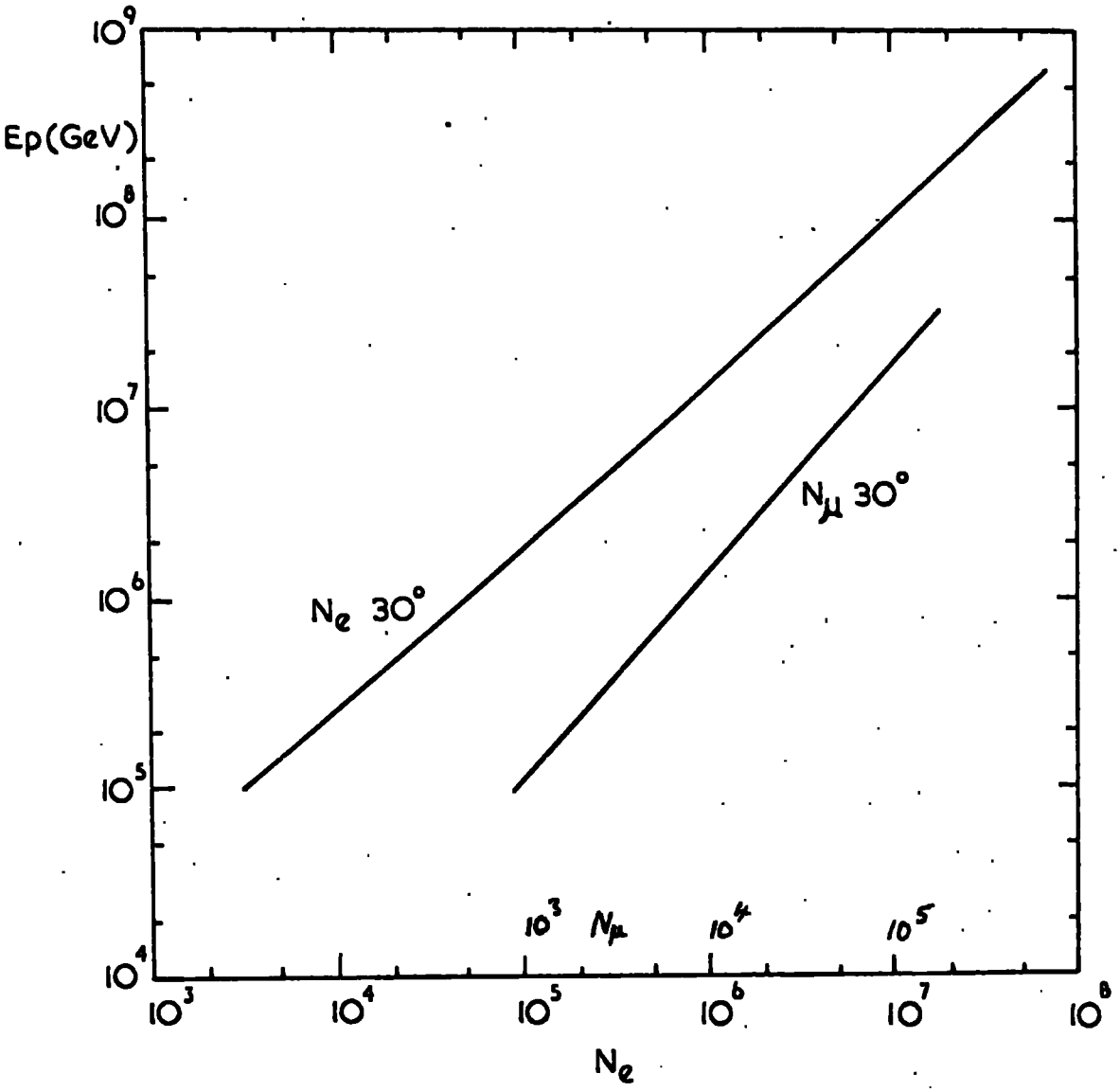

Fig. 5.1.

Sea level electron and muon numbers produced by primary protons at 30° to the zenith.

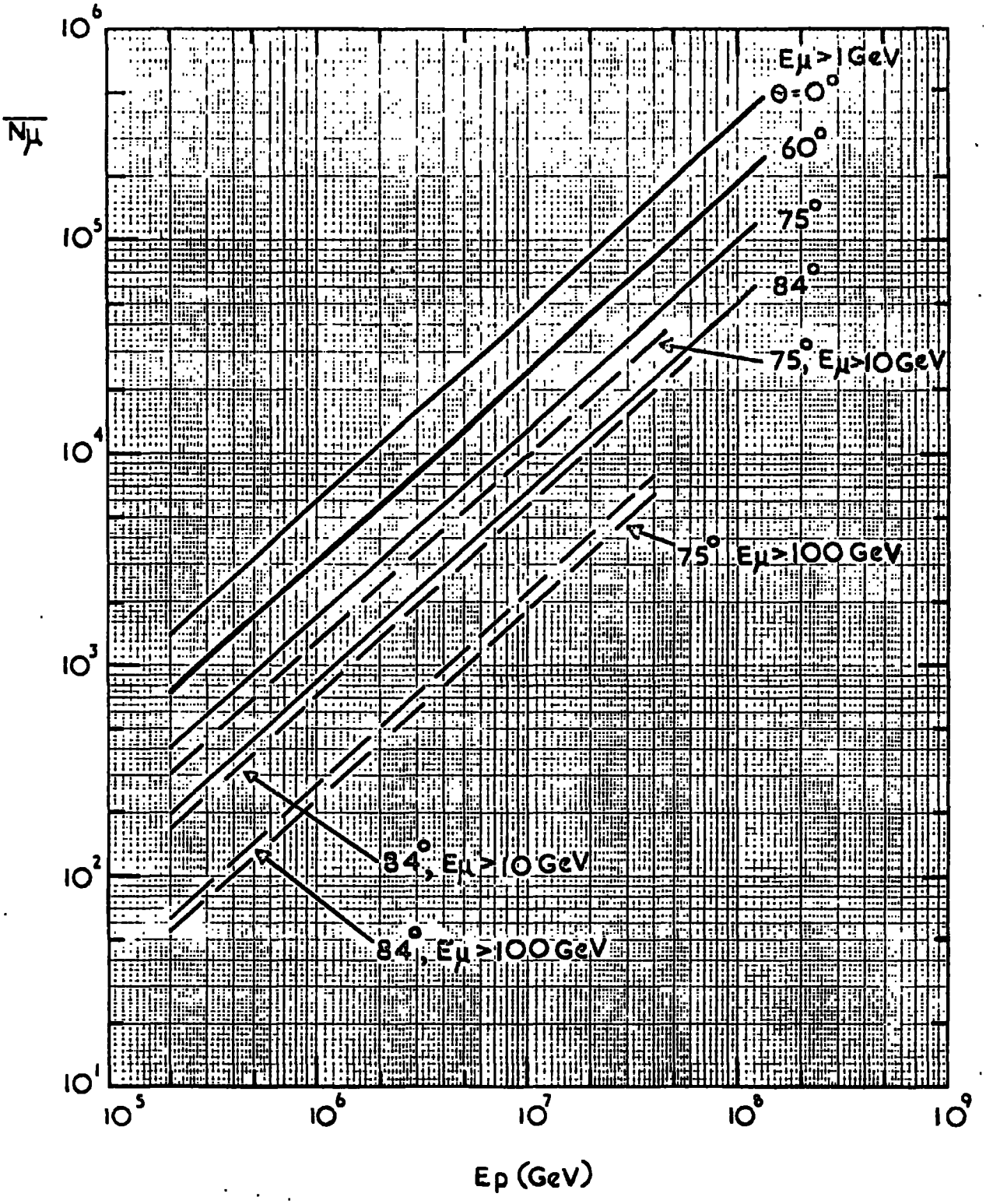

Fig. 5.2. Sea level muon numbers produced by primary protons for various zenith angles and muon threshold energies.

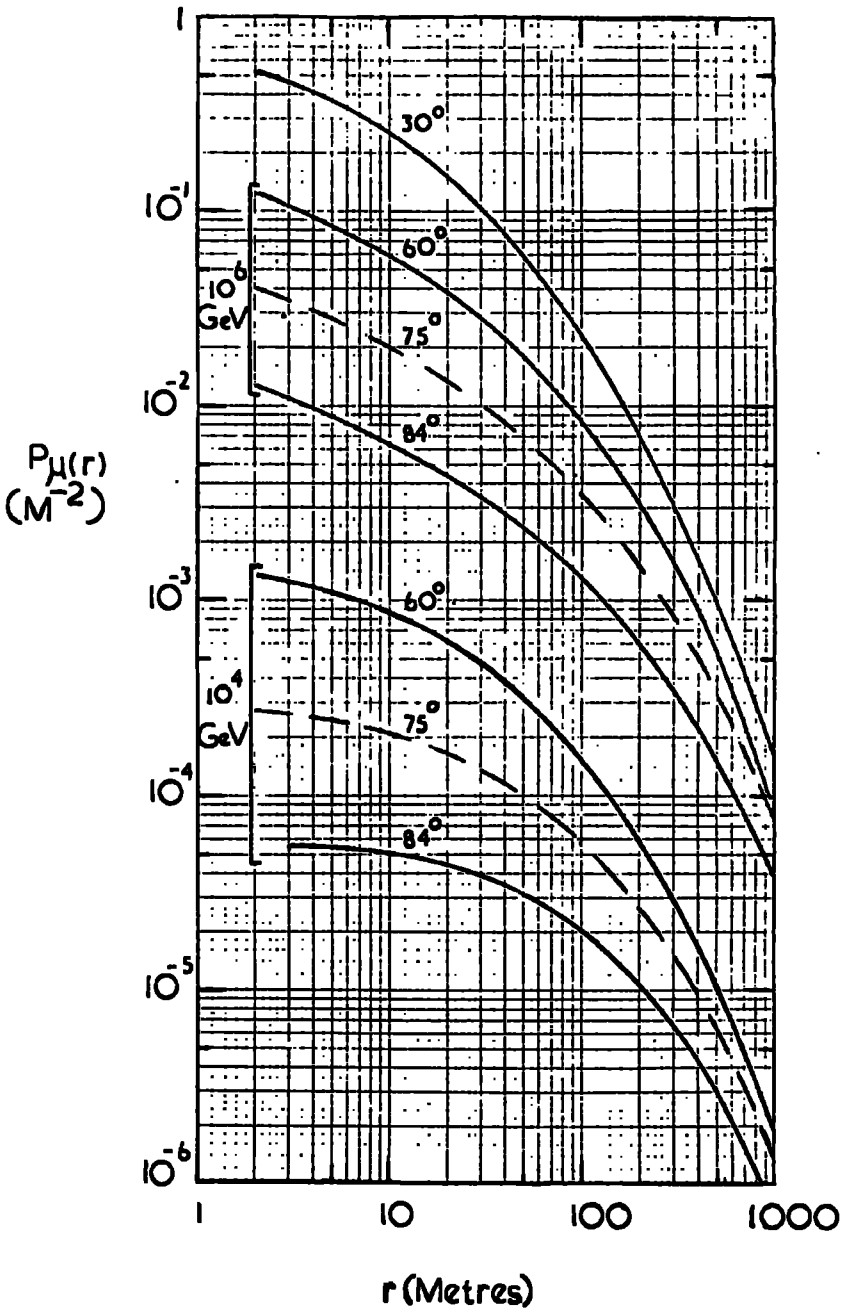

Fig.5.3.

Muon lateral density distributions at different zenith angles for two primary proton energies.

Figure 5.3 shows the muon lateral density distributions for protons at 30°, 60°, 75° and 84°. The lateral distribution varies slightly for different primary nuclei, this variation has been ignored in the following work and the proton lateral distribution used throughout.

5.3 The Principle of Superposition for Heavy Primaries:

The method of calculating the sea level electron and muon numbers for heavy primaries has been to regard an E.A.S. due to a primary of mass A and energy E as equivalent to a superposition of A showers of energy E/A. This implies the assumption that the first interaction of the primary in which it breaks up into separate nucleons produces few pions equivalent to the muon energy region of importance. The general applicability of this assumption has been questioned recently (Orford & Turver, 1968) but in the region of muon energy and radial distance with which we are concerned, the first interaction is of little importance.

It is in general true that the relation between the energy of a primary proton E and the total number of particles in the shower at sea level N can be written $N = E^{\alpha}$, where α is greater than 1. This follows from the fact that as the primary energy increases, the region of maximum development in the shower moves downwards towards sea level. Similarly the number of muons at sea level may be written $N_{\mu} = E^{\beta}$ and

β is less than 1 because as the energy rises the probability that a pion will interact rather than decay to a muon increases.

When dealing with a primary of mass A and energy E the energy per nucleon is E/A. The number of electrons produced at sea level is $N = A\,(E/A)^{\alpha}$ which may be written $N = E^{\alpha}\,A^{1-\alpha}$. Thus, since α is greater than 1, as A increases N decreases for the same total nucleus energy E. In this way the number of electrons in a shower produced by a primary proton is greater than in the case of one produced by a heavy primary.

The opposite effect appears when considering the number of muons. Here $N\mu = A(E/A)^{\beta}$, which can be written $N\mu = E^{\beta}\,A^{1-\beta}$ and β is less than 1. Thus $N\mu$ increases as A increases for the same nucleus energy. In this way a primary proton produces fewer muons at sea-level than a heavy primary of the same energy.

In principle therefore it is possible to obtain a measure of the primary mass from a comparison of the number of electrons in a shower with the number of muons.

5.4 The Variation of the Width of Fluctuations in Ne with Primary Mass.

De Beer et al II (1968) calculate that the relative width of fluctuations varies with primary energy for protons as $\sigma\, ne/\overline{Ne} = 7.0\, Ep^{-0.15}$. Thus as the energy increases

the relative width of the fluctuations falls. These authors find that the main contribution to the fluctuations comes from fluctuations in interaction point. As the maximum of the shower moves down towards sea level so the effect of the variations in interaction point becomes less.

In the case of heavy primaries we may again use the principle of superposition and make use of the result $\left(\frac{\sigma}{Ne}\right)_A = \left(\frac{\sigma}{Ne}\right)_p A^{-\frac{1}{2}}$ from the calculations of De Beer et al. II. (It should be noted that this result applies for the same nucleon energy). Thus the width of the fluctuations decreases as the mass increases, because many interactions occur at any level so that the effects of variation in interaction point are less.

5.5 The Variation of N_e & N_μ with E_p taking into Account Fluctuations with Mass as a Parameter.

To facilitate calculations of electron and muon numbers at sea-level from the two model primary spectra it is necessary to derive a relationship between primary energy and these numbers with mass as a parameter. This derivation must include the effect of fluctuations.

It is well known that the effect of fluctuations in electron size is to decrease the mean primary energy corresponding to a given measured size. This arises because of 'spillage' on the steeply falling primary spectrum.

Thus in calculating the electron size for a given primary energy there is an effective enhancement in size due to fluctuations. As the width of these fluctuations decreases due to increasing energy, or primary mass, this enhancement also decreases. This factor works in the same direction as the principle of superposition, decreasing the number of electrons at sea-level with increasing primary mass. Thus fluctuations enhance the variation of electron size with primary mass.

The method adopted to calculate the enhancement factor was to assume a constant exponent of -1.6 (integral) for the primary spectrum. This introduces inaccuracy at the higher energies where the spectrum is steeper, however the enhancement factor itself is decreasing with increasing energy so that this effect is not serious. The factor was calculated for protons of energy 10^{14} eV and found to be 3.0. The relations quoted in 5.3 of De Beer et al. (1967), were then used to give the variation of this factor with the energy and mass of the primary.

The variation of shower size with primary energy was first derived from the relations given in 5.2, and from figure 5.1 for different primary nuclei. This was then corrected for the effect of fluctuations by the enhancement factor described above. The result is shown in figure 5.4

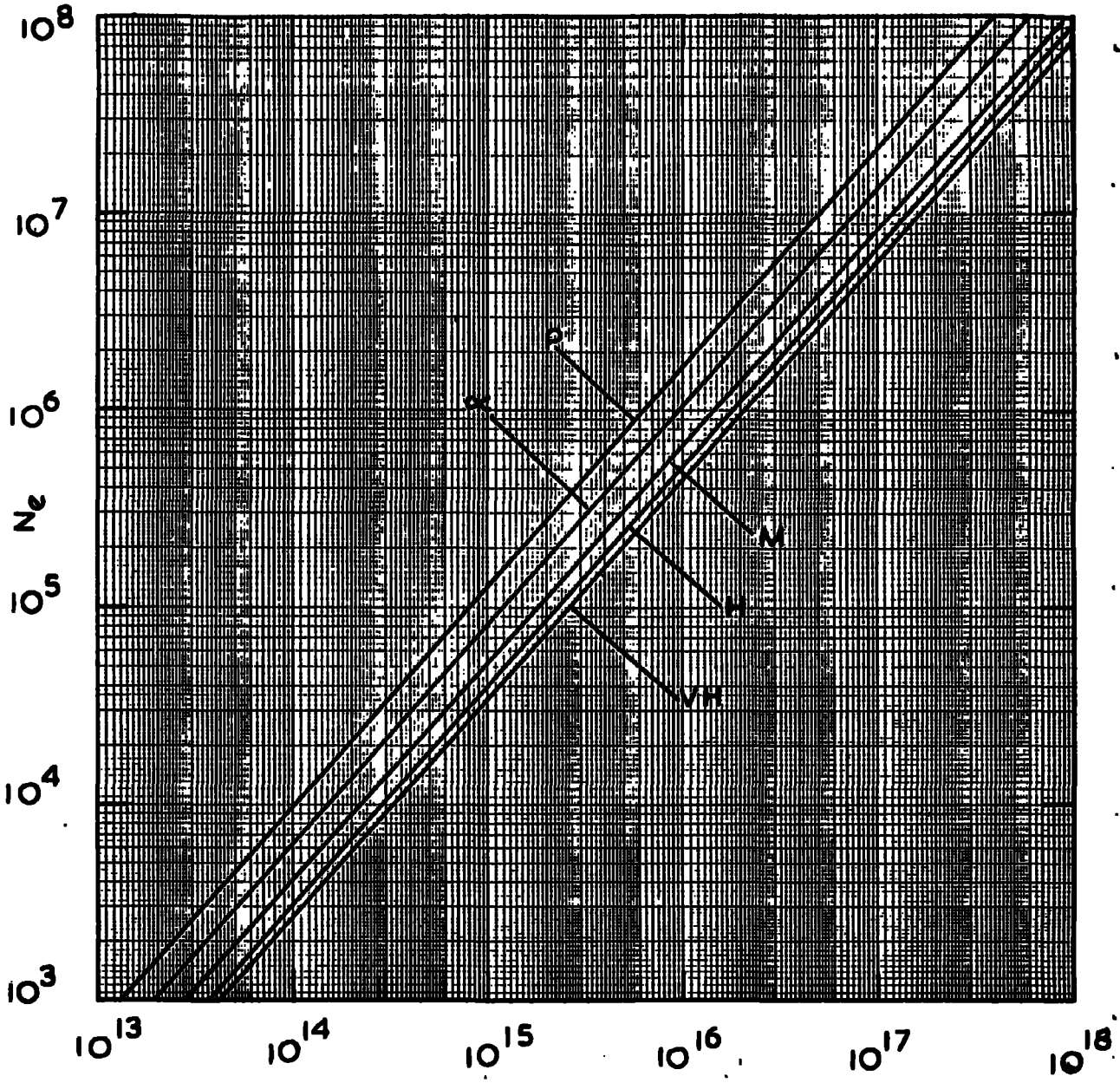

Fig. 5.4.

Sea level electron numbers produced by various primary nuclei as a function of nucleus energy, corrected for the effect of fluctuations.

where the relation between primary nucleus energy and electron size at sea-level is given with primary mass as a parameter.

The calculation of the relation between muon number at sea-level and energy, with mass as a parameter, was carried out in the same way. Here however it was unnecessary to include the effect of fluctuations because these are small for muon numbers. The result is shown in figure 5.5.

5.6 A Survey of Sea-Level Electron Size Spectrum Measurements.

The greater sensitivity of electron size at sea-level to the primary mass, as compared with that at mountain altitudes, requires the sea-level size spectrum to be used as a datum in the following calculations. A collection of experimental measurements has been made, and the result is shown in figure 5.6. These measurements were used to derive a size spectrum covering as wide a range as possible, for reasons described below.

If reliable measurements are available down to very small sizes then it may be possible to compare the primary intensity derived from the size spectrum with that directly measured. The size spectrum of Kulikov (1960), covers the range of shower sizes from 10^4 to 10^6. Thus the derived primary spectrum extends down to about 10^{14} eV and comparison

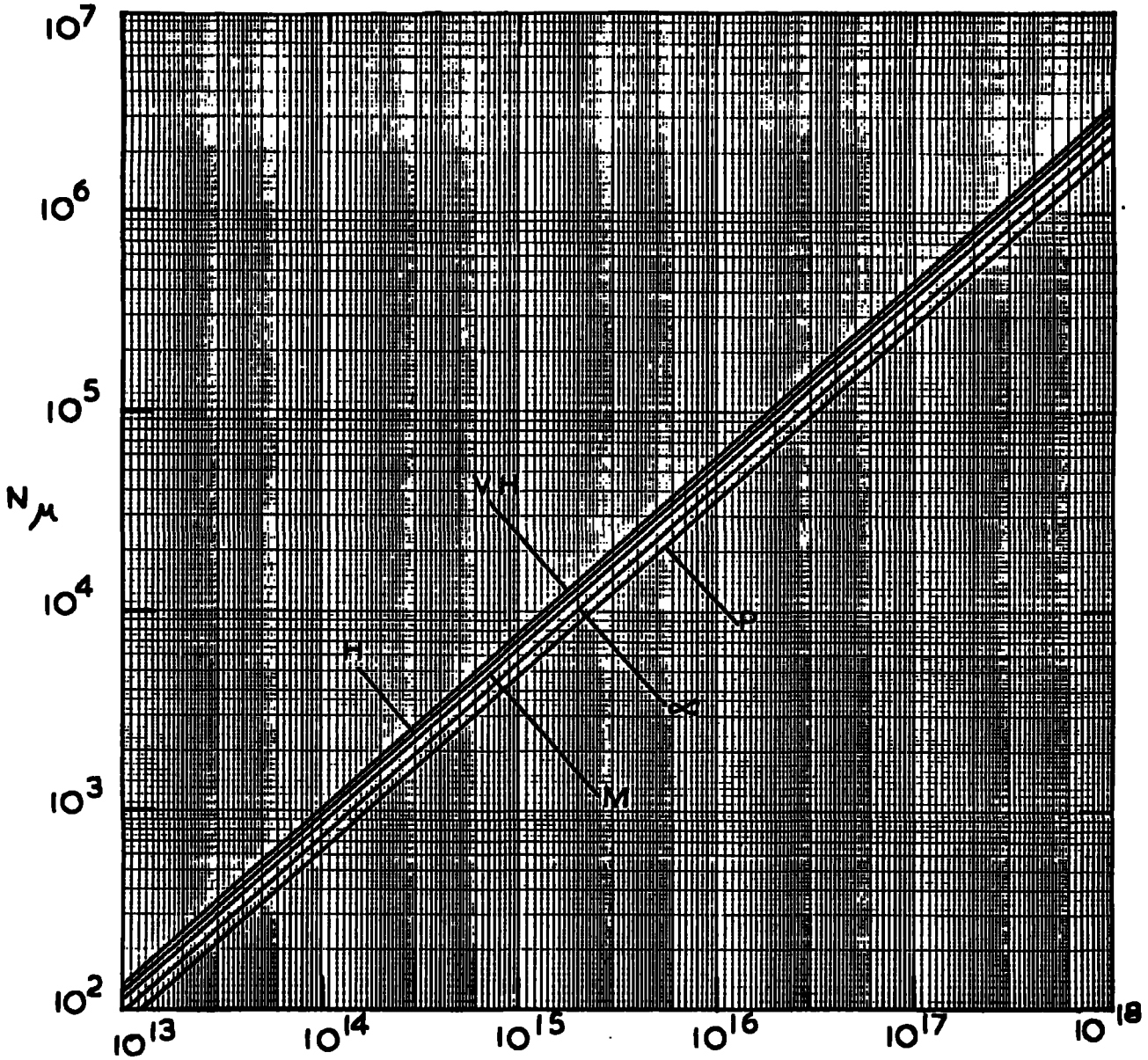

Fig. 5.5. Sea level muon numbers produced by various primary nuclei as a function of nucleus energy.

Figure 5.6 Survey of measurements on the sea-level electron size spectrum.

Key:		
	K_1, K_2, K_3,	Kulikov et al., 1960
	Δ	Greisen, 1966
	●	Cranshaw et al., 1958
	V	Vernov, 1968
	B	Brennan et al., 1958
	T	Tokyo (H.Oda, private communication)
	C	Clark et al. 1957
	R	Rossi, 1960

The composite spectrum used as a datum in the present work was derived as follows. Below 10^5 particles K_1 alone, 10^5 - 10^6 mean of K_2, V, B, and T, at 10^6 all but Greisen, above 10^6 the mean of R and C was taken.

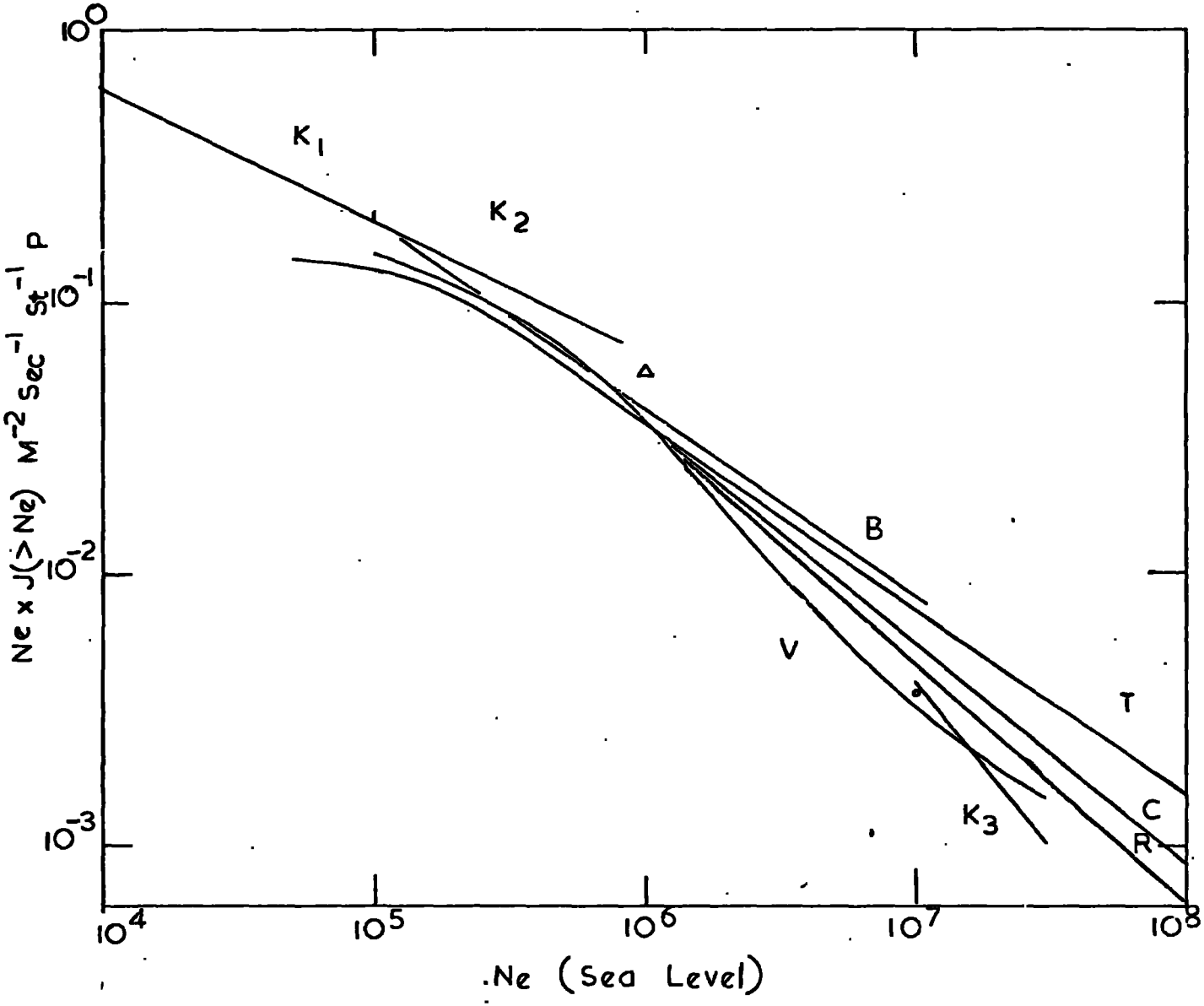
10^0
10^{-1}
10^{-2}
10^{-3}
$Ne \times J(>Ne)\ M^{-2}\ Sec^{-1}\ St^{-1}$
10^4
10^5
10^6
10^7
10^8
.Ne (Sea Level)
K_1
K_2
K_3
Δ
B
V
T
C
R

Fig. 5.6.

may be made with the results of Malholtra et al (1966) who give a primary intensity derived from measurements on gamma-rays, extending to 6 10^{14} eV.

Consideration of errors of measurement in the size spectrum is difficult in view of the paucity of experimental details given by most workers. Where the results of one experiment differ markedly from the average they have been ignored. Otherwise the mean intensity has been taken over all measurements. Unknown systematic errors may exist but at present no correction can be made.

5.7 The Derivation of Two Models of the Primary Energy Spectrum.

With the availability of the E.A.S. model calculations, and the experimental measurements of the sea level size spectrum it is possible to define primary spectrum models with a certain degree of precision. The assumption made here is that the primary spectrum follows a simple power law from the low energy region up to the point where a change in nature results in the observed change of slope of the sea level size spectrum. Also it is assumed that up to this point, the composition remains sensibly constant similar to that measured at low energies.

The sea-level size spectrum gives three pieces of information which can be used to define parameters of the

primary spectrum. The part of the size spectrum below the change in slope, may be used to define the intensity and slope of the primary spectrum using the E.A.S. model, and assuming the normal composition. This may be compared with those measurements, described in Chapter 2, which refer to energies approaching 10^{14} eV. In particular comparison can be made with the spectrum quoted by Malholtra et al,(1966). It will become apparent later in this section that the agreement is good. (figure 5.8). This may be regarded as partial justification both of the assumed composition, and of the E.A.S. model, for the region of energy below 10^{15} eV.

In this way it is possible to produce a model of the primary spectrum, below 10^{15} eV, which agrees with experimental measurements, in slope, intensity and composition. If we wish to modify the primary spectrum above 10^{15} eV, the result must agree with the sea level size spectrum. If the composition were known in this region then the primary spectrum would be uniquely defined by the sea-level size spectrum, and the E.A.S. model, because this directly relates the two under these circumstances.

The composition is treated here as unknown and its variation constitutes the basis of the primary spectrum models. In the first case it is assumed that above a certain energy limit the primaries are all protons and the exponent of the spectrum increases. The two variables in this model

are the position of the energy limit, and the new slope of the spectrum. These can be defined uniquely because we have information from the size spectrum both on the point at which the slope changes, and the new slope, again relating the primary spectrum and the size spectrum by the E.A.S. model. Thus the first model (spectrum A) is defined.

In the second model a rigidity limit is imposed on the primary cosmic rays above which the spectrum of each mass component changes. Again we may obtain a unique model, the only assumption being that the change in the spectrum for each mass component occurs at a constant magnetic rigidity. The two variables in this model are; the magnetic rigidity limit, and the nature of the change in the spectrum of each mass component. These are defined by the requirement of agreement with the sea level size spectrum. Only astrophysically significant forms for the change in spectrum of the mass components have been considered. Three were examined; a sharp cut off, an exponential loss of particles, the exponent depending on the ratio of the rigidity of the particle to the limiting rigidity, and a simple change in exponent of the energy spectrum of each mass component. The first two are alternative ways for the particles to be lost from a large region of uniform magnetic field, the last a form suggested by Ginsburg & Syrovatsky (1964) where they consider escape under conditions where the particles are

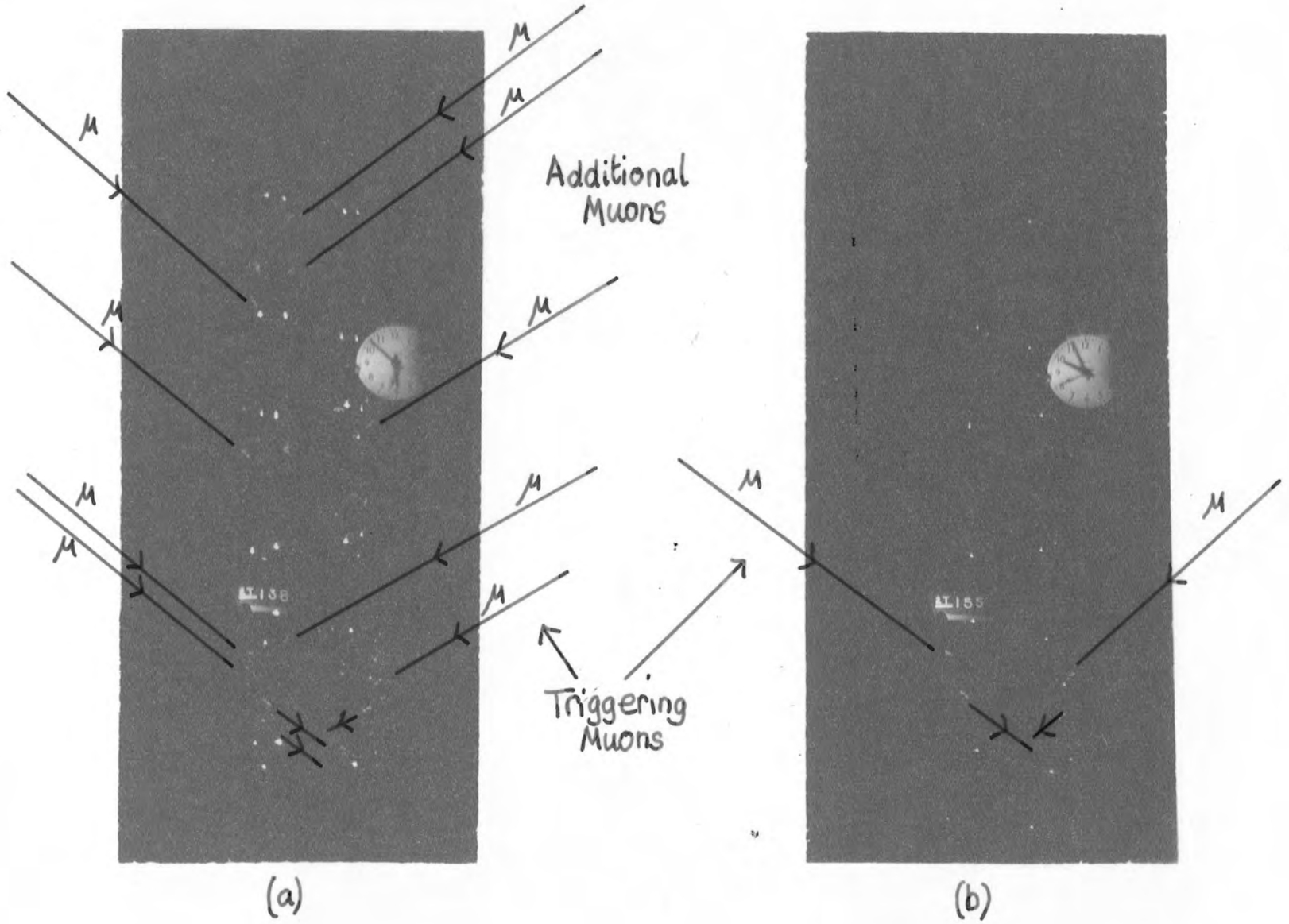
μ
μ
μ
μ
μ
μ
μ
μ
μ
μ
Additional Muons
Triggering Muons
(a)
(b)

contained within the spiral arms by diffusion among the gas clouds (which have magnetic fields attached to them). The only mechanism tried which gives agreement with the sea-level size spectrum is the last where the exponent of the spectrum of each mass component increases by 0.5 above the rigidity limit.

This last finding does not agree with the calculations of Peters (1961). In this paper he shows that the effect of a sharp rigidity cut off, will be equivalent to a sharp cut off at a critical energy per nucleon. Above the electron size corresponding to a proton of this energy, the size will depend solely on the mass of the primaries. In this way, above the kink, the size spectrum becomes characteristic of the mass spectrum of the primaries, which is approximately proportional to A^{-3}. Thus Peters predicts the observed change in slope of the electron size spectrum.

The reason that the present work does not bear this out is that fluctuation effects have been included. These increase the electron size for primary protons, but have only a small effect on that due to heavy nuclei. In this way the exponent of the predicted differential size spectrum, above the kink becomes, larger than -3 (in fact approaching -4.5) and is no longer in agreement with that of the measured spectrum. Thus the inclusion of the effect of fluctuations reduces the number of models of the primary spectrum which

have to be considered to the two models mentioned above, both of which agree with experimental measurements on the electron component. No influx of extragalactic protons has been considered because the energy at which this is expected to occur is outside the energy limits of the present work.

The two model primary spectra are shown in figure 5.7 where the total intensity, and the intensities of the various mass components are shown. Spectrum B, the rigidity modulated spectrum, is shown together with a spectrum based on a pure proton composition throughout. Spectrum A, in which the composition is normal up to the change in slope, and then changes rapidly to a pure proton flux, requires some assumption as to the way in which the heavy primaries are lost. Since at present there are no indications as to how this may occur, an arbitrary transfer is made from the normal composition spectrum below the change in slope, to the pure proton spectrum above. Thus the two models A and B coincide in the energy region below 10^{15} eV.

Comparison is made in figure 5.8 with the spectrum quoted by Malholtra et al. (1966) and with the primary spectra of other workers in figure 5.9.

This latter comparison is of interest for several reasons. In the region below 10^{15} eV both models coincide, and agree with the spectrum given by Greisen (1966a). This

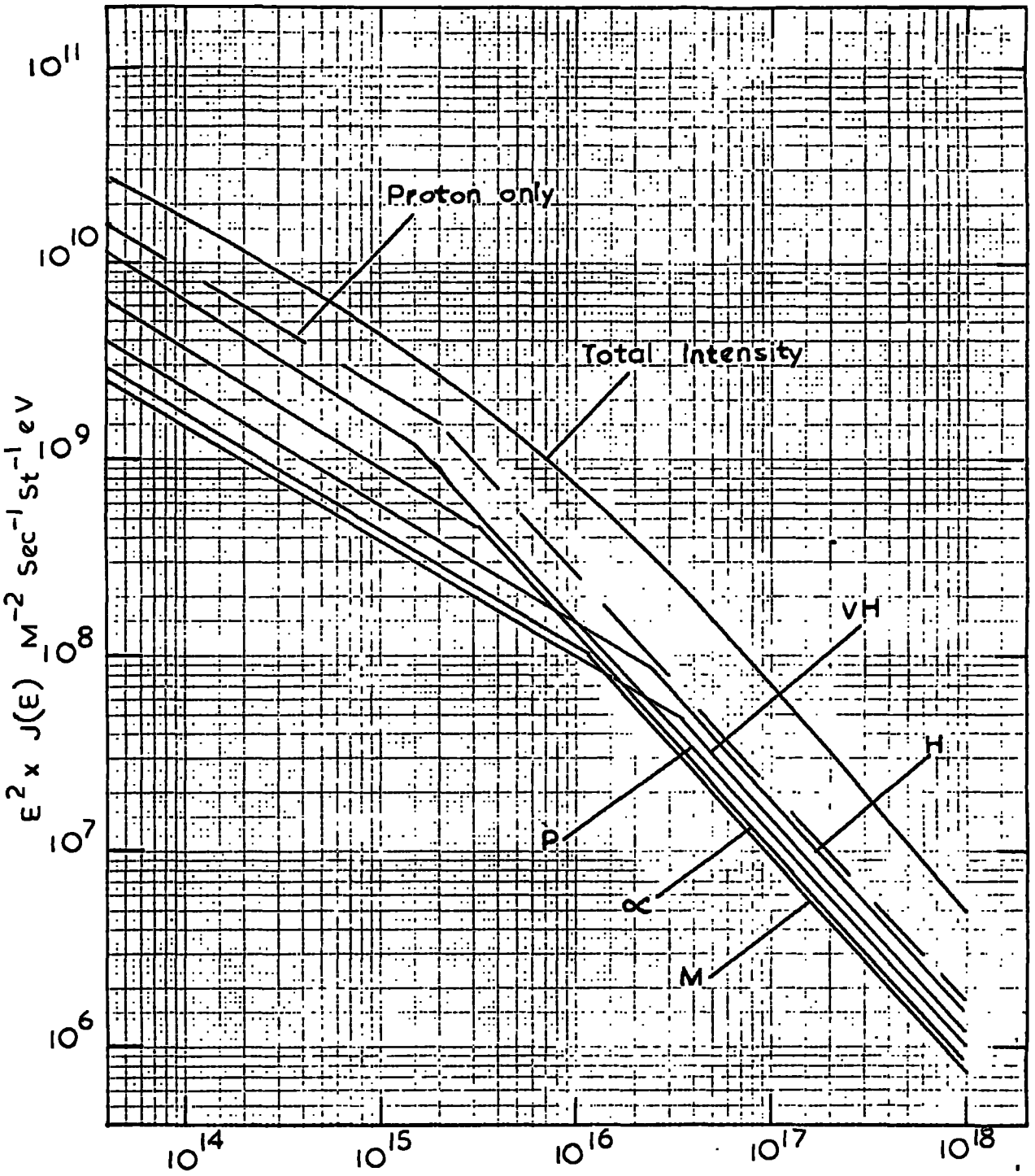

Fig. 5.7.

Model primary spectra giving the agreement with the sea level electron size spectrum.

Figure 5.8 Comparison of the two model primary spectra A and B with the spectrum of Malholtra et al. (1966). Spectrum B is rigidity modulated. Spectrum A changes to a pure proton composition above 10^{15} eV.

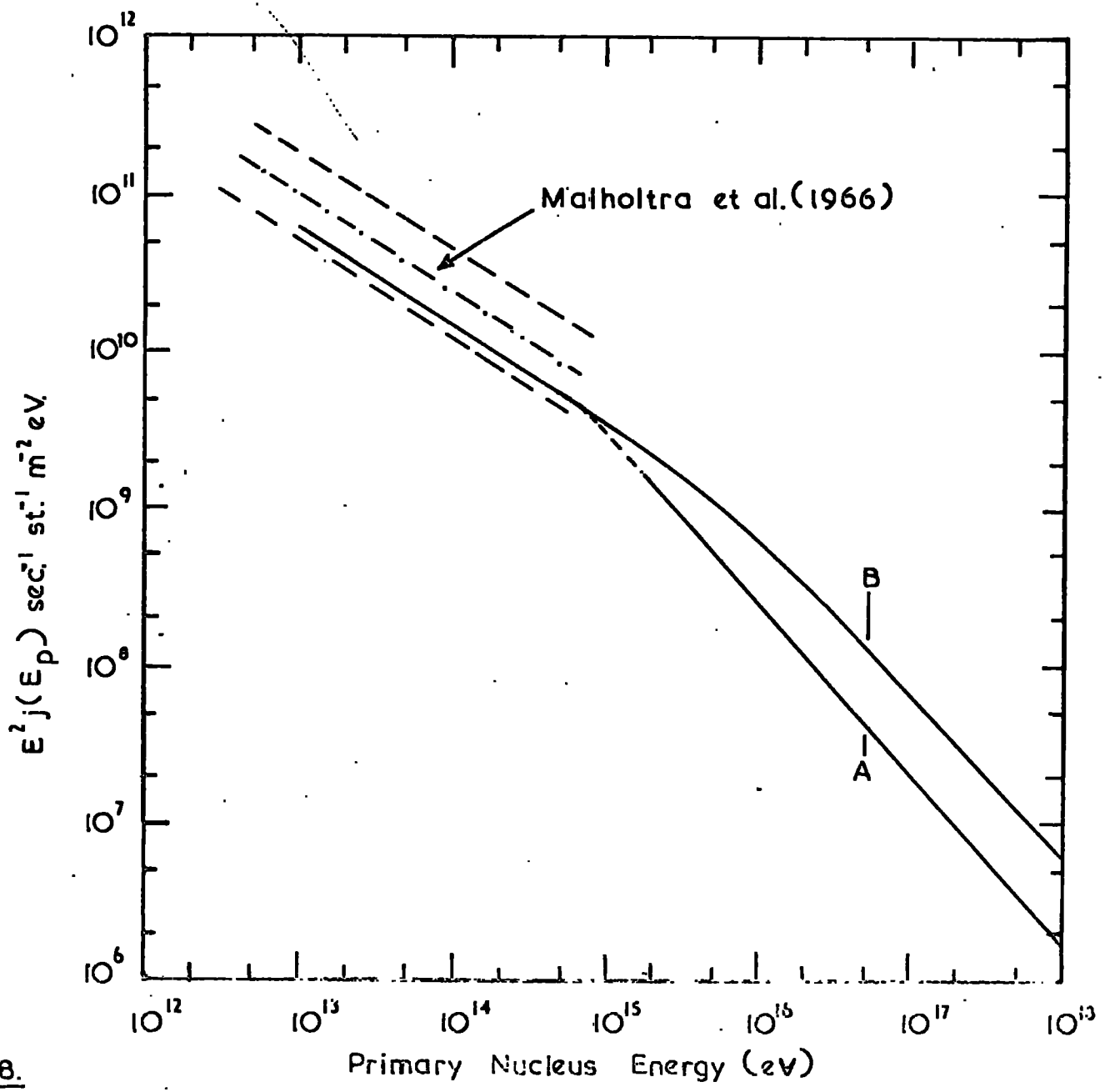
Malholtra et al.(1966)
B
A
$E^2 j(E_p)$ sec.$^{-1}$ st.$^{-1}$ m^{-2} eV
Primary Nucleus Energy (eV)
10^{12}
10^{11}
10^{10}
10^{9}
10^{8}
10^{7}
10^{6}
10^{12}
10^{13}
10^{14}
10^{15}
10^{16}
10^{17}
10^{18}

Fig. 5.8.

Figure 5.9 Comparison of the two model primary spectra with those of other workers based on sea-level, or near sea-level measurements.

G - Greisen 1966

V - Vernov 1968

L - Linsley 1963

Fig. 5.9.

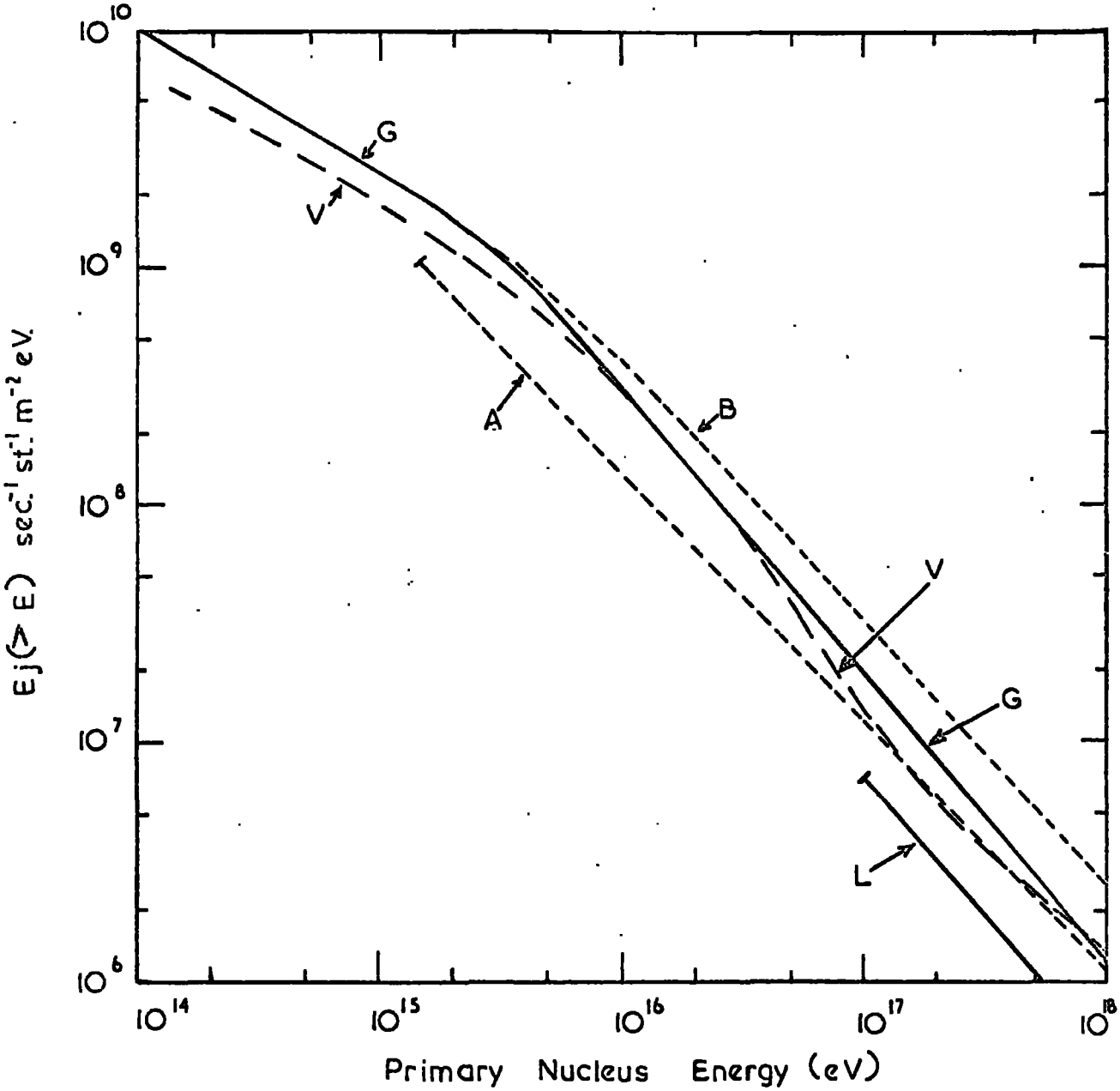
10^{10}
10^{9}
10^{8}
10^{7}
10^{6}
$Ej(>E)$ sec.$^{-1}$ st.$^{-1}$ m^{-2} eV.
G
V
A
B
V
G
L
10^{14}
10^{15}
10^{16}
10^{17}
10^{18}
Primary Nucleus Energy (eV)

agreement shows that the model used does not differ in its predictions from that used by Greisen since presumably the basic data in the two cases are the same. The spectrum of Vernov (1968) is based on his own data, and figure 5.6 shows how this is related to the mean sea-level size spectrum used in the present work. Above 10^{15} eV the difference in intensity between A and B is due to the differing compositions assumed. Further, since the spectra of other workers which are given are based, in the high energy region, on sea-level, or near sea-level measurements, the differences between them and the present work may be attributable to differences in assumed composition.

Since in all cases an E.A.S. model has to be used to relate the sea-level measurements to the primary intensity, either some assumption as to the composition has to be made, or if the composition is not explicitly assumed, the model checked in the low energy region where the composition is normal. Thus all sea-level, or near-sea level measurements on E.A.S. may be regarded as containing the implicit assumption that the composition is normal. This does not apply where measurements are made on E.A.S. at maximum development, because in this case sensitivity of electron size to composition is minimal.

As a check on the above supposition calculations were carried out for a third model spectrum in which the composition

remained universally normal. This spectrum was found to coincide with that of Greisen. The spectrum of Linsley is of interest because he has some evidence that the primaries in this region are protons. Thus the low intensity of spectrum A is in no way in disagreement with experimental measurements.

Related to this is the way in which experiments at sea-level on different components of E.A.S. will give different compositions of the primary flux, because efficiency in production of electrons at sea level decreases with increasing primary mass, and vice versa for muons. Thus an experiment which detects electrons at sea level will be biased toward proton primaries, and one detecting muons towards heavy primaries. If the experiment detects showers at maximum development then no bias occurs. Similarly if some parameter directly related to energy such as Cerenkov light, or atmospheric scintillation is used no bias will occur. This effect is shown in figure 5.10 where the composition at fixed electron size, muon size, and primary energy is shown for the two model spectra A and B.

In this section two model primary spectra have been produced both of which, when incorporated with the E.A.S. model of De Beer et al. (1966), predict a sea-level electron size spectrum which is in agreement with experimental measurements. These primary spectra have been shown to be consistent

The variation of observed composition with E.A.S. parameter measured at sea level for the two composition models A. and B.

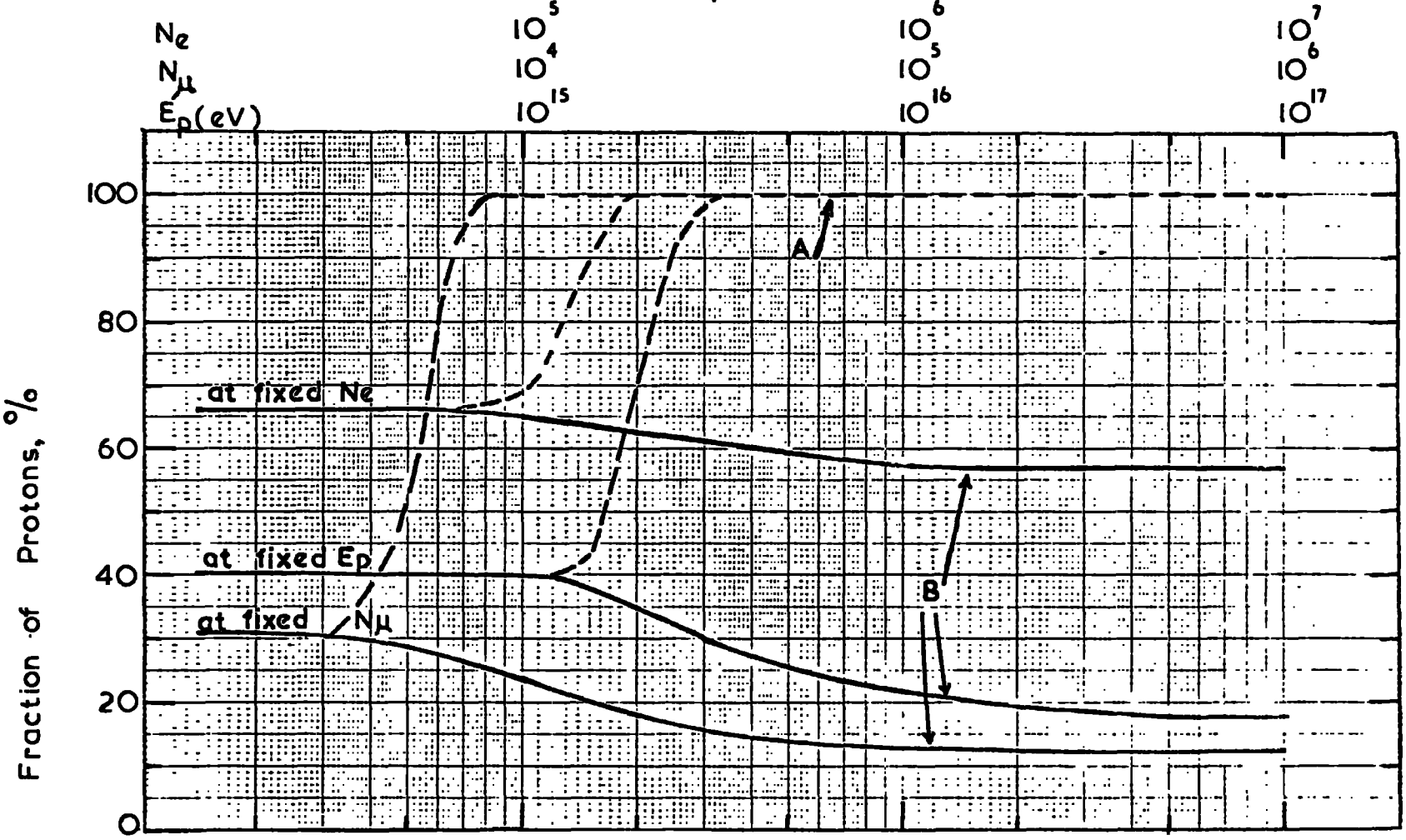

Fig 5.10

with those of other workers, when differences in assumed composition are taken into account.

5.8 Derivation of the Muon Density Spectrum for the Two Primary Spectrums Models A and B

The calculation of the muon density spectrum requires a knowledge of the lateral distribution of muons, and of the relation between the total number of muons in the shower at sea-level, and the primary energy. The model primary spectra can then be folded in to give alternative density spectra. The calculation is first detailed for a primary spectrum of pure proton composition throughout, and then the modifications needed for the spectrum models A and B are indicated.

A point on the integral density spectrum is obtained by evaluating the integral

$$J(>\Delta) = \int_{E_{min}}^{\infty} \pi \left(R(\Delta, E_p)\right)^2 J(E_p)\, d E_p .$$

$R(\Delta, E_p)$ is the radial distance within which a shower of primary energy E_p has to fall to produce a density greater than Δ particles per square metre at the apparatus. The catchment area for such showers is given by πR^2 and the product of this and the primary intensity, integrated over energy gives the total intensity of showers producing a density greater than Δ at the apparatus.

$R(\Delta, E_p)$ is derived from the lateral density distributions, for each primary energy. These in turn are derived from the lateral distributions for various zenith angles given by De Beer et al. (1966, 1969), (figure 5.3), and from the relation between the total number of muons above 1 GeV and the primary energy.

The lower limit of integration E_{min} is set from two considerations. The first is the minimum radial distance, (and hence the minimum primary energy) that can be allowed before the variation of density over the apparatus becomes appreciable. This has been set at 3 metres (the energy limit varying with Δ). The exact value of this limit is not important because the contribution of showers falling close to the apparatus decreases rapidly within 30 metres. The importance of this limit increases as the minimum muon energy increases and the lateral distribution steepens. For muons of energy greater than 600 GeV for example it is no longer valid to use a simple radial cut off and the variation of density over the apparatus has to be taken into account. (De Beer et al. IV, 1969).

The second of the considerations to be taken into account in fixing E_{min} is the existence of a minimum primary energy below which less than two muons survive to sea-level. This is only important for densities less than $10^{-5}\ \rho.m^{-2}$. Again for very high energy muons this limit becomes important.

In the above manner the integral density spectrum can be calculated for a pure proton primary spectrum. To take into account a spectrum of varying composition, it is necessary to evaluate, for each primary energy, the mean number of muons produced at sea-level. This mean number being obtained by combining the muon numbers for each mass component (figure 5.5), weighting the contribution from each by its relative abundance in the appropriate primary spectrum. The result is then used to calculate new lateral distributions for different primary energies and from these $R(\Delta, E_p)$ is obtained and the calculation proceeds as already described. This method assumes that the lateral distributions do not differ in shape for different primary nuclei. The slight differences that do occur are less than the errors involved in calculation.

The results of these calculations appear in figure 5.11 where the integral density spectrum of muons of energy greater than 1 GeV is shown, for the two model primary spectra, and four zenith angles. No allowance has been made in these spectra for the effect of the earths' magnetic field.

5.9 The Geomagnetic Correction.

The effect of the earths' magnetic field becomes increasingly important as zenith angle of the shower increases. Hillas (1966) has calculated that it is no more than 2% near

Fig. 5.11.

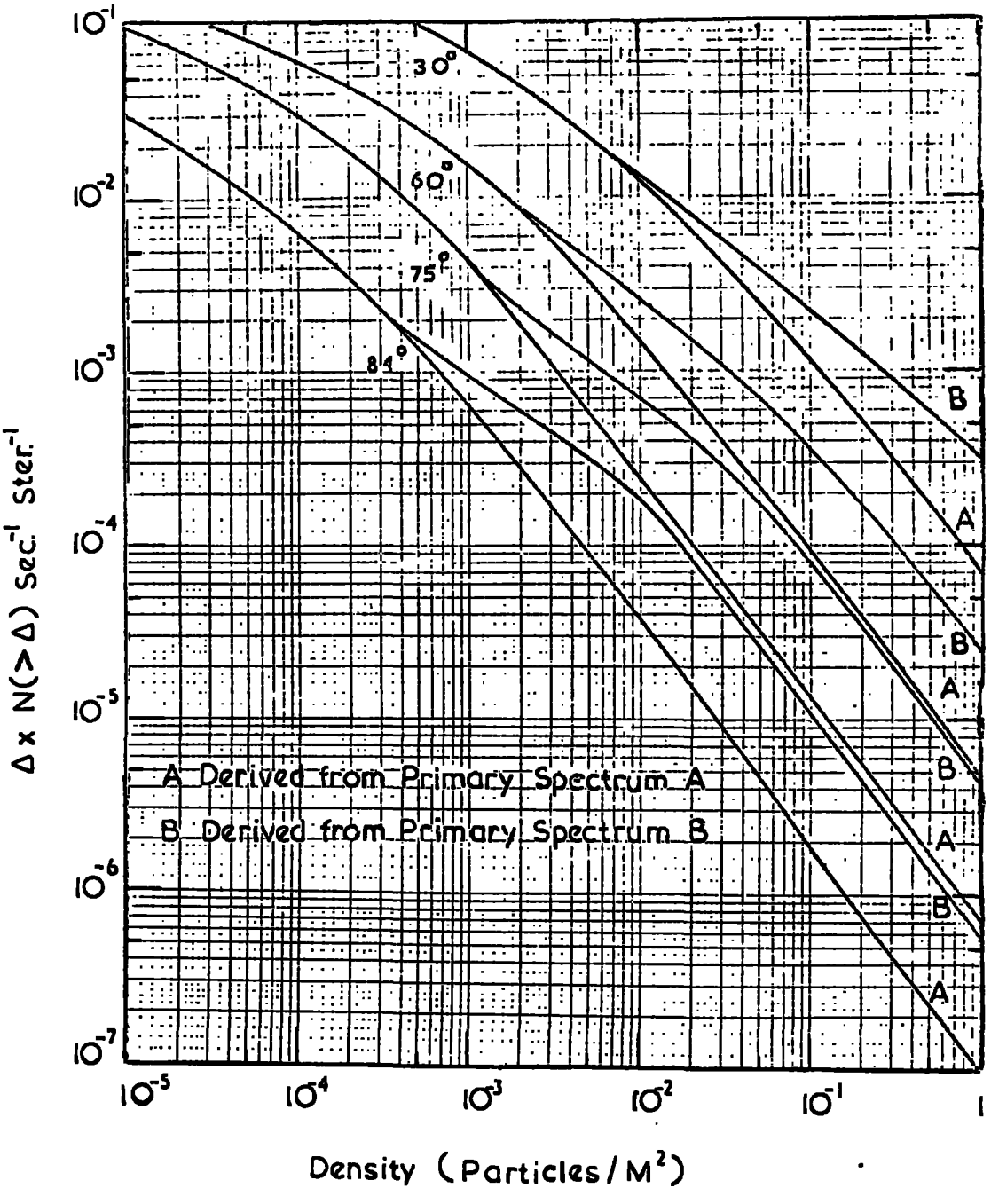

Integral muon density spectra for the two primary spectrum models A and B with no correction for geomagnetic deflection.

the vertical. Calculations by De Beer et al. (1969) show that at 75° the deflection of muons of energy greater than 1 GeV due to geomagnetism is 1.5 times that due to transverse momentum and coulomb scattering. The factor which predominates is the linear height of origin of the muons which increases rapidly with zenith angle.

An exact Model calculation including Geomagnetic effects is prohibitive in terms of computation time. Furthermore the bulk of the data from the experiment falls in a region where geomagnetic effects, though appreciable do not dominate. Therefore it has seemed justifiable to use approximate methods.

A calculation has been done of the lateral distribution of muons at 75° for geomagnetic effects alone. This is in fact a distribution in one dimension only and is similar in shape to the ordinary lateral distribution. Since height of origin is the predominant factor the distribution for other angles can be derived from the variation in mean height of origin with angle.

Two methods of combination of the lateral distribution for magnetic deflection, and that for transverse momentum and scattering have been used. In the first the r.m.s. radii of the two distributions have been added in quadrature to produce a new r.m.s. radius which is applied to the lateral distribution to give that with magnetic correction. This

assumes that the shapes are the same, and that the resultant shower is still radially symmetric. In fact the shower is elliptical in section, however the new radius is a mean between the major and minor axis of the ellipse so that this uncertainty is partly taken into account. This method, despite its crudity seems to give good agreement both with the shape of the observed variation of density spectra with angle in the present work, and (with due allowance for different geomagnetic conditions) with the work of Parker, (1967) out to zenith angles where geomagnetic deflection is several times that due to transverse momentum and scattering.

A second method has been to assume that deflection by geomagnetism is proportional to radial distance due to transverse momentum and scattering. This assumption is roughly true in the middle region of radial distance. Thus each annulus of the lateral distribution has been displaced along the axis of geomagnetic deflection of the shower and the resulting non circular distribution calculated. This has then been combined with the primary energy spectrum to produce density spectra, due allowance being made for the new shape of the shower. This method gives density spectra which agree with those produced by the first method up to a zenith angle of 70°. Beyond this an excess over method 1 is predicted. This is because where magnetic deflection is

large the shower becomes elongated, so that the mean distance at which a given density is observed increases, giving a larger catchment area for a given detector.

The density spectra, corrected for geomagnetic deflection, for showers incident from geomagnetic North, and the field conditions prevalent at Durham are shown in figure 5.12.

5.10 The Variation of the Theoretical Density Spectrum with Zenith Angle.

In order to obtain density spectra at intermediate angles it is necessary to find a method of interpolation. Figure 5.13 shows the variation of intensity, at a constant density, of the density spectrum with zenith angle. The angular scale is in terms of the logarithm of secant θ. This is proportional to the mean linear height of origin of the muons. It can be seen that the variation of the spectrum, uncorrected for geomagnetic deflection, may be represented by two intersecting power laws in cosine θ, and that the spectrum including geomagnetic corrections may be represented by a single power law throughout.

In Chapter 6 it is shown that when the experimental angular variation is corrected for the changing acceptance with angle of the apparatus, this follows a similar law, as do the experimental distributions of other workers. Thus it appears justifiable to use the law so derived to produce

Integral muon density spectra, corrected for geomagnetic deflection for the conditions of the present work. Fig. 5.12.

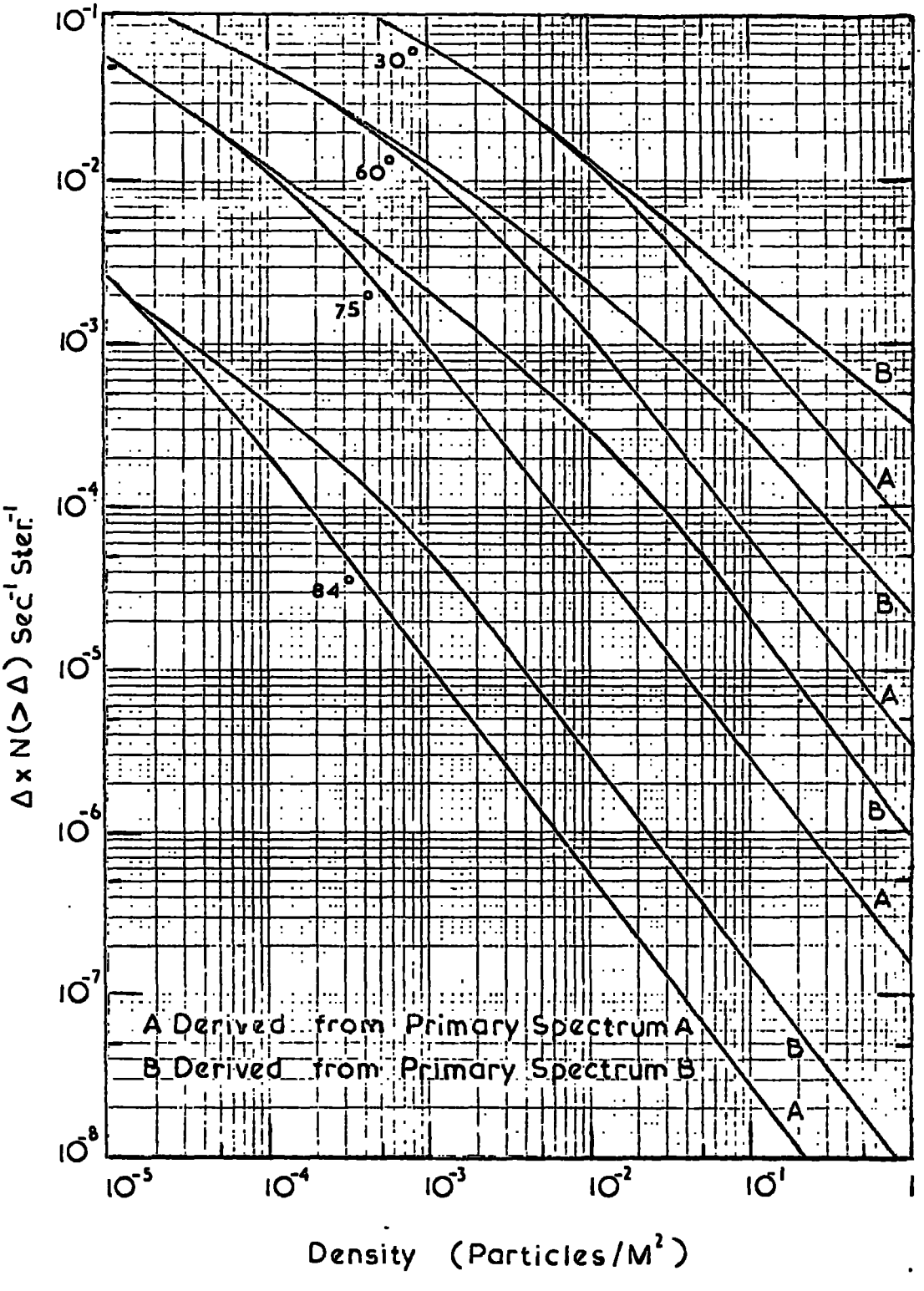

Fig. 5.13.

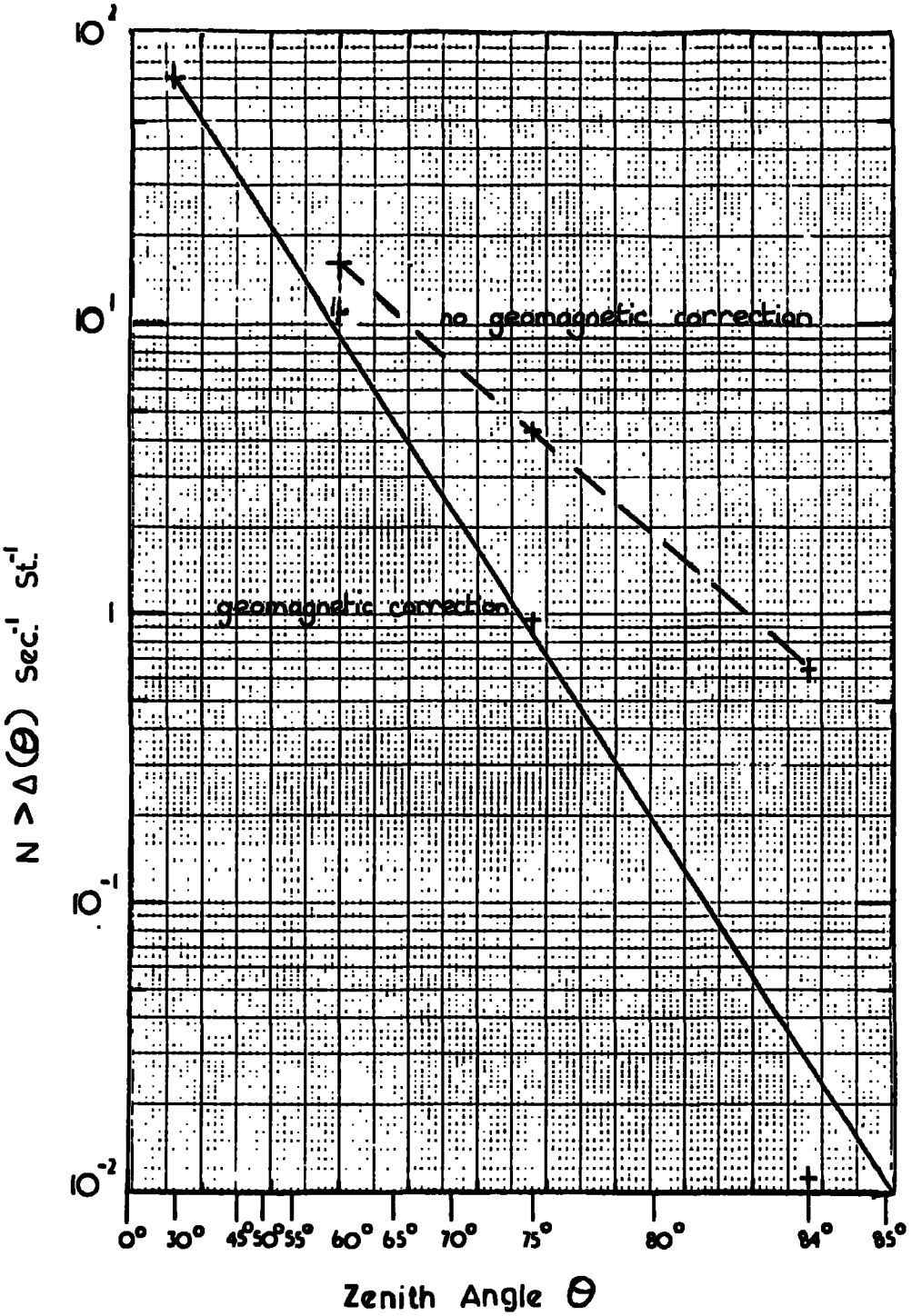

The angular variation of the density spectrum.
The horizontal axis is in terms of Log Sec θ

density spectra at intermediate angles.

5.11 Sensitivity of the Density Spectrum to the Mean Transverse Momentum

The sensitivity of the density spectrum to the parameters used in the model plays an important part. If the density spectrum is sensitive to one parameter, uncertainty in its magnitude may obscure information to be obtained on another.

Figure 5.14 shows the variation of the density spectrum with the value of mean transverse momentum of the secondary pions assumed in the model. It is seen that there is sensitivity to this in the intensity of the density spectrum, but little variation in shape. Thus if all other parameters are fixed independently a comparison with experiment could in principle give information on the transverse momentum associated with these events.

The reason for this sensitivity is that an increase in spread of the shower causes a marked reduction of the density of muons at a given distance. This is such as to cause a reduction of intensity at a given density proportional to the square of the increase in spread. Thus an increase in the mean transverse momentum assumed causes a large decrease in the density spectrum.

Fig. 5. 14

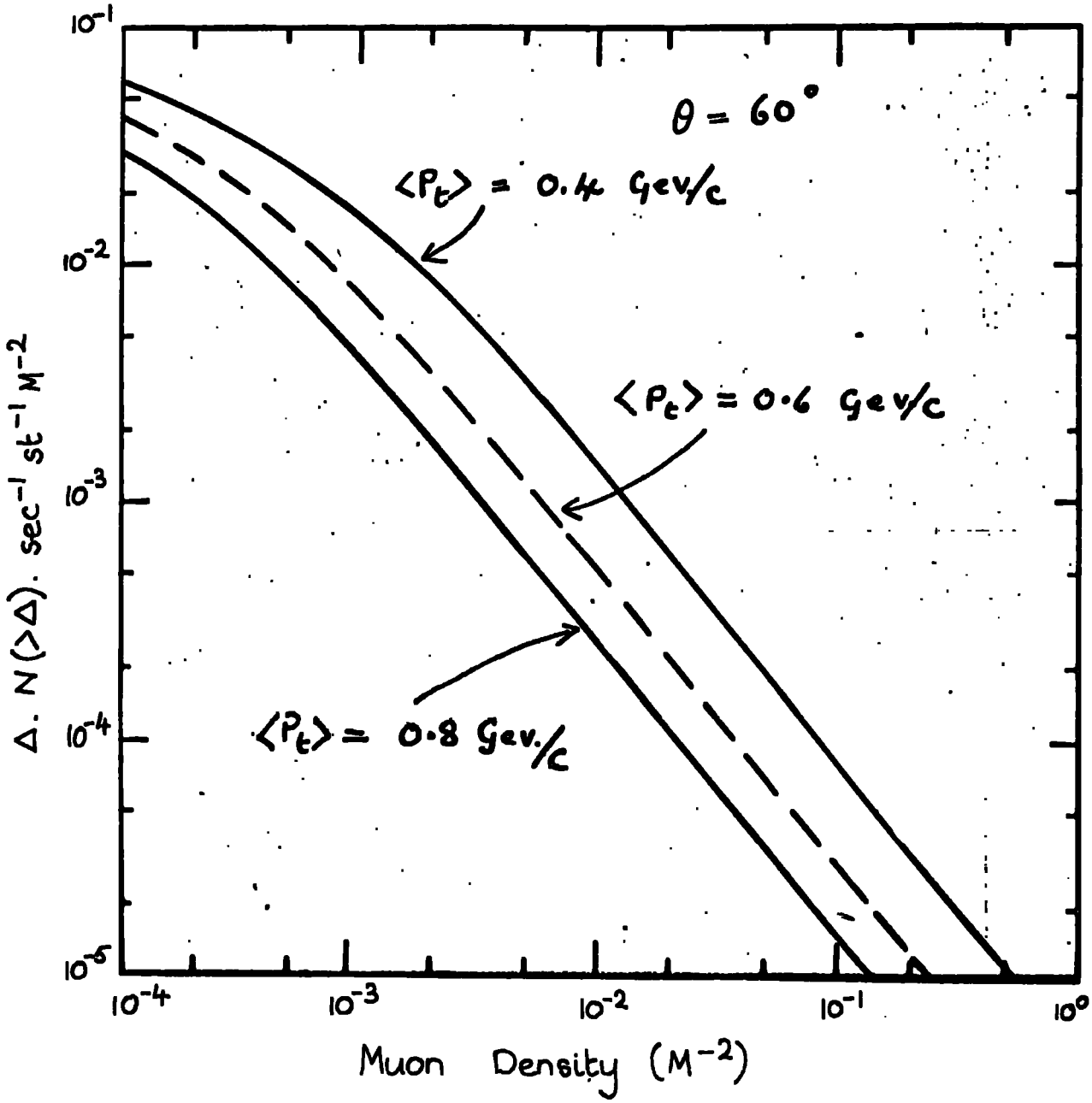

Integral muon density spectra for primary spectrum A and three values of the mean transverse momentum (P_t) at 60°.

5.12 Summary

In this chapter, theoretical density spectra have been produced for two different models of the primary spectrum. These two models both give agreement with the sea-level electron size spectrum. In the following chapter comparison with experiment enables a conclusion to be drawn as to which of these models is to be preferred.

CHAPTER 6

Comparison of the Experimental Results with Theory

6.1 Introduction

The theoretical density spectra obtained in the previous chapter are used to derive the expected rates of muon groups detected by the apparatus as a function of zenith angle and multiplicity. This enables a comparison to be made between the experimental results and the theoretical predictions, and from this, conclusions can be drawn as to which density spectrum gives best agreement and hence which model of the primary flux is to be preferred.

6.2 Theory of Triggering Probabilities.

The derivation of expected rates requires a knowledge of the triggering probability of the apparatus and how this varies with angle and density. This probability may be defined as the probability that at least one particle passes through each detector linked in coincidence with the others, and that no particles pass through any anticoincidence detectors.

For any given density and angle the mean number of particles passing through a detector can be evaluated from

its area projected on to the plane of the shower front. Poissonian statistics then give the values of the probabilities mentioned above. The resultant product gives the probability that a shower making angles θ, and ϕ with the apparatus and producing a density Δ will trigger the detectors.

6.3 The Geometry of the Detectors

The detecting elements of the array are arranged to form two scintillator telescopes and an anticoincidence counter (see figure 3.1 a and b). The triggering probability depends on the overlap area of the telescopes at any particular angle. Figure 6.1 shows the detail of the telescopes and the geometrical relationships. These are used to give the following expression for the variation of projected overlap area. The angles θ and ϕ are the zenith and azimuth angles made by the shower axis.

$$A(\theta,\phi) = [h - d\,(\cot\theta - \tan\alpha)][l - s.\tan\phi]\cos\phi\sin\theta$$

The projected area of the anticoincidence counter varies simply as $A = \cos\theta$, each counter having an area $1\,m^2$.

6.4 The Triggering Probability

This is obtained by evaluating the function

$$P(\theta,\phi,\Delta) = (1 - \exp(-\Delta A(\theta,\phi)))^2\,(\exp(\Delta))$$

over all values of θ, ϕ, Δ

where $A(\theta,\phi)$ is defined in section 6.3; values

Fig. 6.1

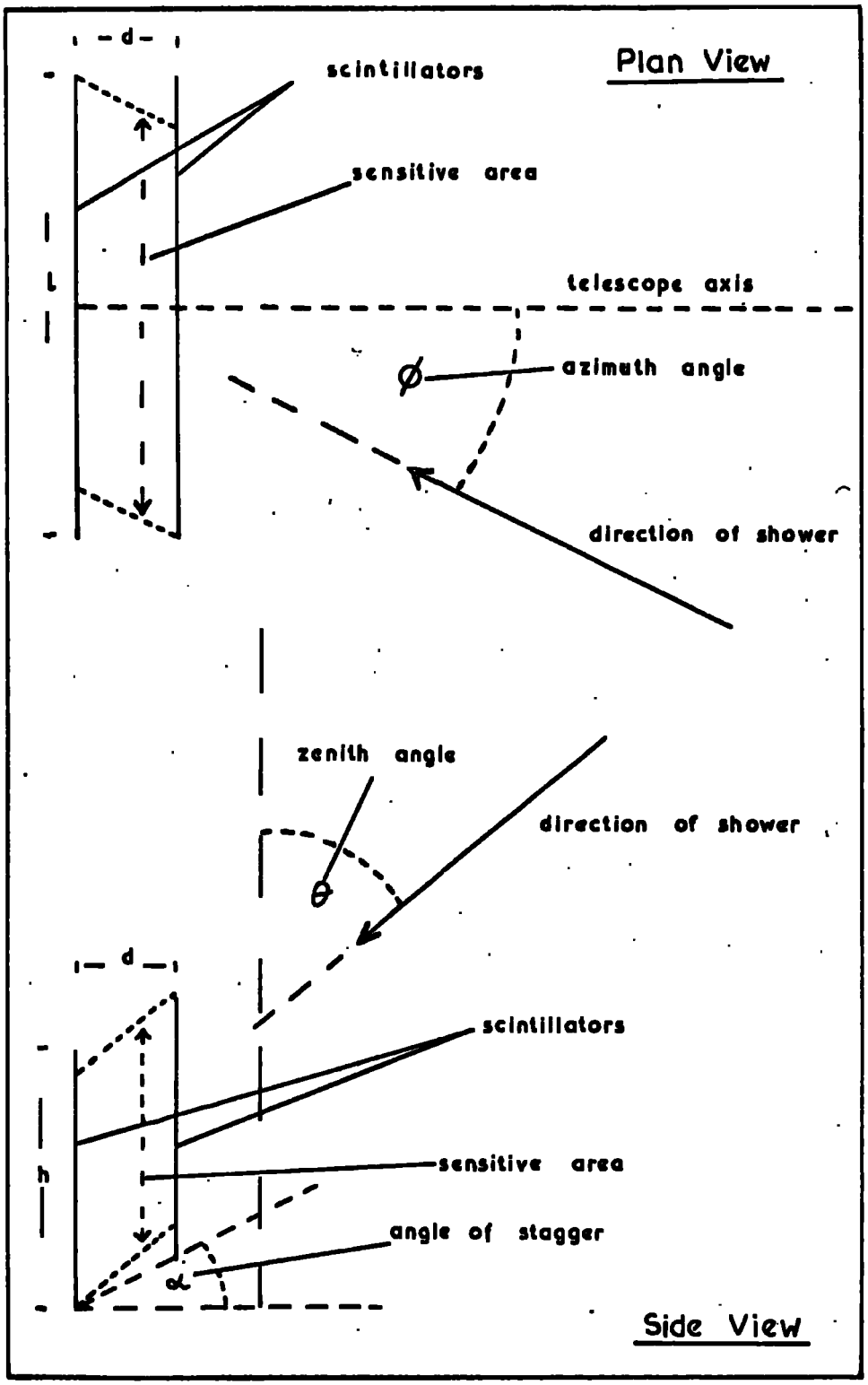

Detail of a telescope, showing geometrical relationships.

of $P(\theta, \phi, \Delta)$ are shown in Figure 6.2.

6.5 Derivation of the Effective Density Spectrum for Given Values of Zenith and Azimuth.

Each of the density spectra given in figure 5.12 is differentiated and converted to an effective density spectrum. This may be defined as the differential density spectrum of showers which have the minimum requirements for triggering the apparatus, and is obtained by multiplying the intensity at each density by the triggering probability for the appropriate zenith and azimuth angles. The effective density spectrum is thus a function of both zenith and azimuth. The former variation is both inherent in the showers and the apparatus, the latter only in the apparatus.

6.6 Accurate Derivation of the Effective Density Spectrum for a Given Projected Zenith Angle.

The apparatus measures the zenith angle of the showers projected in the plane of the flash tube windows. This introduces a further complication because for a constant projected zenith angle, different azimuth angles correspond to different true zenith angles. Thus the events observed at a given projected zenith angle are composed of groups of muons which have passed through varying thicknesses of atmosphere.

The problem is solved by calculating for each projected

Fig. 6.2.

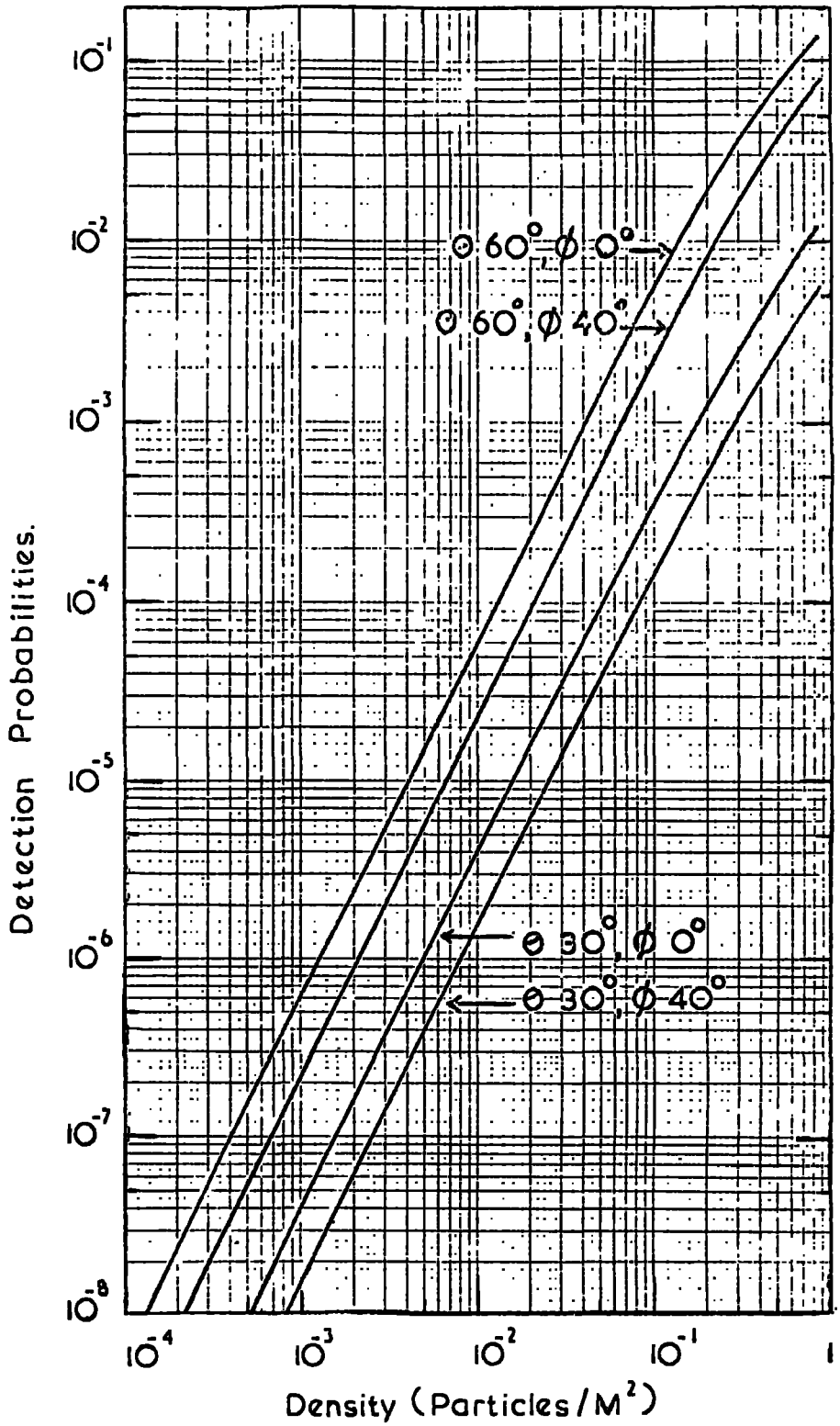

Triggering Probabilities.

zenith angle the variation of true zenith angle with azimuth. These are related by $\tan\theta_p = \cos\phi \tan\theta$, where θ_p is the projected zenith angle. The respective effective density spectra are then summed to give the total contribution to that cell in projected zenith angle.

In order to weight the various contributions correctly the solid angle of each cell of azimuth must be used. This is calculated to be $d\omega = \frac{\sin\theta}{\cos\phi} \cdot \frac{\sec^2\theta_p}{\sec^2\theta} \cdot d\theta_p \, d\phi$. The geometrical relations are shown in figure 6.3.

Thus the true variation of the expected differential density spectrum is obtained by summing each effective density spectrum weighted by its solid angle. Figure 6.4 shows a typical effective density spectrum.

6.7 Approximate Derivation of the Effective Density Spectrum in Projected Zenith Angle.

The above mentioned calculation has been carried out for several different zenith angles, however for repeated calculations it has been found possible to use an approximate method.

The variation of trigger probability with azimuth is relatively sharply peaked in the direction normal to the array. This, coupled with the rapidly falling zenith angular variation, and the decrease in solid angle for large azimuth angles, means that the contribution from large azimuth angles is small. Thus the variation of shape of

Fig. 6.3

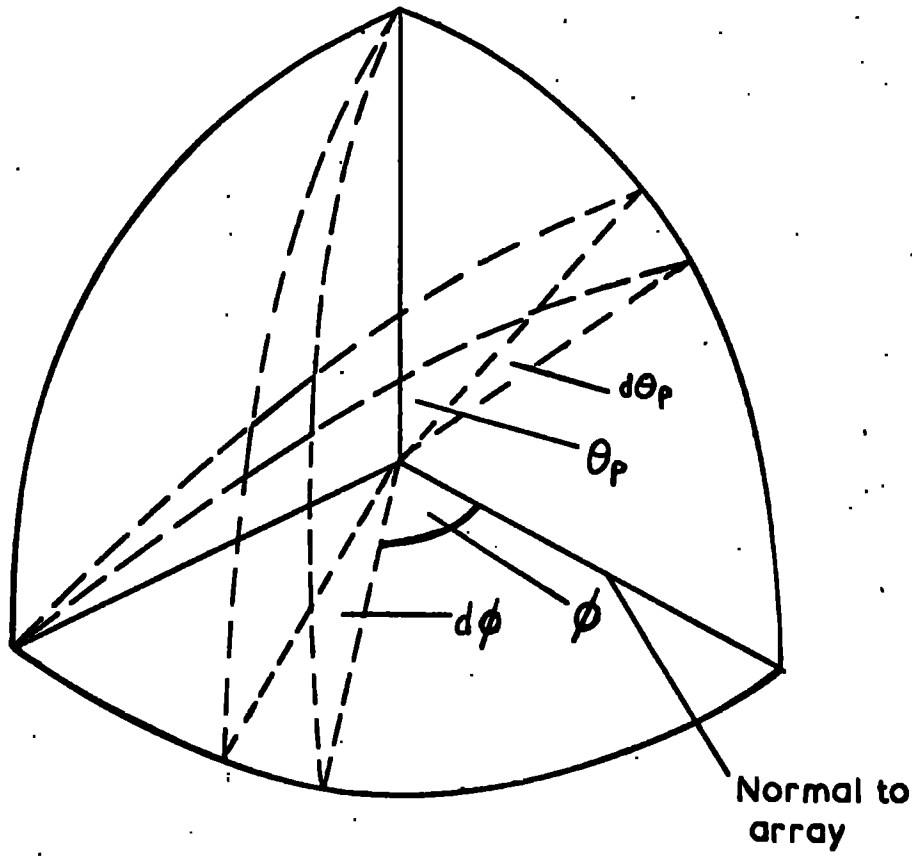

Geometrical relations for solid angle,

and projected zenith angle.

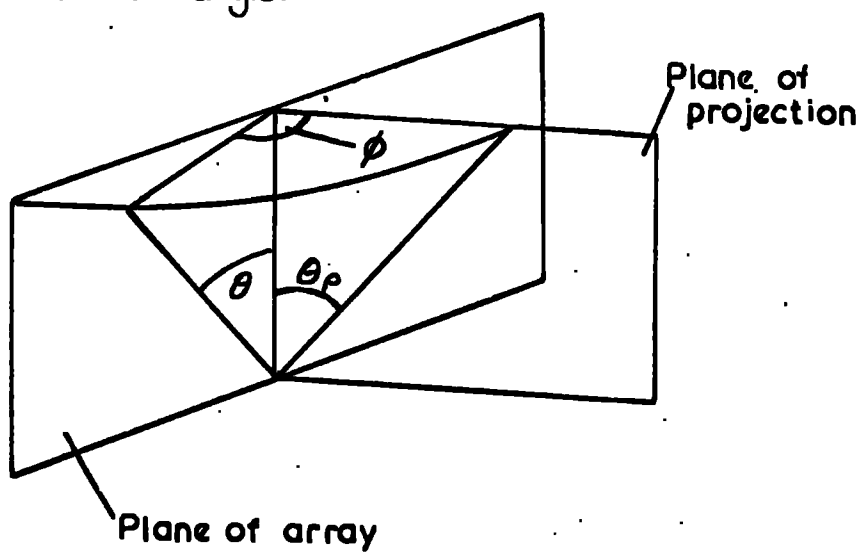

Fig. 6.4.

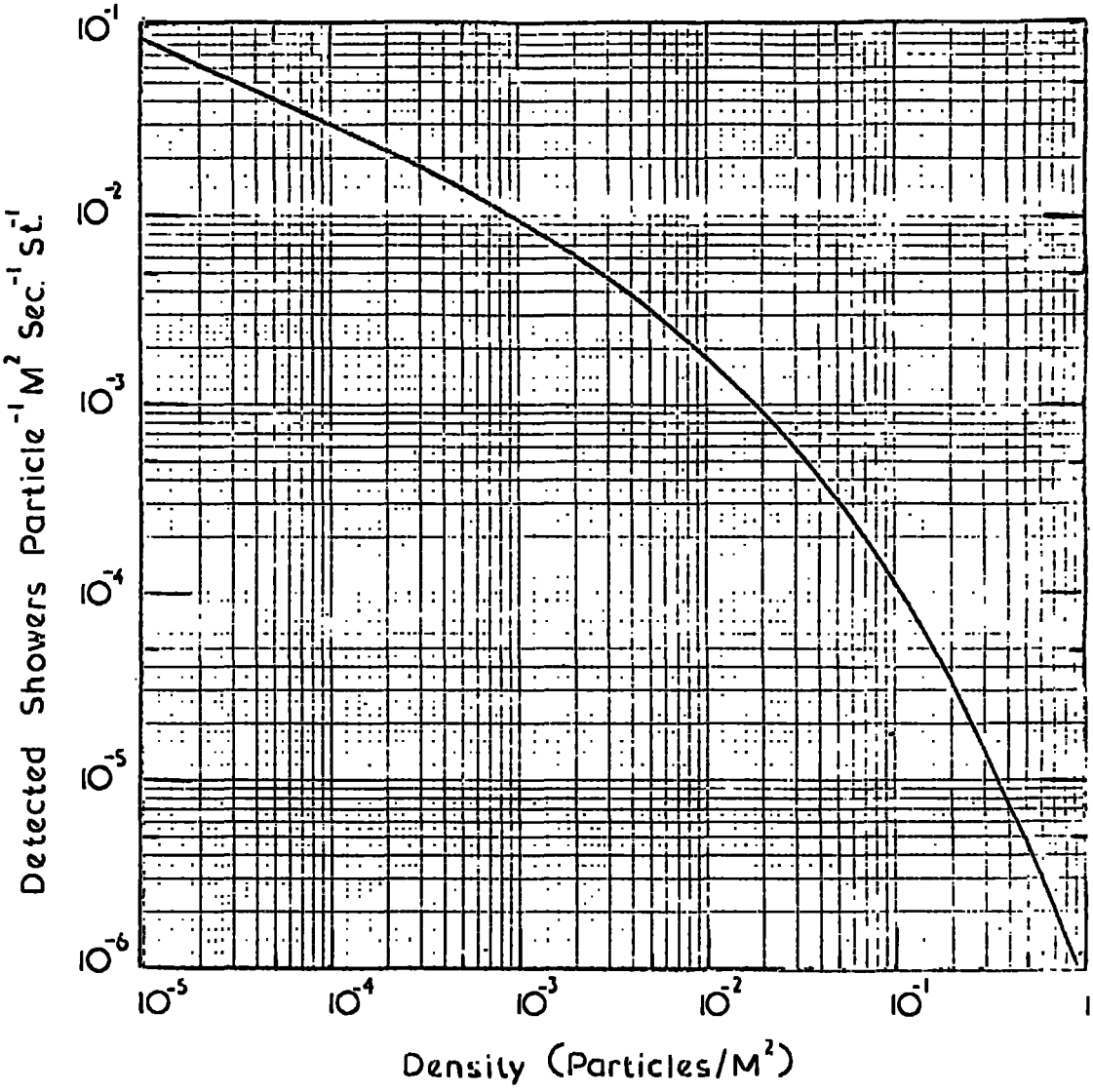

A typical effective differential density spectrum.

the density spectrum with azimuth may be neglected. It has been found that if the effective density spectrum at the true zenith angle equal to the projected zenith angle, is taken with a value of 40° for the azimuth, the resulting effective density spectrum differs by less than 5 per cent from that calculated by the accurate method, due allowance being made for solid angle. This method having been proved is used in all subsequent calculations.

6.8 The Expected Rate of Triggering of the Apparatus as a Function of Zenith Angle.

Integration of the effective density spectrum(derived by either of the two above methods) over density leads to the expected rate of triggers by muon showers at the given projected zenith angle. This may be expressed as the number of showers per second, triggering the array, at projected zenith angle θp per $d\theta p$.

The integral of the effective density spectrum of muons greater than one GeV converges at low densities. This is not necessarily the case with other density spectra at higher threshold energies. The convergence arises because of the loss by μ-e decay of the low energy muons, combined with the use of a two-fold coincidence system (which varies in efficiency with Δ^2). Experiments on high energy density spectra require 3 fold coincidence techniques to give a finite value of the

integral over density.

6.9 The Problem of Small Densities and Poissonian Fluctuations.

A typical effective density spectrum (figure 6.4) shows that the median density triggering the array is about 10^{-3} particles/M^2 so that the mean number of particles crossing the apparatus is considerably less than one. Thus the observation of one or more muons in the apparatus is in the majority of cases the result of an upward fluctuation in the number of muons in that area. This is because the rapidly falling density spectrum gives many more events in which the mean number is less than one, so that the contribution to the observed rate from small mean densities with an upward fluctuation is much greater than the contribution coming from the density giving a mean number in the region of the number observed. This gives a very different distribution in number observed than that which is derived directly from the effective density spectrum.

6.10 Derivation of the Multiplicity Spectrum for a Given Projected Zenith Angle.

Multiplicity is defined here as in Chapter 4 as the total number of muons observed in an event including those particles which trigger the scintillation counters. The number of triggers as a function of density, is expressed by

the effective density spectrum. This therefore already includes events containing at least two muons i.e. of multiplicity $\geqslant 2$. The probability of observing 0, 1, 2,— n additional particles in the main array, as a function of density, is obtained from the poissonian probability

$$P_n = \frac{m^n}{n!} \exp(-m).$$

where m is the mean number of particles crossing the array, i.e. the product of the density, and the area of the array, projected on to the shower front. This probability is then folded in with the effective density spectrum for each value of n. A series of curves results, each representing, as a function of density, the differential intensity of events of multiplicity n + 2. A group of such curves is shown in figure 6.5. Integration of each curve then gives the theoretical multiplicity distribution. This distribution is calculated for each cell of projected zenith angle thus enabling comparison to be made with theory. A typical result is shown in figure 6.10.

6.11 The Variation of Median Primary Energy with Density and Angle.

In Chapter 5 it was shown that the contribution to each density comes from a variety of primary energies. In deriving information about the primary energy spectrum from the experimental results the median primary energy has

Fig. 6.5.

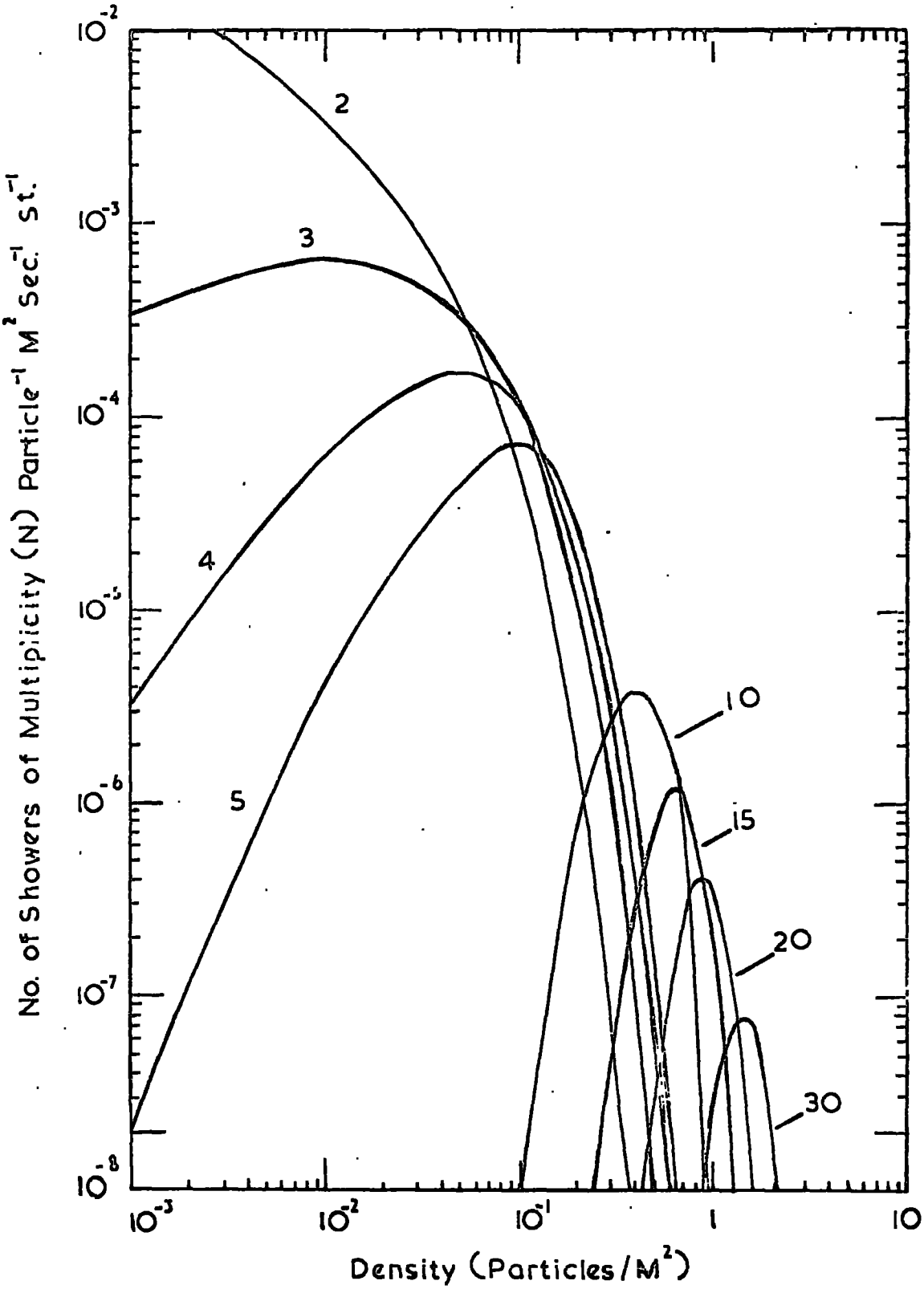

The contribution to each multiplicity from the density spectrum.

been used as this measure suffers least from obscurities in definition.

The median primary energy corresponding to any point on the density spectrum for any given angle is obtained readily from the integration of the function $\pi R^2 J(E_p)$ given in Chapter 5 (5.8) This median is shown plotted against density for various angles in figure 6.6.

6.12 The Variation of Median Density with Multiplicity and Angle.

In section 6.10 it was shown that because of fluctuations in density the contributions to the intensity at a particular multiplicity come from a range of densities. The median density corresponding to a particular multiplicity is obtained from the integration of the probability function given in 6.10. A typical plot of median density against multiplicity is shown in figure 6.7.

The two preceeding sections give the functions necessary to relate the observations at any multiplicity and zenith angle with the median primary energy producing that multiplicity thus enabling deductions to be made on the nature of the primary particles at that energy, by a comparison of experiment, with the two theoretical predictions based on primary spectra A and B (Chapter 5).

Fig. 6.6.

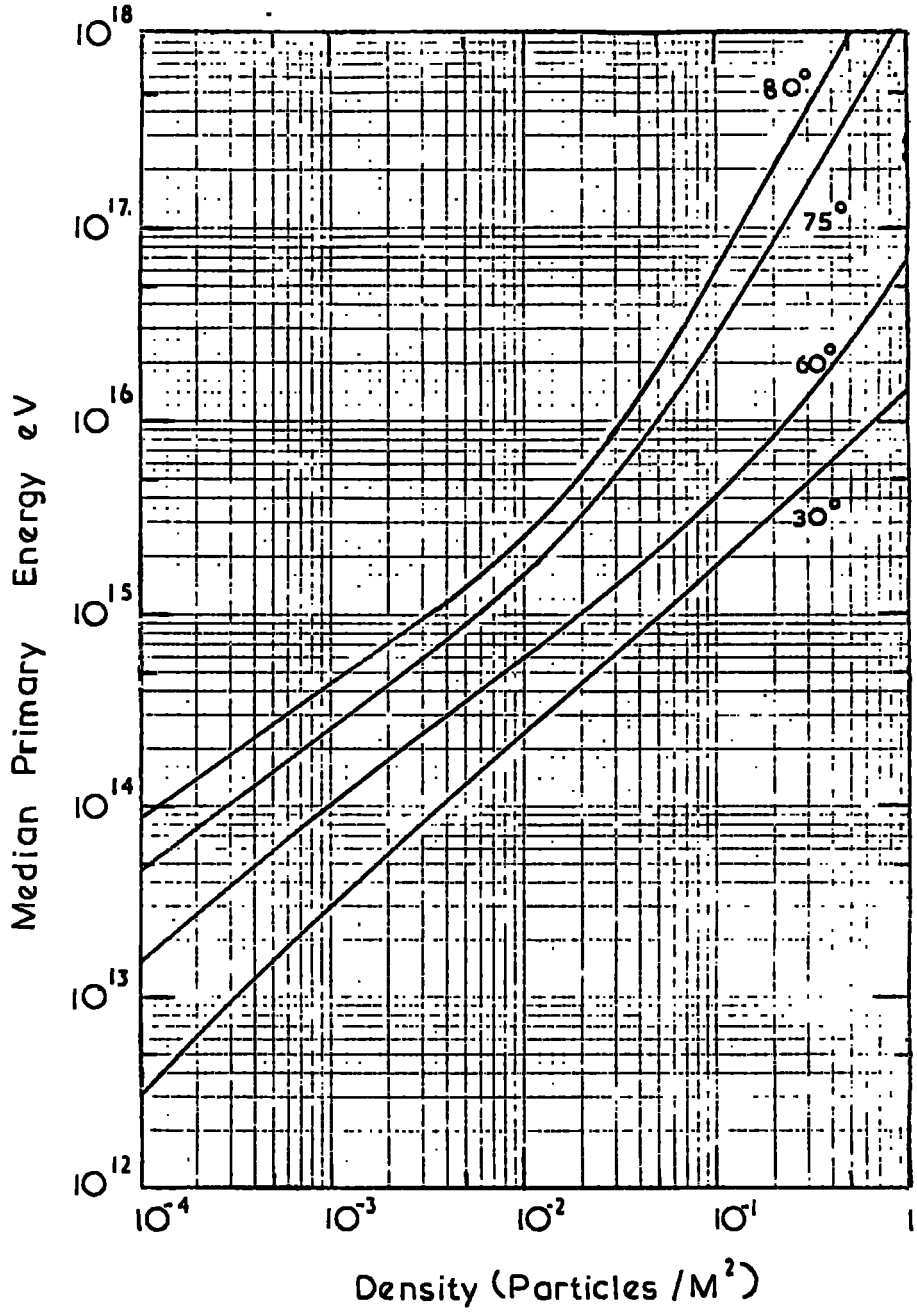

Median primary energy as a function of density and zenith angle.

Fig. 6.7.

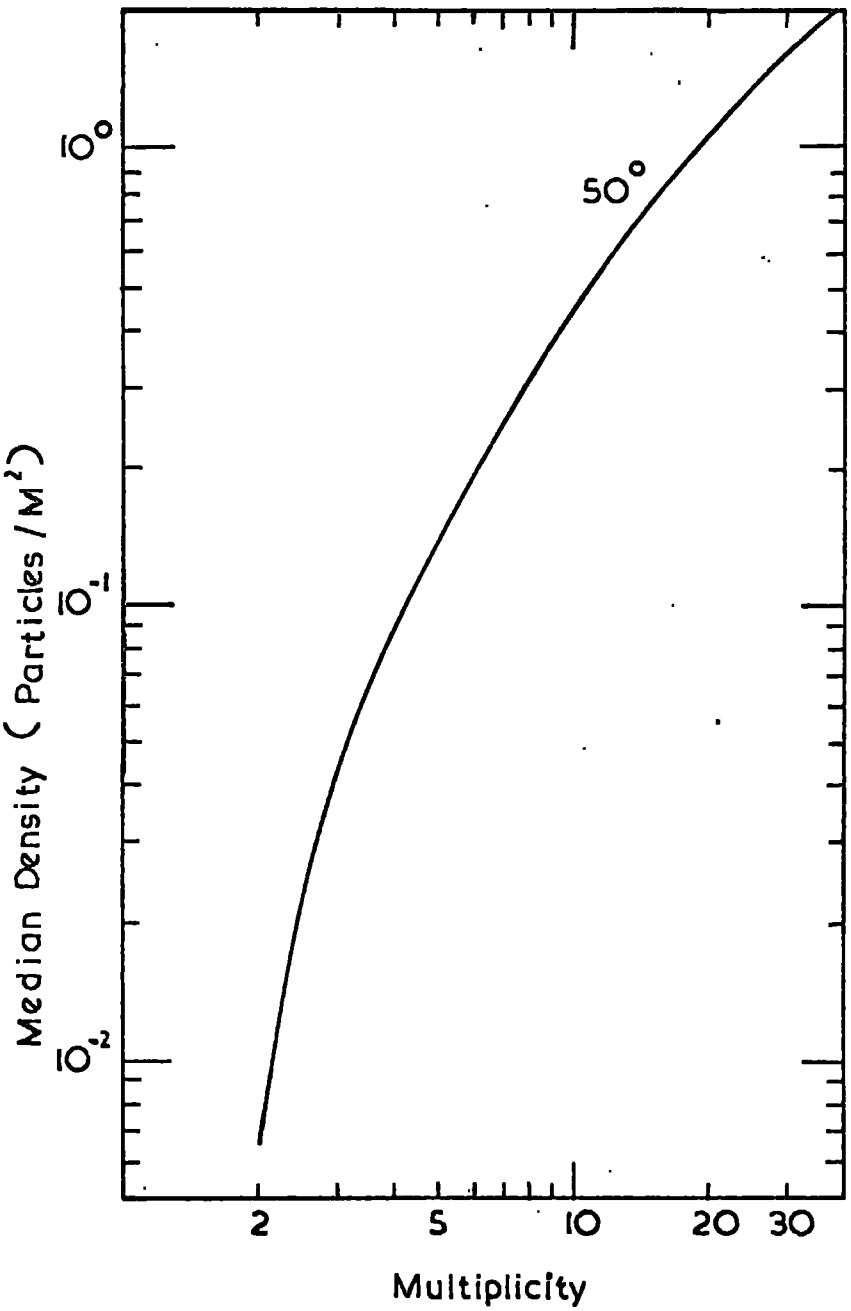

Median density as a function of multiplicity and angle.

6.13 Comparison of the Experimental Angular Distribution with the Theory.

The position has now been reached where direct comparison can be made between the experimental results analysed in Chapter 4 and the theoretical predictions. Figure 6.8 shows the experimental distribution in projected zenith angle. The details of its derivation are given in Chapter 4.

In order to make comparison with theory the integral under the effective density spectrum is first obtained for each cell of zenith angle. This represents the intensity of events triggering the apparatus. There is only a very small contribution to this integral from the region where the predictions of primary spectra A and B differ so in this comparison these predictions effectively coincide. This integral is then multiplied by the solid angle and running time to give the predicted total number in each cell of projected zenith angle. The result appears on figure 6.8 as the solid line the results of a similar calculation appear for the density spectra with no geomagnetic correction, and for those with an assumed value of the mean transverse momentum of 0.8 GeV/C.

It should be stressed that this comparison is direct, that no normalization has been used, and that the theoretical predictions have been treated throughout in the same way as

Comparison of theory and experiment, angular spectrum. Fig. 6.8.

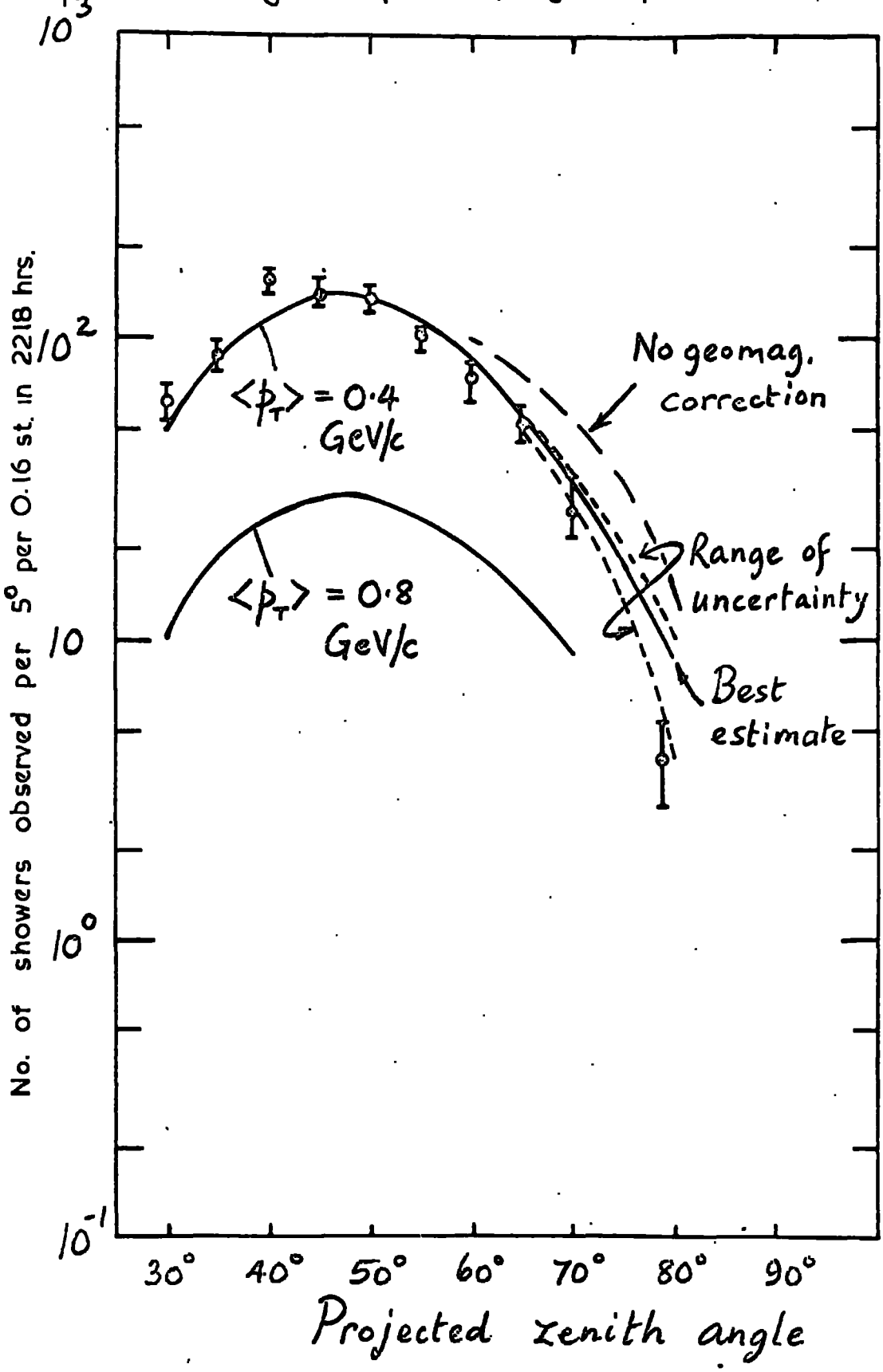

the experimental data.

Several points arise from this figure. The geomagnetic correction plays only a small part in the region where the bulk of the data lies, and thus any inaccuracies in this will not be important. The agreement between the prediction and experiment is extremely good both in spectral shape and intensity. As mentioned in Chapter 4 the bulk of these events are pairs of muons, for which the median primary energy is about $3\ 10^{14}$ eV. Thus this comparison relates to a region of the primary energy spectrum where the composition is expected to be normal. This agreement therefore acts as a strong support for the validity of the E.A.S. model calculations, and especially their ability to predict correctly the interelation between the electron component in the vertical and the muon component at angles away from the vertical.

The sensitivity of the density spectrum to the mean transverse momentum of secondary pions has already been mentioned in Chapter 5. Here we see that this sensitivity is carried through to the comparison with experiment, and that the evidence is strongly in favour of the assumed value of 0.4 GeV/c.

6.14 The Form of the Incident Angular Spectrum of Muon Showers.

Other workers (Barton, 1968), have found it necessary

to assume a form for the angular spectrum of muon showers, in order to combine measurements made at different zenith angles. So it is of interest to see what the present results give for the incident angular spectrum of pairs of muons. Figure 6.9 shows the experimental and theoretical points of figure 6.8 divided by the triggering probability, at the median density for the events ($\sim 10^{-3}$ p/m^2). This unfolds the effect of the variation in sensitivity of the apparatus with angle (to a first approximation). The experimental results are seen to obey, rather closely a power law in Cos θ over the whole range of angles. The exponent is close to -4, the value assumed by Barton (1968). This figure corresponds to figure 5.13 which shows the variation of the theoretical density spectrum with angle.

6.15 Comparison of the Theoretical and Experimental Multiplicity Distributions.

The events in each cell of the angular distribution were divided into cells of increasing multiplicity, as described in Chapter 4, and compared with the theoretical multiplicity distribution for that angle. A typical distribution is shown in figure 6.10. This comparison has been made for all angular cells. However the density spectrum is so steep that the statistical accuracy is poor. This comparison is important, if deductions on the mass composition

Fig. 6.9.

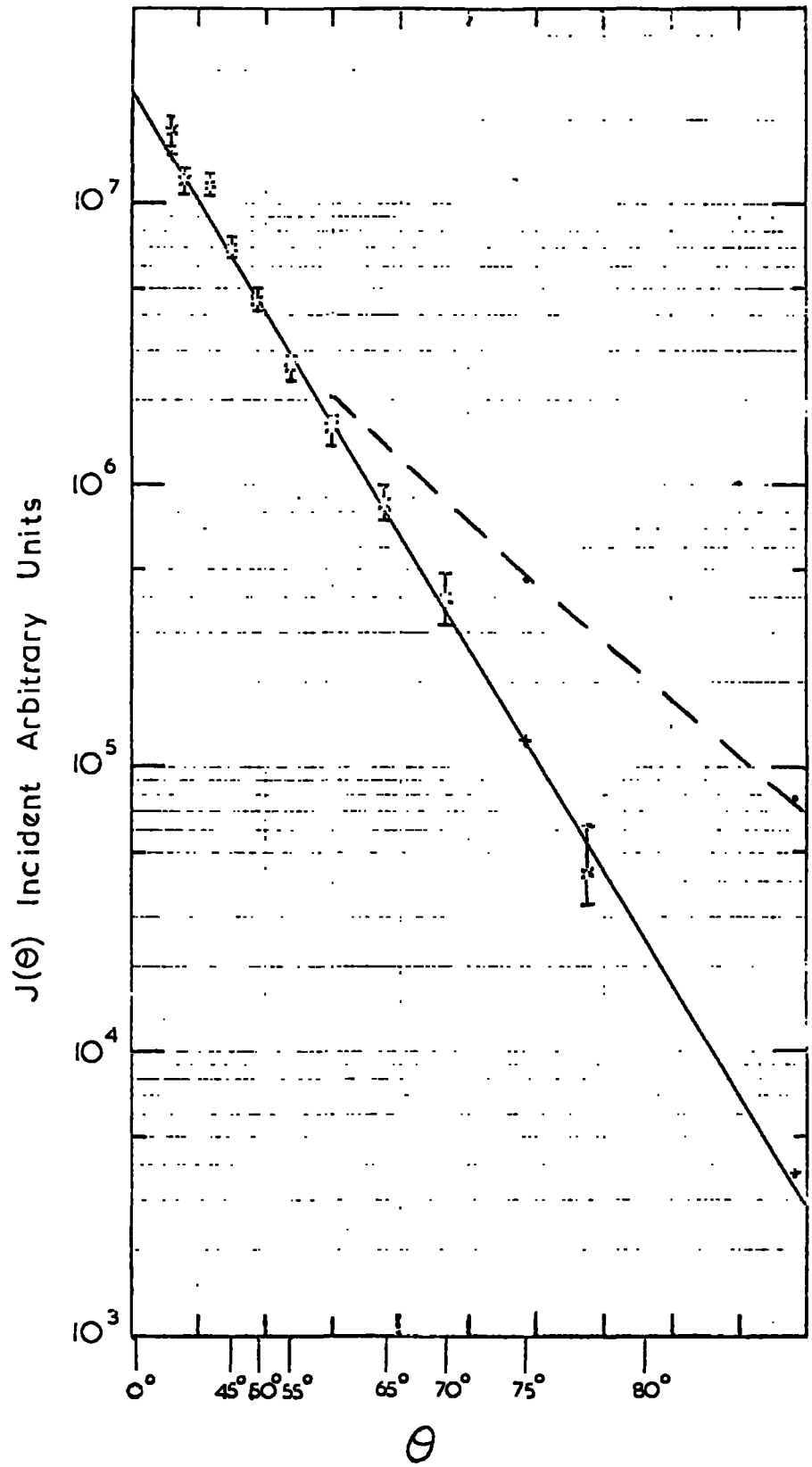

The incident angular spectrum of muon showers.

A typical multiplicity distribution

Fig. 6.10.

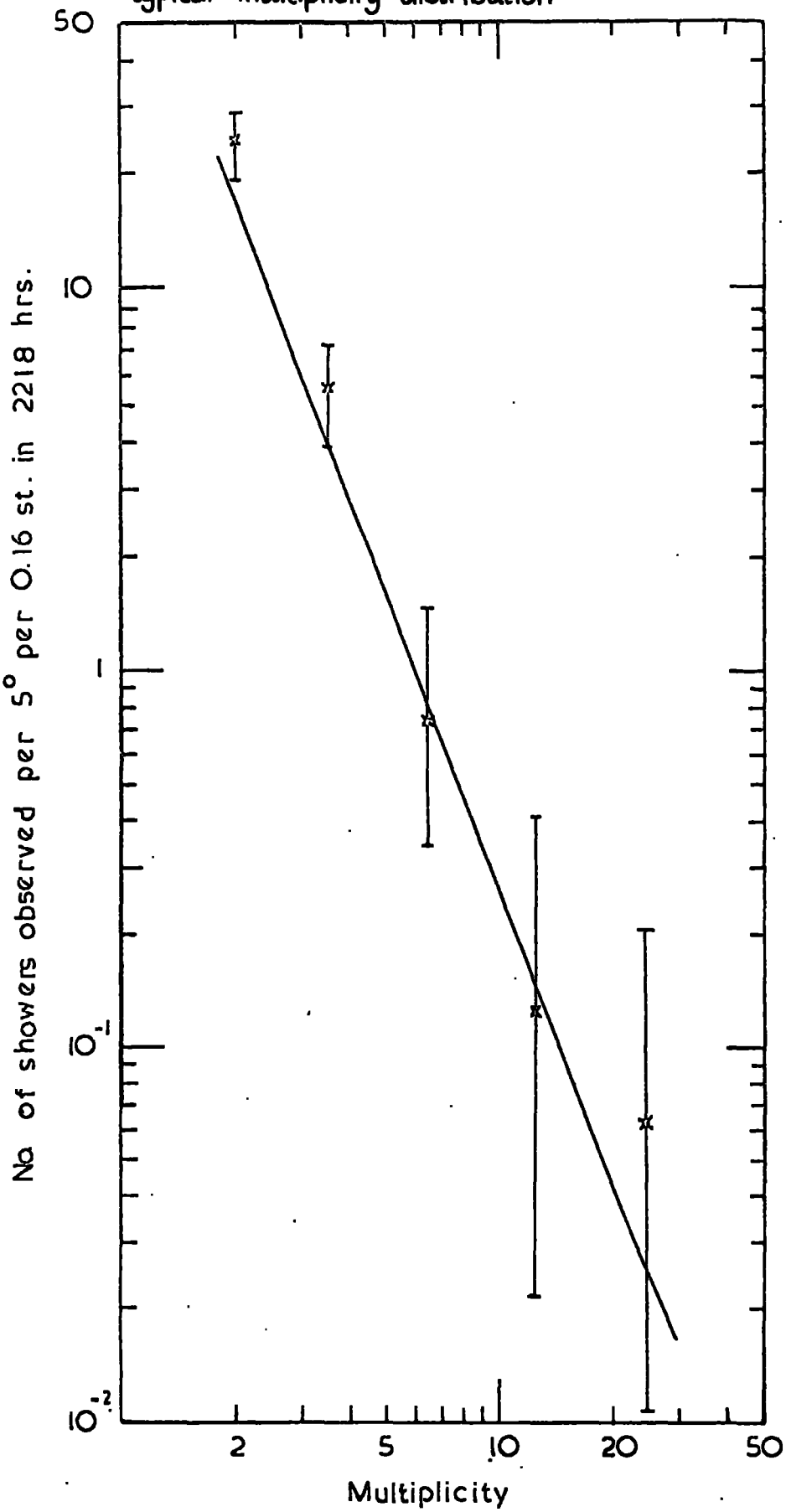

at high primary energies are to be made, as large multiplicities correspond to high primary energies.

The variation of median primary energy with multiplicity and zenith angle has been given in section 6.11. Since interest in the primary energy spectrum is paramount over the density spectrum, if some measure of the agreement between experiment and theory may be obtained as a function of primary energy then deductions on the composition can be made from the better statistical accuracy so achieved.

The measure of agreement adopted was the ratio observed rate/expected rate, for each multiplicity cell in each angular distribution. These cells represent individual entries in table 4.1. The median primary energy for each cell was derived from the curves shown in figures 6.6 and 6.7.

The ratio was then plotted for each cell of multiplicity and angle, at the appropriate median primary energy. This energy varies slowly with zenith angle, and rapidly with multiplicity. In this way all the data were incorporated, and the points so obtained were grouped into a few cells of good statistical accuracy.

The result is shown in figure 6.11 for the two alternative primary spectra A and B. The precision of the points is sufficient to make a clear distinction between them.

The immediate implication is that below 10^{15} eV, where

The ratio of observed to expected frequencies of multiple muons as a function of median primary energy. Fig. 6.11.

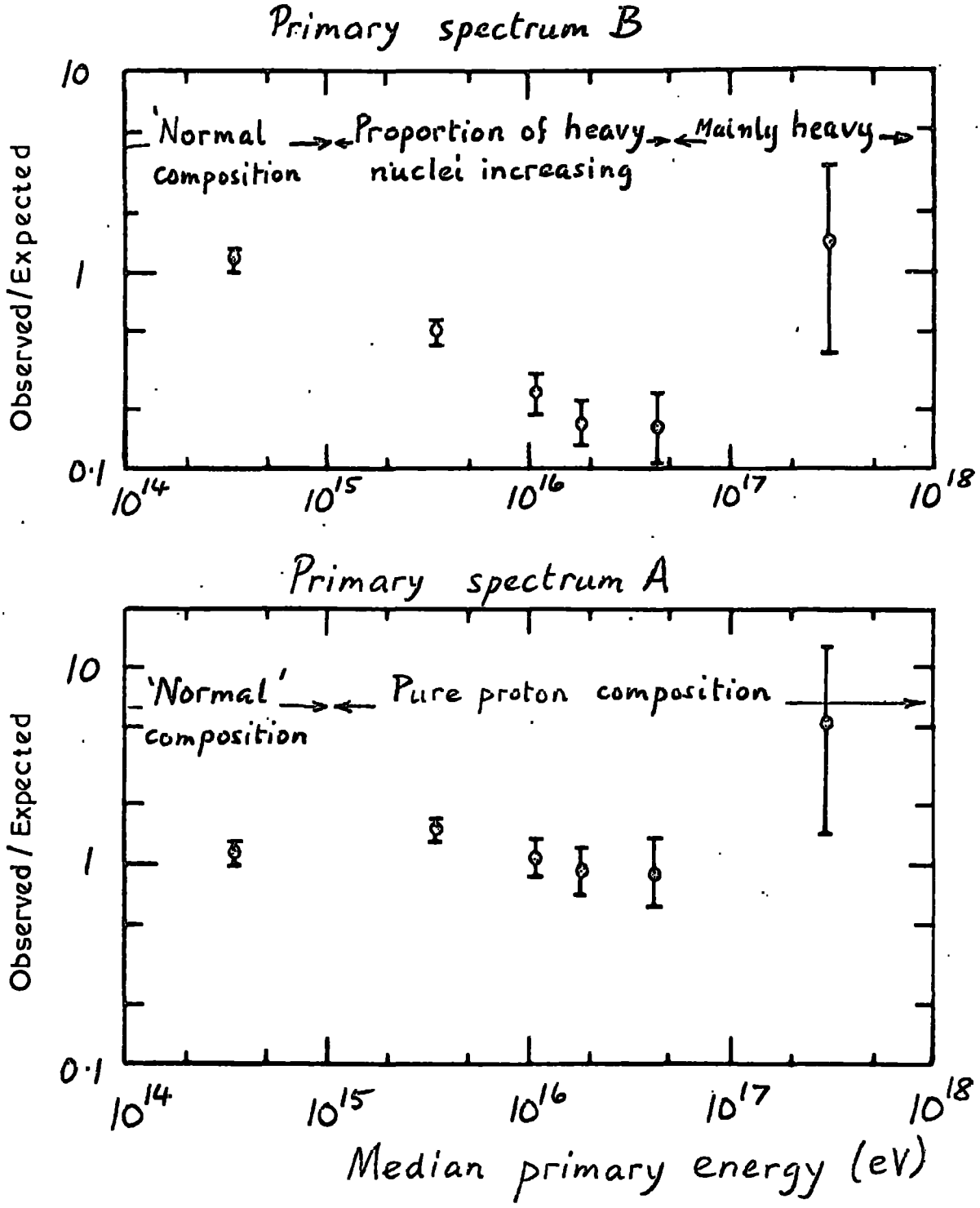

the two models coincide agreement is good. This follows directly from the results on the angular spectrum because the bulk of the data lie in this region. Beyond 10^{15} eV, it is clear that spectrum A is favoured by this experimental data, and that spectrum B is not. Thus there is no evidence for an increase in the mean mass of the primaries beyond 10^{15} eV. It should perhaps be noted that the models A and B were chosen to be extreme cases, and that with the present data, it is not possible to distinguish any more subtle variations in the primary composition.

It has been mentioned previously that Orford and Turver (1968) have found it necessary to postulate a mean mass for the primaries at about 10^{17} eV, of more than 10, and a multiplicity law rising as fast as $E^{\frac{1}{2}}$. Although the weight of the present work is minimal at this energy, the implication that the mass of the primaries increases beyond 10^{15} eV arising from the work of Orford and Turver is in opposition to the present conclusions. It was therefore thought necessary to examine the effect of an $E^{\frac{1}{2}}$ multiplicity law on the results presented in figure 6.11.

The E.A.S. model calculations of De Beer et al. (1966) included consideration of the effects of such a law, although to a lesser accuracy than in the main calculations. Qualitatively it can be seen that this type of law, deposits the energy of the shower into the electron-photon cascade

higher up in the atmosphere and thus produces fewer electrons at sea-level. Also the higher multiplicity results in an increase in the muon number at sea-level.

The results of these calculations have been used to predict density spectra and comparison has been made with experiment, the results are shown in figure 6.12. It can be seen that the agreement between theory and experiment is poor for both primary spectrum models, and is worse for the model containing an increasing primary mass beyond 10^{15} eV. Thus the present work does not support the use of an $E^{\frac{1}{2}}$ multiplicity law.

In conclusion it can be stated that the experimental results on muon showers relating to primary energies below 10^{15} eV are in agreement with the theoretical predictions and that this agreement lends strong support to the validity of the E.A.S. model calculations. When the results of these calculations are extended to the energy region above 10^{15} eV, then the agreement between theory and experiment is good for primary spectrum A, and the results do not support primary spectrum B where the mean mass of the primaries increases beyond 10^{15} eV.

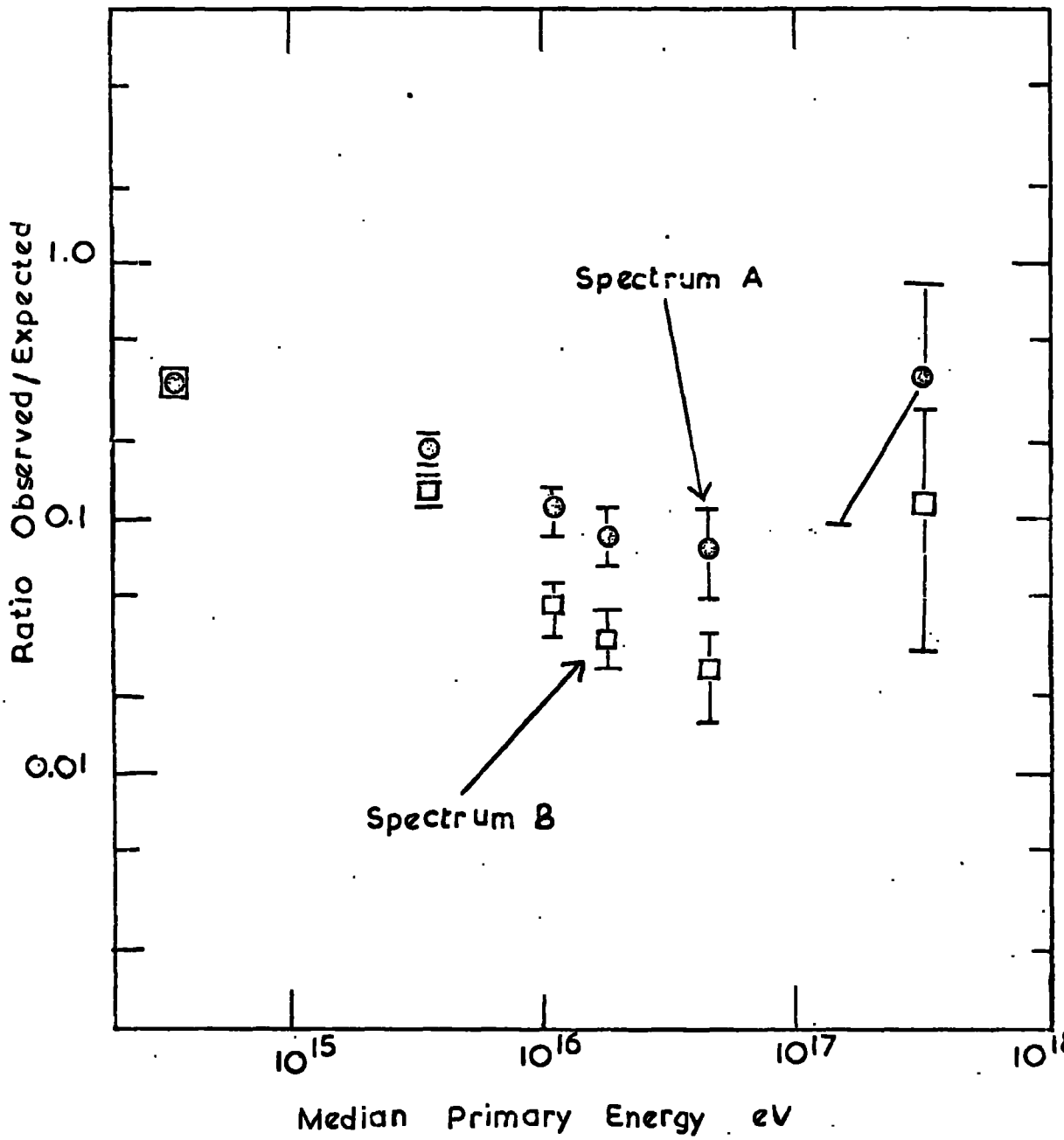

Fig. 6.12. The effect on 6.11. of an $E^{1/2}$ multiplicity law.

CHAPTER 7

Comparison with the Results of Other Workers

7.1 Introduction

Only two experiments seem to have been carried out on muon showers away from the vertical. Other work has been done on near vertical showers, and on muon showers underground. In this chapter comparison will be made with all these results. Such comparison is important because the amount of agreement with the present results found in the work of others will give an indication of the weight to be placed on the findings with respect to the composition of the primaries.

Unfortunately very little work has been done on the multiplicity spectrum of muon showers and the main comparisons can only be made with work done on pairs of muons. As shown in the previous chapter these correspond to primary energies below 10^{15} eV.

7.2 The Utah Prototype Neutrino Detector

In the development of the Utah neutrino detector (Bergesson et al. 1968) a prototype was built and operated at sea-level. In the course of this work 1200 muon showers were detected at zenith angles greater than 45^{o}. Most of these events were

pairs of muons. This work was carried out by Parker (1967).

Figure 7.1 shows a diagram of the apparatus. The detecting elements are two water Cerenkov counters designed to detect muons and also to give their direction. Each consists of a concrete tank 3 metres deep, 1 metre wide and 7.6 metres long filled with water. The front and back walls of the tanks have a series of vertical tubular wavelength converters each with a photo-multiplier attached. A cone of Cerenkov light falling on these detectors gives a signal, the wall from which this signal comes indicating the direction of the particle.

The track delineating elements are cylindrical spark counters. The position of the spark in the counter is obtained by a sonic ranging technique.

A trigger of the counters occurs whenever a signal is received from either the front walls of each counter, or the back walls, indicating the passage of a muon through the tanks. The data from the spark counters is fed directly on to magnetic tape, and the tape is scanned by a computer programme to select muon shower events.

The angular distribution obtained by Parker is shown in figure 7.2. The angular acceptance variation of the apparatus has been taken out by him and corrections made for loss of events due to triggering of both walls of the Cerenkov counter by some muons.

Fig. 7.1

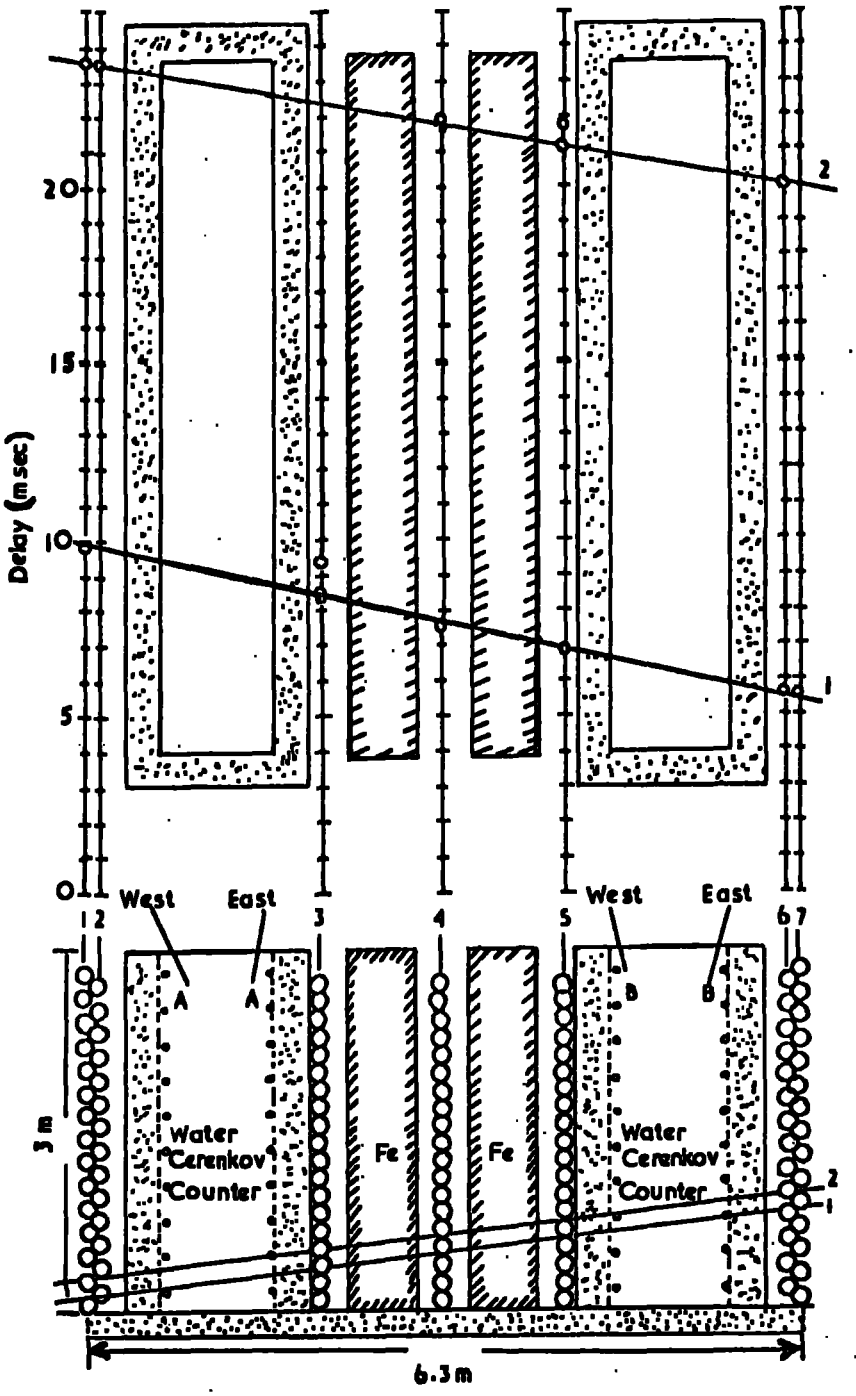

The Utah Prototype Neutrino Detector

Comparison of the present work with that of Parker (1967) Fig. 7.2

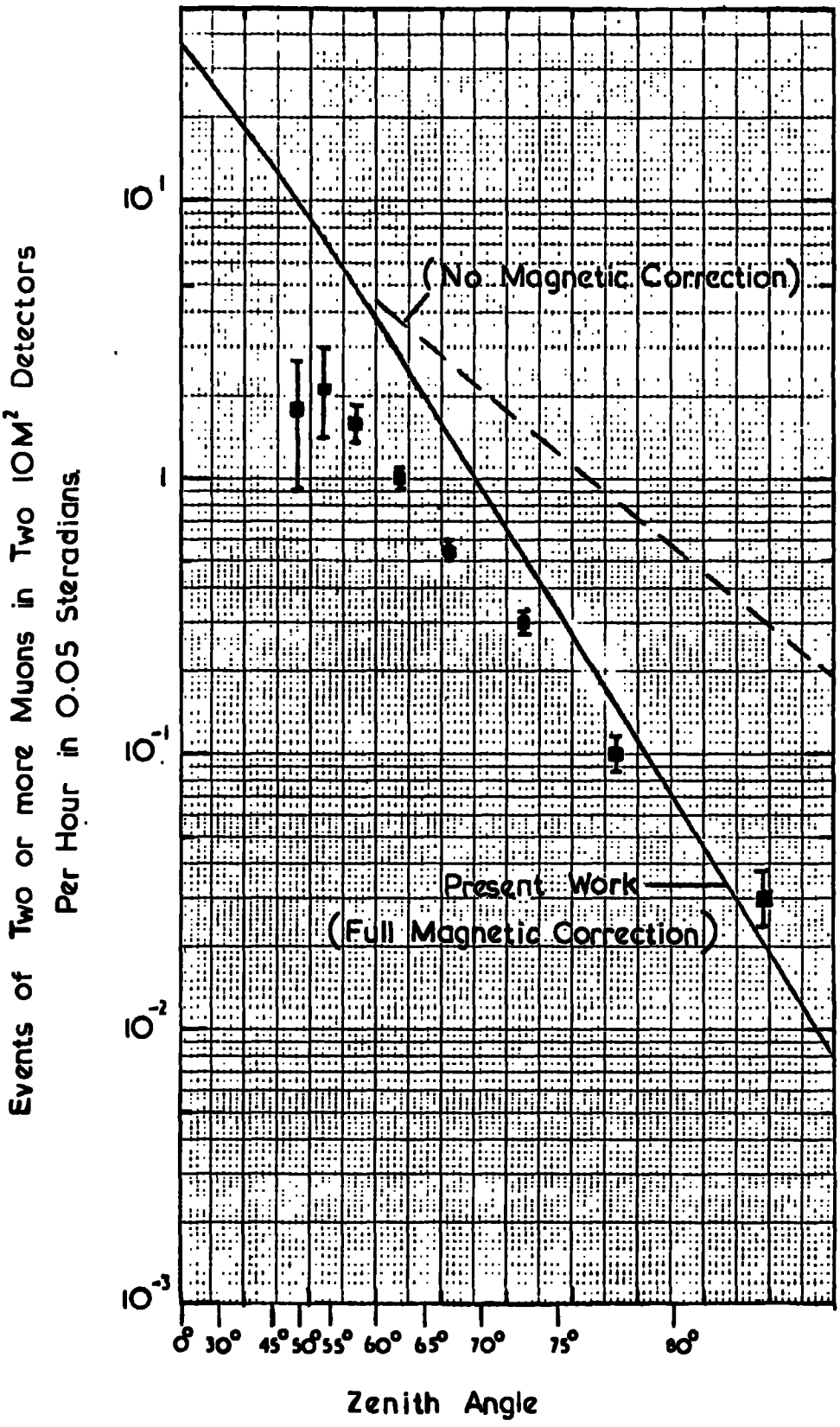

This data was obtained during a time when the absolute acceptance of the apparatus was unknown and was later normalized to an absolute rate obtained from a run carried out at one zenith angle (64^{o}). The reason for this choice is that Parker was interested in making comparison with the results of Sekido (1966), (see next section). Sekido expressed his results in terms of the rate of pairs of muons in 2, 10 square metre detectors. Parkers' apparatus had an overlap area of 10 square metres at 64^{o}.

In making comparison with the present work the theoretical calculations have been used as these represent rather well the angular distribution obtained in the present work. This avoids the dubious preceedure of unfolding the experimental acceptance function to obtain the incident spectrum. The geomagnetic correction has been calculated for the conditions of the Utah experiment and found to be very close to that prevalent at Durham. A small correction has also been made for the energy threshold of the Utah apparatus (2 GeV).

It can be seen that while the spectral shapes are similar, the absolute intensities differ by a factor of 2. The comparison was made by calculating the rate in terms of the units quoted by Sekido (see next section), and using Parkers' own estimate of his absolute intensity given in the same units. An attempt has been made by the author to resolve this discrepancy, which also appears between the results of Sekido and Parker, by re-estimating the efficiency of the

Utah detector from the published scale diagrams and data.

The area used by Parker to calculate his absolute acceptance (10 M^2), refers to the area of the central three layers of spark counters. The Cerenkov detectors lie on either side of these and as they are of comparable size their overlap area must be smaller than this. Since they trigger on single muons the efficiency varies as the overlap area. An estimate of this efficiency, has been made and appears to be 0.73, assuming that the whole volume of the counters is sensitive. However the quoted efficiency is 0.93 so that a discrepancy exists. A more realistic estimate of the Cerenkov counter efficiency, assuming that some path length in the water is essential for triggering, would give an estimated efficiency near 0.5. Such a factor would resolve the discrepancy, however this may be fortuitous, and it has not been possible to consult the author on this.

7.3 Cosmic Ray Telescope No.3.

Sekido (1966) has measured the rate of pairs of cosmic ray muons at angles of 45°, 60° and 75° to the zenith using a pair of air Cerenkov detectors. The major interest in this work was the search for directional anisotropies in muon rich air showers, but good measurements were also obtained on the variation of rate with zenith angle.

Figure 7.3 shows a diagram of one of the pair of telescopes. Each consists of a closed tube, 13 M long and 5.5 M in diameter. The front of each tube is covered with 5 cm of lead, and a large parabolic mirror made up of small convex mirrors is placed at the base of the tube. The focus of the mirror falls on a bank of photomultipliers.

A muon of sufficiently high energy traversing the tube will produce a narrow beam of Cerenkov light. This will be brought to a focus on the bank of photomultipliers. Because the angle of emission is small, about 1.5^{o}, the light will closely follow the path of the muon and the point on the photomultiplier bank at which the light falls, depends only on the angle which the muon makes with the axis, not on the position of the track in the tube. Thus the apparatus behaves like an optical telescope. From the records of which photomultipliers are triggered the angle the muon makes with the axis is derived.

The use of two such telescopes in coincidence in principle enables parallel muons to be selected. In practice, since the variation of detection efficiency across the photomultiplier bank is quantized, and muons in E.A.S. have an average scatter of 3^{o}, a pattern of triggered photomultipliers is demanded which allows for such variations. Inevitably there is some inefficiency in such a system, and recently Sekido (private

Fig. 7.3

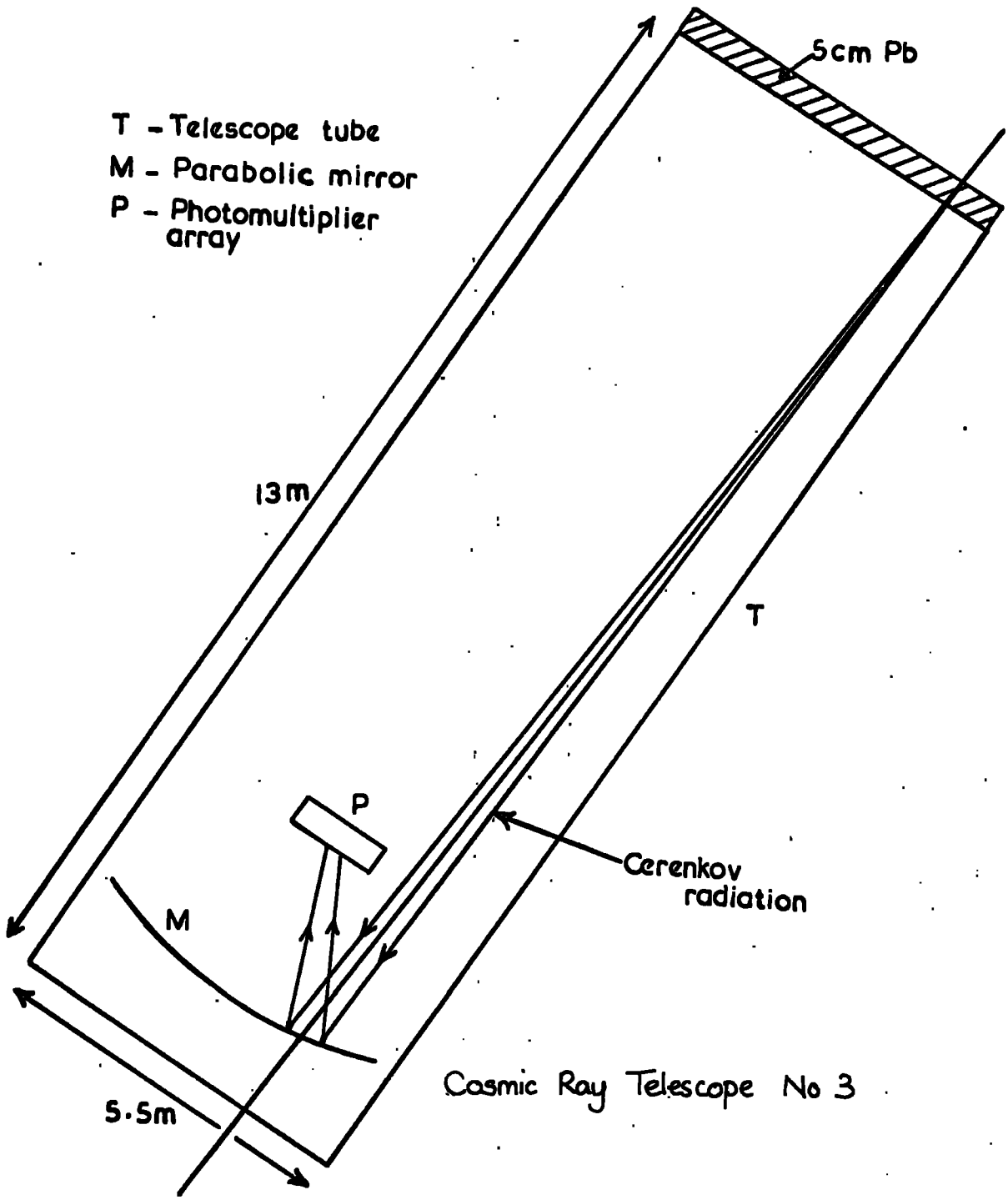

Cosmic Ray Telescope No 3

communication) has given a revised estimate of the absolute efficiency of his apparatus, which is approximately 70% lower than in the original publication (1966). The estimates of the true rate through his apparatus is shown in figure 7.4 together with the predicted rate derived from the present work.

7.4 Comparison with the Present Work

Because the apparatus relies on Cerenkov light the energy threshold for muons, having passed through the lead shield, is 10 GeV. This has a rather small effect at large zenith angles where the mean energy of muons in E.A.S. is high c.f. 16 GeV at 60°. However at 45° Sekidos' smallest zenith angle, an appreciable number of muons are less than 10 GeV. A calculation of the density spectrum of muons $>$ 10 GeV was made using lateral distributions given by De Beer et al. (1966) and using the angular variation derived in the present work. The frequency of at least two muons through Sekidos' apparatus was calculated using his values of area and acceptance. The detector cannot distinguish 2 muons in one telescope from one, so allowance was made for this. The results are given in terms of the rate of pairs of muons detected in two 10 M^2 detectors over 0.05 steradians.

The result is shown in figure 7.4. It can be seen that agreement is good. At large zenith angles a correction has

Fig. 7.4

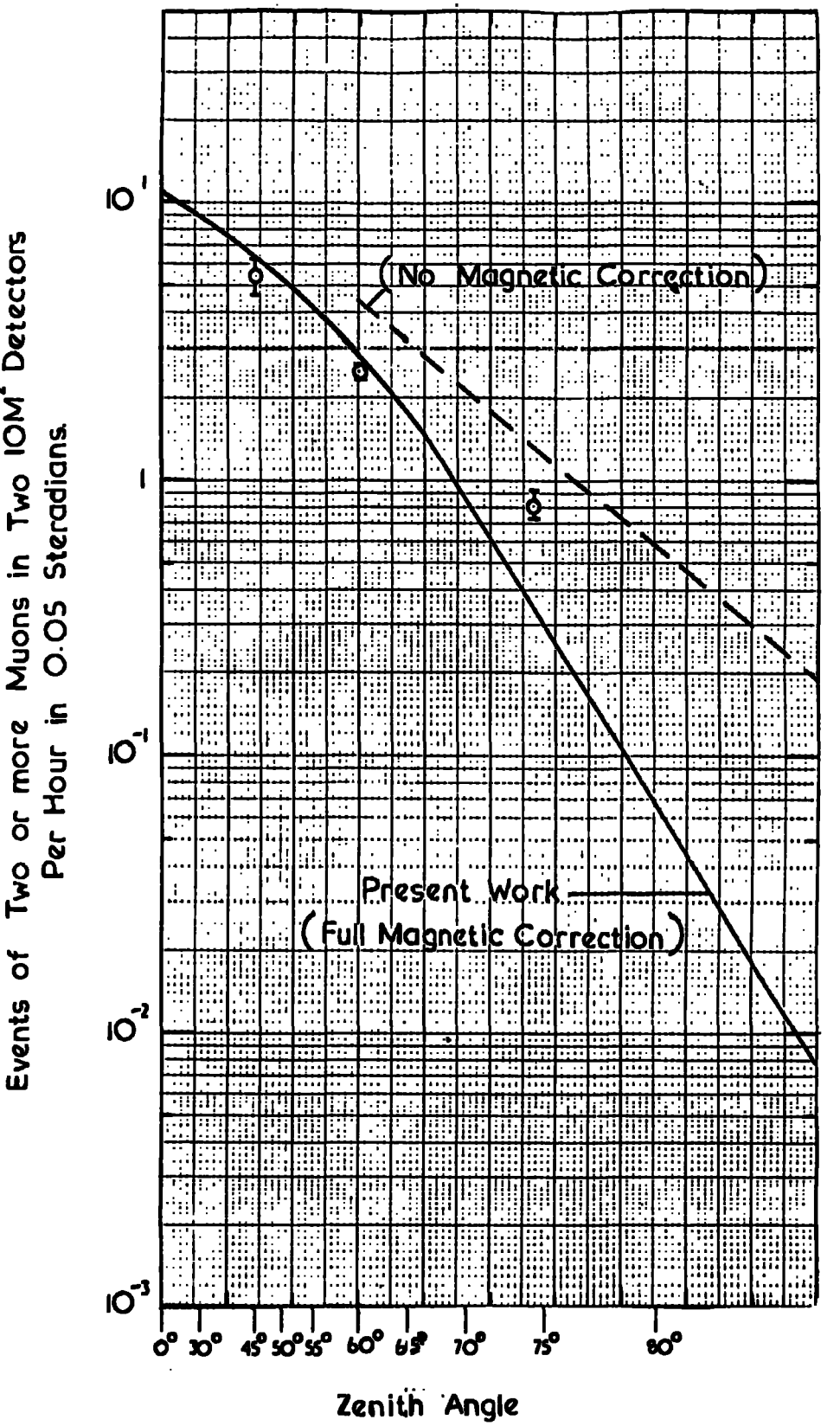

Comparison of the present work with that of Sekido et al (1966)

been made for geomagnetic scattering as before, using the geomagnetic conditions prevalent at Nagoya. However some difference remains at 75^{o}, but this is well within the possible error in the geomagnetic correction. It has been suggested by Parker (1967) that the high value at 75^{o} may be due to triggering of the apparatus by vertical E.A.S. passing transversly through the telescopes.

The agreement between these results and the present work, although not perfect is sufficient to give support to the conclusions expressed in Chapter 5. Also it suggests that the discrepancy between the Utah work and the predictions made from the Durham results may well be due to the factors discussed in 7.2.

7.5 Comparison with the Work of Barton (1968)

Barton (1968) has carried out observations of the vertical flux of groups of muons at a depth of 60 m.w.e. underground. The apparatus consisted of a vertical stack of six 1.12 M^2 scintillation counters interleaved with layers of lead 1.3 cms thick. A further two counters of the same size could be operated in coincidence with the stack at varying distances from it. The use of a lead shield over the counters served to absorb the soft component emerging from the roof of the laboratory.

Muon events were selected on the basis of pulse height

analysis of the scintillator outputs. The rate of such events detected has been expressed in terms of the vertical intensity of muon pairs through a horizontal lamina of area 1 square metre per day, per steradian.

Barton has given a table, in which he collects the results of other workers on underground muon showers, re-interpreting the data where necessary to give the intensity expressed in the above form. This involved the use of the $\cos^4 \theta$ law for the variation in intensity with zenith angle mentioned in Chapter 6.

In order to compare the present work with this data a calculation was carried out, based on the density spectra used in Chapter 6. This gives the intensity of muon pairs of energy greater than 1 GeV in the standard units used by Barton. This calculation depends on an extrapolation of the angular variation law given in Chapter 6 to zero zenith angle which may not be justifiable. However the difference in intensity between 30° and the vertical is small so this should be a second order effect. Calculations have also been carried out for muons of energy greater than 10 GeV.

The results of these two calculations are given in table 7.1 together with the results of Barton, and those of the workers he quotes referring to threshold energies near 10 GeV. It can be seen that agreement is fair, and considering both

the risk of contamination of the experimental results by electrons (none of the work quoted used visual detectors), and possible inaccuracies in the extrapolation of the angular variation some support for the validity of the present work is gained.

Since pairs of muons are involved here the primary energy region is below 10^{15} eV and so no information is available from this work on the composition above this energy. Also, as with other comparisons, the theoretical density spectra have been used as representing rather accurately the present experimental results.

Table 7.1 (after Barton, 1968)

Observers	Depth (m.w.e.)	Energy Threshold (GeV)	Multiplicity	Intensity (m^{-2} day^{-1} st^{-1})
George et al. (1953)	60	12	2	260 ± 20
Kessler & Maze (1957)	65	13	2	32 ± 11
Hunter & Trent (1962)	37	7.4	2	94 ± 8
" "	60	12	2	76 ± 8
Vavilow et al. (1963)	S.L	~ 1	2	56 ± 9
Bingham and Kellerman (1965)	50 cm Pb	11	2	83 ± 19
Barton (1968)	60	12	2	62 ± 14
Present Work (Theoretical Prediction)	-	1	2	94
" "	-	10	2	36

7.6 Comparison with Other Work on the Multiplicity Spectrum

As mentioned in the introduction, data on the multiplicity spectrum of muon showers is sparse. Parker gives the following relative frequencies for multiple muon events corrected for loss of events due to showers triggering both walls of the counters.

Multiplicity	2	3	4
Number	572	24.5	2.3 (1 event)

This extremely steep spectrum is the result of the triggering conditions of the Utah apparatus. The apparatus triggered on single muons, thus no restriction was placed on the recording of pairs of muons and the relative rate is high. With apparatus of the Durham type, where a two-fold coincidence is required the number of pairs triggering the apparatus is much reduced relative to the number of events of higher multiplicities. The precision of the above data does not justify the extensive computations required to obtain a direct comparison.

Barton (1968) has quoted an observed multiplicity spectrum with which comparison may be made since the triggering conditions are similar to those of the Durham apparatus. The spectrum quoted is based on events recorded on a two-fold trigger, the

multiplicity being measured in the stack. There may be some ambiguity in the measurement of multiplicity based as it is on pulse heights in the scintillator stack. The exponent quoted for the differential multiplicity spectrum is -2.6 ± 0.2.

The exponent of the Durham multiplicity spectrum varies somewhat with angle, steepening as the zenith angle increases so that lumping of the data together is not permissible.

Comparison may be made with the theoretical multiplicity spectrum for 30° zenith angle, this being the smallest angle for which calculations have been done. The exponent here is -2.4, within the error limits of Bartons' figure. In fact the exponent should be larger than this, because of the steeper lateral distribution for 10 GeV muons, and hence the steeper density spectrum. Thus it would seem that there is reasonable agreement between the present work and that of Barton.

7.7 Conclusions

Unfortunately the comparisons made above do not enable direct checking of the Durham multiplicity data with sufficient precision to support the deductions on the mass composition of the primaries made in Chapter 6. Thus this data must stand on its own.

With regard to the data on pairs of muons it appears that there is reasonable agreement between the present work, and that of Sekido and Barton in absolute terms. The spectral shape of the angular variation agrees with that of Parker, but an absolute discrepancy remains of a factor of 2. This is of importance because of the excellent statistics obtained in this experiment. The absolute intensity does rely on a single measurement however and may be subject to the possible inefficiencies pointed out in 7.2. Even if this discrepancy remains, the present work is supported by its agreement with that of Sekido and of Barton.

CHAPTER 8

Conclusions.

8.1 Introduction

The object of the present work was to attempt a study of the primary mass composition in the energy region 10^{14} - 10^{17} eV. From the results of this study it was expected that a test could be made of the hypothesis that the change in exponent of the primary energy spectrum at about 10^{15} eV was due to a rigidity cut off imposed on the primary flux.

The firmness with which conclusions can be drawn is strongly dependent on the various assumptions used throughout the work. This is because the relationships between the energy and mass of the primary nucleus and the parameters of the E.A.S. measured at sea-level, are not straightforward, and depend on many factors which cannot be defined uniquely. Thus in order to give due weight to the present conclusions a consideration of the various factors involved is necessary.

8.2 The validity of the E.A.S. model

In the sense that all E.A.S. models involve assumptions which cannot be tested independently there is no ultimate

justification for their use. However, a certain amount of support for a particular model is forthcoming from a consideration of a number of points.

The E.A.S. model used in the present work is conservative in that the assumptions used have values which are smooth extrapolations of trends observed at machine energies. As such the model must be regarded as reasonable. Futher support for the model may be found from the agreement of predictions made with experimental observations on certain parameters of E.A.S.

The energy spectrum of muons predicted by the model is found to agree with experimental measurements at all zenith angles. This shows the ability of the model to predict correctly the longitudinal development of E.A.S. There is not such good agreement with experimental determinations of the lateral distribution of muons, especially at energies above 40 GeV. For all energy thresholds it appears that within 10 metres of the shower core an excess of muons is predicted. This has been ascribed by the authors (De Beer et al., 1966), partly to experimental errors in core location, and partly to a restriction on transverse momentum transfers less than 0.1 GeV/c.

At muon energies greater than 40 GeV there is a significant excess of experiment over theory at distances

approaching 100 metres. However the model predicts, with some success, the lateral distribution of muons greater than 1 GeV, in the region 10 - 500 metres from the shower core, and in the present work, the density spectrum of such muons is used, which is sensitive to the form of the lateral distribution only in the region 50 - 150 metres from the core. In addition it can be stated that fluctuations in the lateral distribution will have a minimal effect because these are least in the above mentioned radial distance region.

The agreement between the predicted angular variation in the present work and the experimental observations support the model in two aspects. The fact that the angular variations agree, suggests that the predictions at different zenith angles are successful. The agreement in absolute intensities gives support to the model in a vital aspect. The use of the vertical electron size spectrum as a datum, working back to the primary spectrum, and using this to predict the density spectra of muons at the various zenith angles was expected to reduce the sensitivity of the results to model parameters. The validity of such a step depends on the models' ability to relate correctly the behaviour of the vertical electron component and the muon component at all zenith angles. The agreement in intensity supports this aspect of the model. This comment applies to primary energies in the region 10^{14} -

10^{15} eV.

Thus it would appear that although the model has some limitations, for the particular purpose of the present work, where the properties of the bulk of the muons in E.A.S. are considered, the tests described above show that the model behaves in a satisfactory manner.

8.3 Consideration of the Effect of Variations in E.A.S. Model Parameters.

It is clear that variations in model parameters could in principle result in a reversal of the tentative conclusions drawn in Chapter 6, by altering the predicted density spectra, even though such variations may have no a priori justification. Of the parameters used the most sensitive are the multiplicity law and the mean transverse momentum (P_t). The effect of using a different multiplicity law has been considered in Chapter 6 where it is shown that the use of an $E^{\frac{1}{2}}$ law, gives poor agreement with both composition models (A & B) the agreement being worse for spectrum B where the mean mass of the primaries increases beyond 10^{15} eV.

It could be supposed that if P_t were allowed to increase rather rapidly with primary energy, the corresponding decrease in the predicted density spectra would reverse the conclusions drawn in Chapter 6 and favour spectrum B. However there is experimental evidence from the present work (described fully

in appendix 2) which makes such an increase unlikely.

If other parameters are assumed to be fixed, then any differences between experiment and theory may be ascribed to changes in P_t. The angular spectrum (figure 6.8) shows remarkable agreement at all angles although the mean muon energy varies from approximately 5 GeV at 30^o to 70 GeV at 70^o and as a result the mean energy of the interactions producing their parent pions increases from 200 to 2000 GeV. This implies that P_t remains nearly constant at 0.4 GeV/c over this range of interaction energies. Furthermore, the median primary energy remains nearly constant at approximately 10^{14} eV.

If the multiplicity data is considered in the same way it is found that the mean muon energy and hence the interaction energy increases with multiplicity, in this case however the median primary energy also increases, the range of interaction energies covered being the same. Thus, if an increase in P_t with median primary energy is postulated in order to give agreement with spectrum B, the variation of P_t with interaction energy does not agree with that derived from the angular data. Thus an inconsistancy arises within the experimental data if heavy primaries and an increasing P_t are assumed.

Table 8.1 shows the present work and other muon studies

Table 8.1 Muon Studies

(i) The lateral distribution of muons in E.A.S. threshold energy 40 GeV, primary energy approximately 10^{17} eV. (Earnshaw et al. 1968, Orford and Turver 1968)

Composition	$\bar{A}$	Multiplicity Law	Interaction Energy (eV)	P_t (GeV/c)	Comments
(1)* protons	1	$E^{\frac{1}{4}}$	$5\ 10^{10}$-$5\ 10^{12}$	0.4-1.0	Selection bias
			" "	0.6-3.0	No selection bias
(2) heavies	56	$E^{\frac{1}{4}}$	" "	0.4-0.6	Turver 1969 (private communication).
(3)* protons	1	$E^{\frac{1}{2}}$	" "	0.4-0.6	
(4) heavies	10-20	$E^{\frac{1}{2}}$	" "	0.4	Orford and Turver (1968)

*Interpretation by De Beer et al. (1968b) and Wdowczyk and Wolfendale 1968 (private communication)

De Beer, J. et al. 1968(b) Can. J. Phys. 46, S737

Earnshaw J., et al., 1968 Can. J. Phys. 46, S122.

(ii) Muon showers deep underground, threshold energy (S.L.) 1000 GeV, primary energy 10^{14} - 10^{16} eV.

(Porter and Stenerson, 1969, Interpretation by Adcock et al. 1969)

Composition	$\bar{A}$	Multiplicity Law	Interaction Energy (eV)	P_t (GeV/c)	Comments
(5) protons spectrum A (modified)*		$E^{\frac{1}{4}}$	10^{14} - 10^{16}	0.5-0.8	*Slower change to protons.
(6) heavies spectrum B		$E^{\frac{1}{4}}$	" "	required value of P_t increases progressively ↓	
(7) protons spectrum A (modified)*		$E^{\frac{1}{2}}$	" "		*faster change to protons
(8) heavies spectrum B		$E^{\frac{1}{2}}$	" "		

Porter, L.G. and Stenerson, R.O. 1969. J. Phys. A, 2, 374.

Adcock, C., Wolfendale, A.W., Wdowczyk, J., J. Phys. A. 2 (in the press).

(iii) Present Work, threshold energy 1 GeV, primary energy 10^{14} - 10^{17} eV

Composition	$\bar{A}$	Multiplicity Law	Interaction Energy (eV)	P_t (GeV/c)	Comments
(9) protons spectrum A		$E^{\frac{1}{4}}$	10^{11} - 10^{12}	0.4	
(10) heavies spectrum A		$E^{\frac{1}{4}}$	" "	0.4-0.8	prohibited by experimental measurements of P_t variation.
(11) protons spectrum A		$E^{\frac{1}{2}}$	" "	< 0.4	at variance with machine measurements
(12) heavies spectrum B		$E^{\frac{1}{2}}$	" "	< 0.4	

which draw conclusions on the primary mass. The effect of different combinations of multiplicity law and P_t on the derived composition is shown. The primary energy and muon threshold energy varies between the different experiments.

There is no general consistency among the three sets of results. (ii) and (iii) may be regarded as not inconsistent since the interaction energies do not overlap thus these suggest a favoured combination of $E^{\frac{1}{4}}$ and $P_t = 0.4$ rising very slowly with interaction energy. (i) is inconsistent with this because the interaction energy range is the same as in (iii), however the primary energy is higher in (i) and also muons at large distances from the core play a large part. It may be possible that these muons have some anomaly in their production which does not appear in the muons closer to the core, important in case (iii). General conclusions are not possible, except to note that while several combinations of model parameters and primary mass appear possible in the case of high primary energies, and high muon threshold energies, one only seems to give agreement in the present work where low energy thresholds are used at moderate primary energies.

The above considerations show that conclusions on the primary mass are sensitive to the model parameters and that

differing combinations of these give different conclusions as to the mass composition. In the case of the present work the combination of parameters appears to be unique this being dependent on the validity of the present analysis of the data.

8.4 The Effect of the Sea-Level Size Spectrum and Experimental Errors in the Present Work.

Since the primary spectra A and B depend on the adopted sea-level size spectrum any variation on this could alter the conclusions drawn. In the derivation of the spectrum used as a datum no provision was made for inclusion of such variation and a mean spectrum was taken. It is possible that some bias is present and a change in the adopted size spectrum would be reflected in a proportional change in the intensity of the predicted density spectrum. In particular a decrease of a factor of 5 in the intensity at 10^6 particles would reverse the present conclusions, giving a result in favour of heavy primaries. While not impossible such a large decrease in intensity, particularly at this size where many experimental measurements are used seems unlikely.

Experimental errors in the present work which could reverse the conclusion are those which tend to cause a loss of high multiplicity events. From the considerations given in Chapter 4 this would seem unlikely, any errors tending

to enhance multiplicity, for example the inclusion of knock-on electrons and unassociated muons. Also, any inefficiency in the apparatus would tend to decrease with increasing multiplicity. Thus it would appear that any errors which are known at present would tend to bias the conclusion toward spectrum B.

8.5 Comparison of the Conclusions of the Present Work with those of other E.A.S. Experimental Studies.

The conclusion to be drawn from the present work, subject to the limitations discussed above is that primary spectrum A is favoured over primary spectrum B. Thus the present experimental evidence is against the view that the mean mass of the primaries increases beyond 10^{15} eV in accordance with the rigidity modulation hypothesis. In terms of origin this is consistent with production of energetic cosmic rays in a region where the radiation field is intense, and relativistic nuclei are quickly fragmented by photo-disintegration (Zatsepin & Kuzmin, 1968, Kinsey, 1969).

A comparison of this conclusion with those of other E.A.S. workers is shown in table 8.2. In the case of muon studies already presented in table 8.1 the prefered interpretations of the authors have been given.

A general conclusion is not possible from this table as

Table 8.2 E.A.S. Studies

Authors	Method	Primary Energy (eV)	Conclusions	Comments
(1) Maze et al., 1969(private communication)	Muon/ electron ratio	10^{15}-10^{16}	Rapid modulation within the energy range from normal to heavy, then to protons	The change to heavies is less certain than the change to protons
(2) Chatterjee, 1964	Muons and hadrons in E.A.S.	10^{14}-10^{16}	Change from heavies to protons at approximately 10^{15} eV.	
(3) Swinson & Prescot 1965	Electron density spectrum	$< 10^{15}$	Energy/ nucleon cut off at 10^{15} eV.	
(4) Linsley & Scarsi, 1962	Fluctuations (and shower development)	$>10^{17}$	Pure mass composition (probably protons).	
(5) Toyoda et al. 1966	Fluctuations	$>10^{17}$	"	

Authors	Method	Primary Energy (eV)	Conclusions	Comments
(6) Bray et al.	Multiple Cores	10^{15}	Rigidity cut off at 10^{15} eV	Doubt cast on conclusions, notably by (7)
(7) Samorski et al. 1969	Multiple Cores	10^{15}	Multiple cores do not reflect primary mass.	
(8) Adcock et al., 1968	Fluctuations and muon/electron ratio	10^{14}-10^{18}	Test of hypothesis (6) inconclusive with present statistics	Theoretical analysis and comparison with experiment
(9) Orford & Turver, 1968	Muon lateral distribution	10^{17}	Mean Mass 10-20	$E^{\frac{1}{2}}$ multiplicity law
(10) Porter & Stenerson 1969	Muon showers deep underground	10^{14}-10^{16}	Slow change to protons near 10^{15} eV	Slow increase in P_t

Analysis by Adcock et al. 1969, 1970

Authors	Method	Primary Energy (eV)	Conclusions	Comments
(11) Present Work	Muon showers at large Zenith angles	10^{14}-10^{17}	Change to protons above 10^{15} eV (or normal composition throughout)*	*Cannot be ruled out with the present analysis

a wide divergence exists between the conclusions of the various workers. Entries 1, 2, 4, 5 and 10 are broadly consistent with the present work, 3, 6, and 9 are inconsistent, the remainder being inconclusive or consistent with either.

Acknowledgments

The author is grateful to Professor G. D. Rochester F.R.S. for provision of facilities for this work and for his interest in it.

The help and guidance of Dr. M. G. Thompson throughout the period of the work is acknowledged with gratitude. Professor A. W. Wolfendale is thanked for much good advice on all aspects of the work.

Dr. B. Holyoak and Dr. J. Wdowczyk are thanked for useful discussions as are other past and present members of the cosmic ray group especially Dr. K. E. Turver, Dr. I. W. Rogers, Mr. C. Adcock and Mr. D. Alexander.

Professor Y. Sekido and Dr. J. L. Parker are thanked for their useful correspondence.

The technical staff of the Physics Department are thanked for their assistance in construction of the apparatus especially Mr. W. Leslie and Mr. E. Lincoln. Particular thanks are due to Miss P. A. Wallace for her consciencious and accurate execution of many calculations.

Mrs. E. Lincoln is thanked for her typing of this thesis.

Appendix 1

The Electron Component at Large Zenith Angles.

During preliminary runs with the apparatus, the electron component at large zenith angles was found to be more intense than expected. Early measurements on the electron density spectrum have been published in Alexander et al., 1968. The work to be considered here refers to data on these showers obtained during a sensitive time of 800 hours, with the apparatus arranged as shown in figure (1). Events were selected which showed clear evidence of a core in one of the central flash tube trays. The number of particles observed in the rest of the array was recorded together with the mean zenith angle of the particles. The angular distribution of the events, from the South (unshielded) and from the North (shielded with 1.5 radiation lengths of iron), is shown in figure (2).

Because the expected number of ordinary E.A.S. at large Zenith angles with an appreciable electron content, is small, It is to be expected that these events are due to electromagnetic interactions of muons. This is borne out by the angular spectrum which shows an increase at very large zenith angles, which follows that in the muon energy spectrum at large zenith angles due to enhanced pion decay.

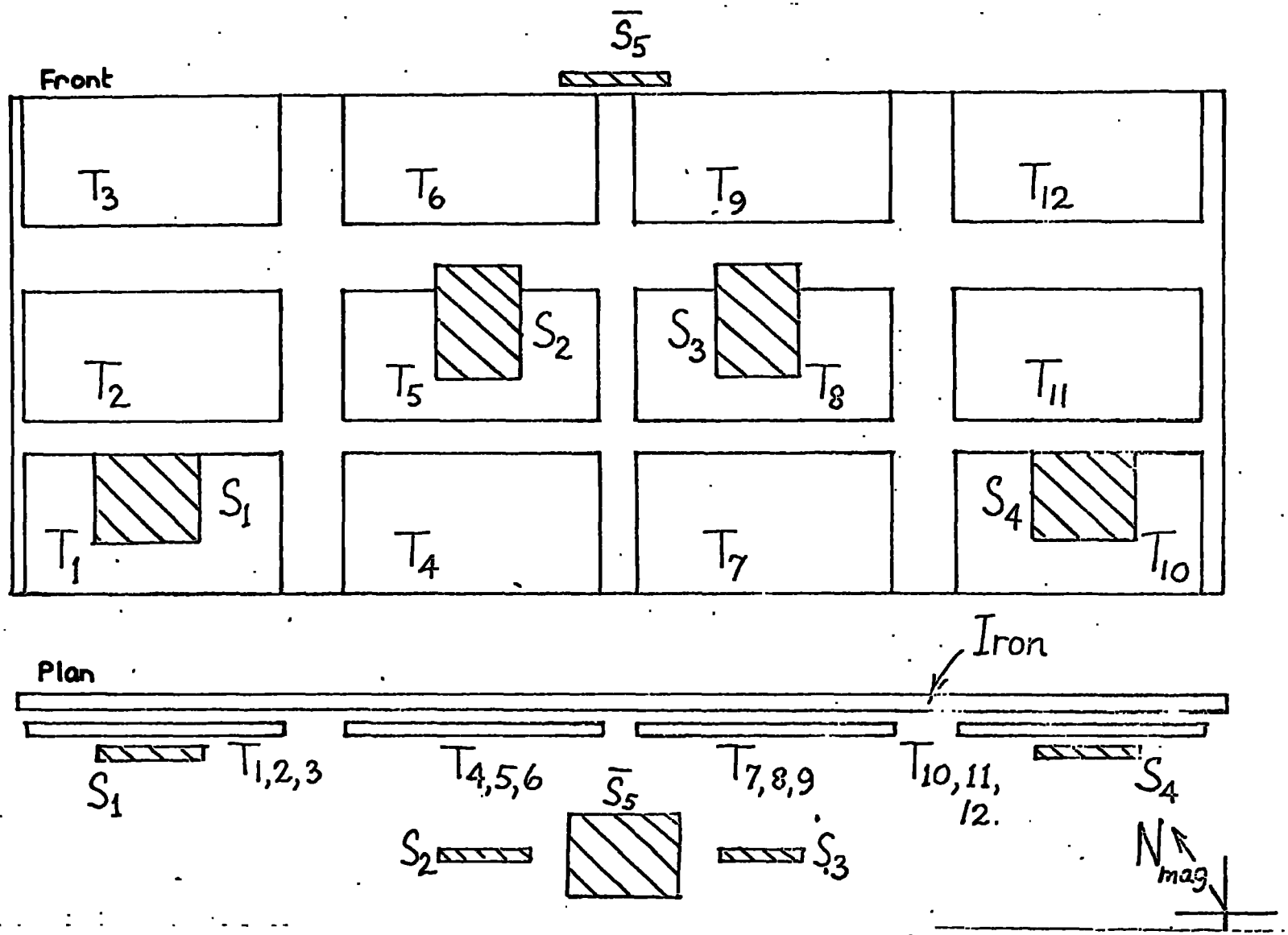

Fig (1) The apparatus.

Fig.(2) Angular distribution of detected events

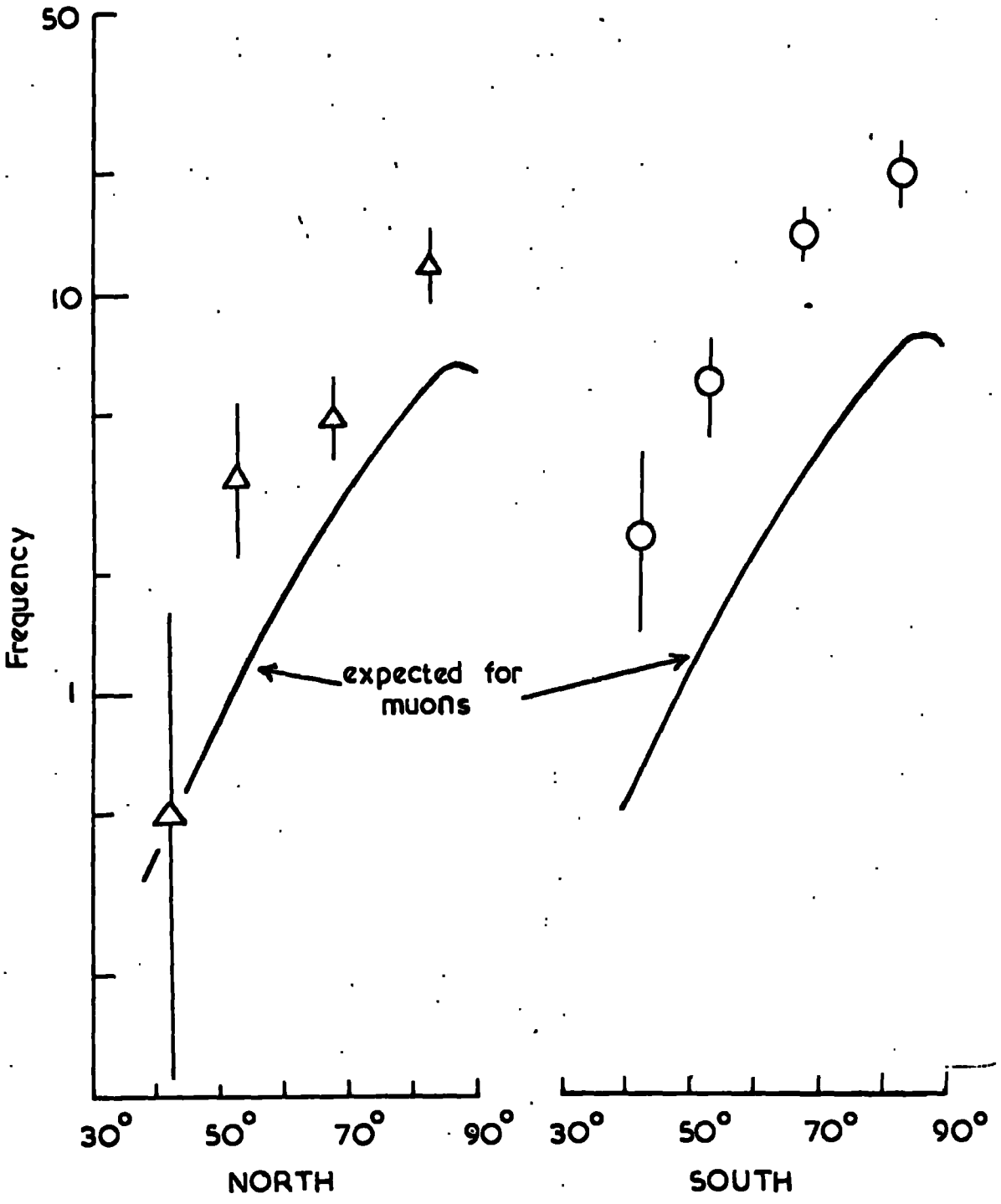

Accordingly calculations were carried out of the integral frequency of such showers to be expected due to muon bremstrahlung. (Knock on effects were considered, but are small, as are those of pair-production). The integral size spectrum produced was found to agree with that calculated by Matano et al., 1968 in the region where the two calculations overlap (above 10^3 particles). The present calculations covered a size range of 80 to 10^4 particles.

In order to estimate the incident shower size of the present results use was made of the lateral distribution functions of Nishimura and Kamata 1950, 1951, 1952 for pure electromagnetic cascades. The integration of this function over the array was compared with the number of particles actually observed and in this way the shower size was estimated.

Of great importance is the fact that the age parameter of the shower varies with radial distance. The region of the shower within 10 metres of the core developes quickly and the density reaches a maximum (s = 1.0) when the age parameter for the rest of the shower is about 0.6. This means that an array of small dimensions, like the present apparatus, detects showers while, in terms of the bulk of the particles, they are still young. Thus the size deter-

mined above is smaller than the size at maximum development by a factor of between 1.5 and 2. This factor has to be allowed for when comparison is made with theory. All these remarks apply only to pure electromagnetic cascades where there is no nuclear active core to distort the lateral distribution.

In order to compare the derived size spectrum with the theoretical calculations the triggering probability has to be calculated. Unlike a conventional E.A.S. array this is very small for many of the detected showers. The probability of detection, by the 4 fold coincidence scintillator arrangement, was calculated for showers whose axes fell in the central flash tube trays, based on the expected particle densities. Examination of the film records of the events however showed that in many events at least one of the scintillators was triggered by a particle which did not appear in the flash tube tray behind. A fraction of these may be due to the triggering particle passing through a gap between the trays, however it appears that many could be explained by the photons in the electromagnetic cascade. Estimates of the photon intensity based on the ratio given by Greisen, 1956, do not give a sufficient flux of photons, however these were for showers at maximum development and it may be that the flux of photons in the showers observed

in the present apparatus is higher than this.

Estimates of the triggering probability were prepared based on the enhanced photon flux derived from the examination of the experimental records. These differ from those based on the normal definition of size only in the region below 300 particles.

In this way the incident size spectrum was estimated from the experimental data. This is shown in figure (13.) compared with the experimental results of Matano et al. (1968b) (marked I.N.S.). It is clear that there is a marked discrepancy between theory and experiment. This applies both to the I.N.S. results and the Durham results. The fact that the two groups agree both in the experimental results, and the theoretical calculations, suggest that this excess is genuine. It has been shown by Etim & Picchi (1969) that the contribution from the photo-nuclear interaction of muons is small with a cross section of 500 micro-barns, and it appears that a cross section of 20 m.b. is required to explain the excess (Alexander et al., 1970). Thus no explaination of this result is forthcoming at present, however the Kiel group (Trumper, 1969 private communication) are in the process of operating apparatus, similar to that at Durham and confirmation of these results may be obtained in the near future.

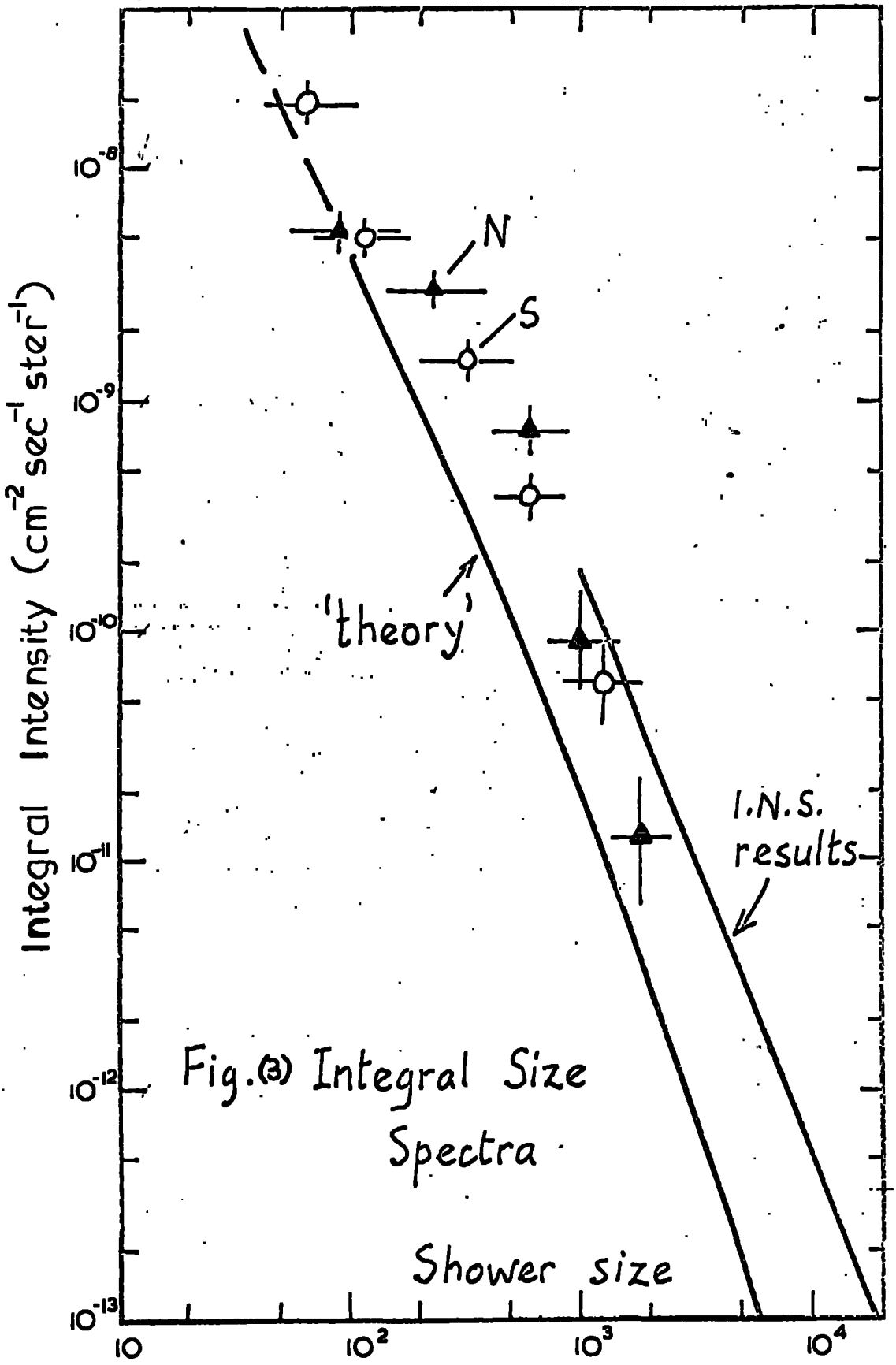

Fig.(3) Integral Size Spectra

APPENDIX 2

1. The Mean Energy of the Muons Observed in the Apparatus.

The mean energy of muons in E.A.S. is expected to be higher than that of single muons. It has not been possible to measure the energy of muons in individual events, but by dividing the events into a few angular cells it has been possible to obtain an estimate of the mean energy of these muons from their probability of interaction in the iron.

Each triggering particle passes through two seperate layers of iron and is observed emerging from each. Non triggering particles pass through one layer only. The frequency of observation of electron showers produced by the muons emerging from the iron has been determined for 3 angular cells and multiplicity cells of 2, 3 & 4, $\geqslant 5$ muons.

The conversion from frequency of production of showers to mean energy has been done using the observations of Said (1966) on the frequency of production of such showers in a solid iron spectrograph by muons of known momentum. Corrections were made to convert from these results, effectively for an infinite thickness of iron, to the present case of 4.5 radiation lengths, varying with angle. In this way the

mean energy of the muons observed was calculated.

A comparison is made in figure 1 between the experimentally determined mean energies and a theoretical prediction based on the De Beer et al. E.A.S. model. The precision of the experimental points is not good, but there is general agreement with the theory. Thus the observed particles behave as muons in E.A.S.

2. The Effective P_t as a Function of Interaction Energy

If all other parameters are assumed to be fixed then differences between theory and experiment may be ascribed to differences in P_t. The value of P_t, chosen to give agreement between theory and experiment may be defined as the effective P_t.

The mean energy of the muons; determined experimentally or from theoretical analysis, may be used to estimate the energy of the interactions producing their parent pions. Osborne (1966) gives a relation between the interaction energy E^*_π and the mean energy of the pions produced, in which allowance for fluctuations in inelasticity is made.

$$E^*_\pi = 5{\cdot}8\ \bar{E}_\pi^{\,1{\cdot}27}$$

The energy of the muons produced is on average $0.76\ \bar{E}_\pi$ so that E^*_π may be written in terms of $\bar{E}_\mu$ as

$$E^*_\pi = 5{\cdot}8\ (\bar{E}_\mu / 0{\cdot}76)^{1{\cdot}27}$$

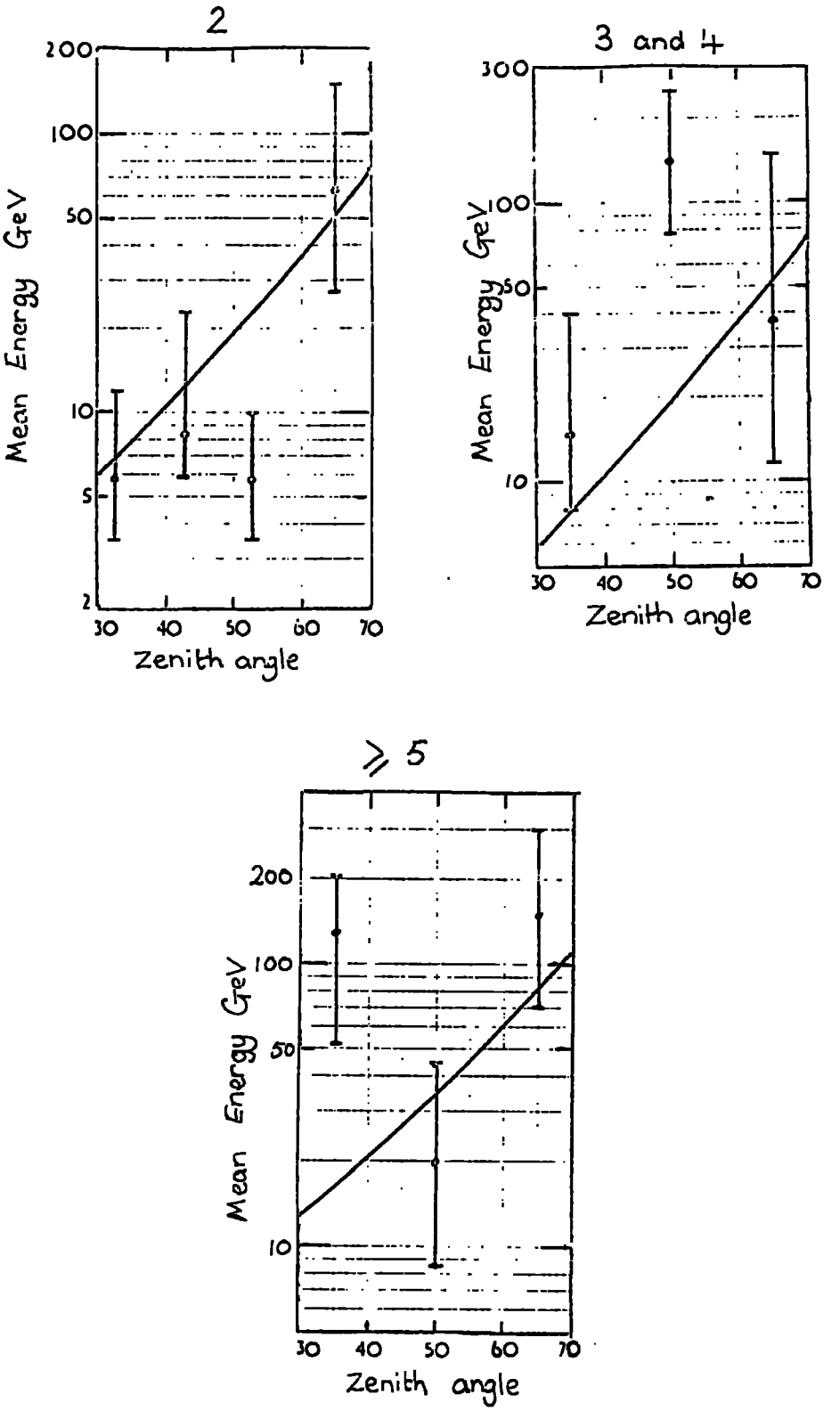

Fig. 1. Mean energy of muons in E.A.S.

In this way E_π^* has been estimated for each angular cell, the effective P_t derived from the difference between theory and experiment in the angular distribution, and plotted against E_π^* (figure 2).

Also shown in this figure are points in which P_t and E_π^* are derived from the multiplicity data in the same way, assuming primary spectrum A. The agreement between the two analyses effectively precludes the use of P_t increasing with primary energy to give agreement with primary spectrum B.

The apparent slow rise in P_t with E_π^* is in agreement with that derived by De Beer et al. (1968b) from a world survey of measurements.

3. The Pressure Coefficient of the Observed Events.

The pressure coefficient of the observed events is an indication of the rate of attenuation of the showers observed. The variation of rate of selected events with atmospheric pressure is shown in figure 3. The pressure coefficient may be defined by the relation

$$\text{Rate} = A\, e^{-\alpha \Delta p}$$

The result of a least squares fit to the data gives a value of $\alpha = 0{\cdot}04$. This small value is entirely

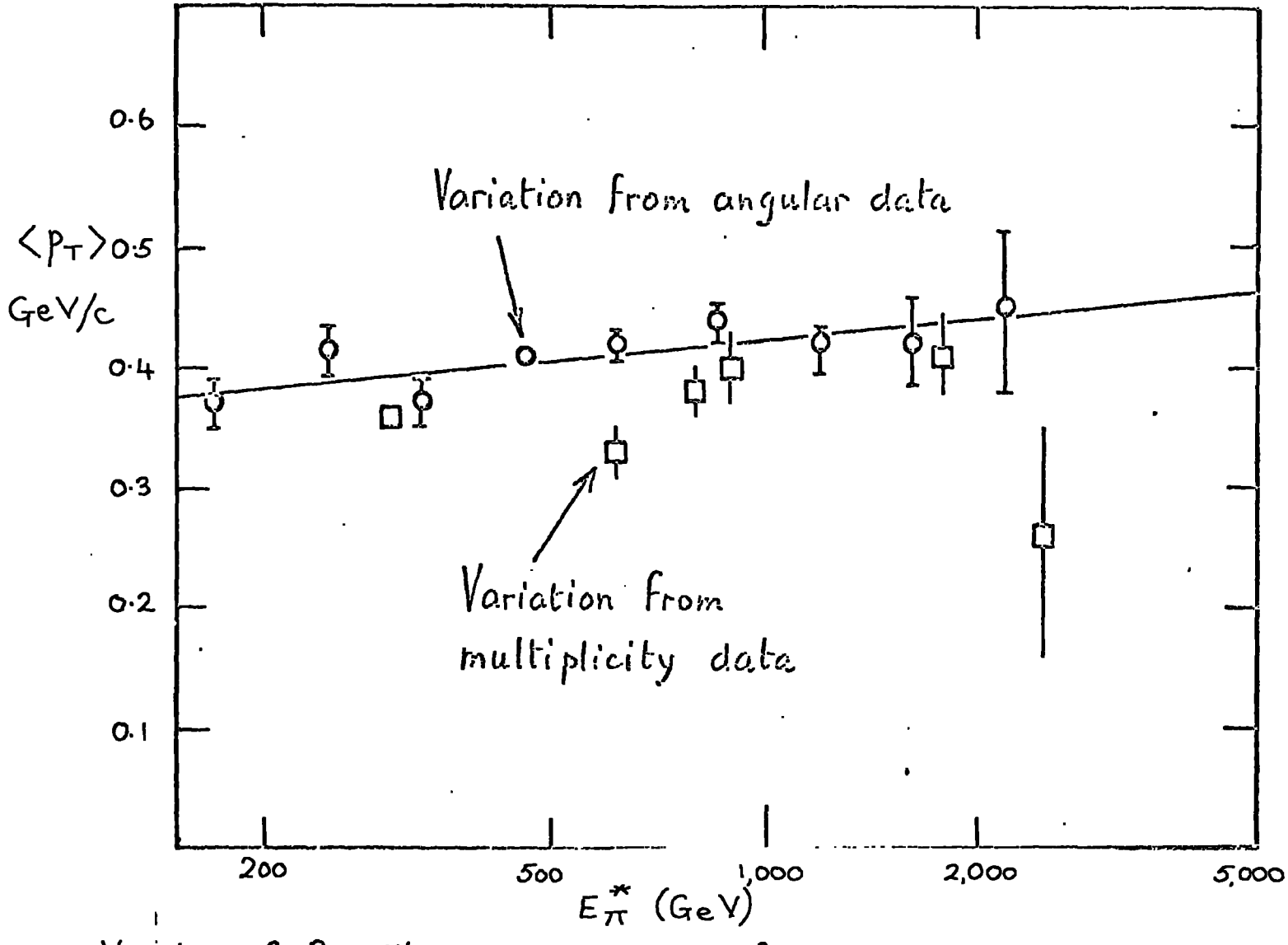

Fig 2. Variation of P_t with interaction energy from angular and multiplicity data.

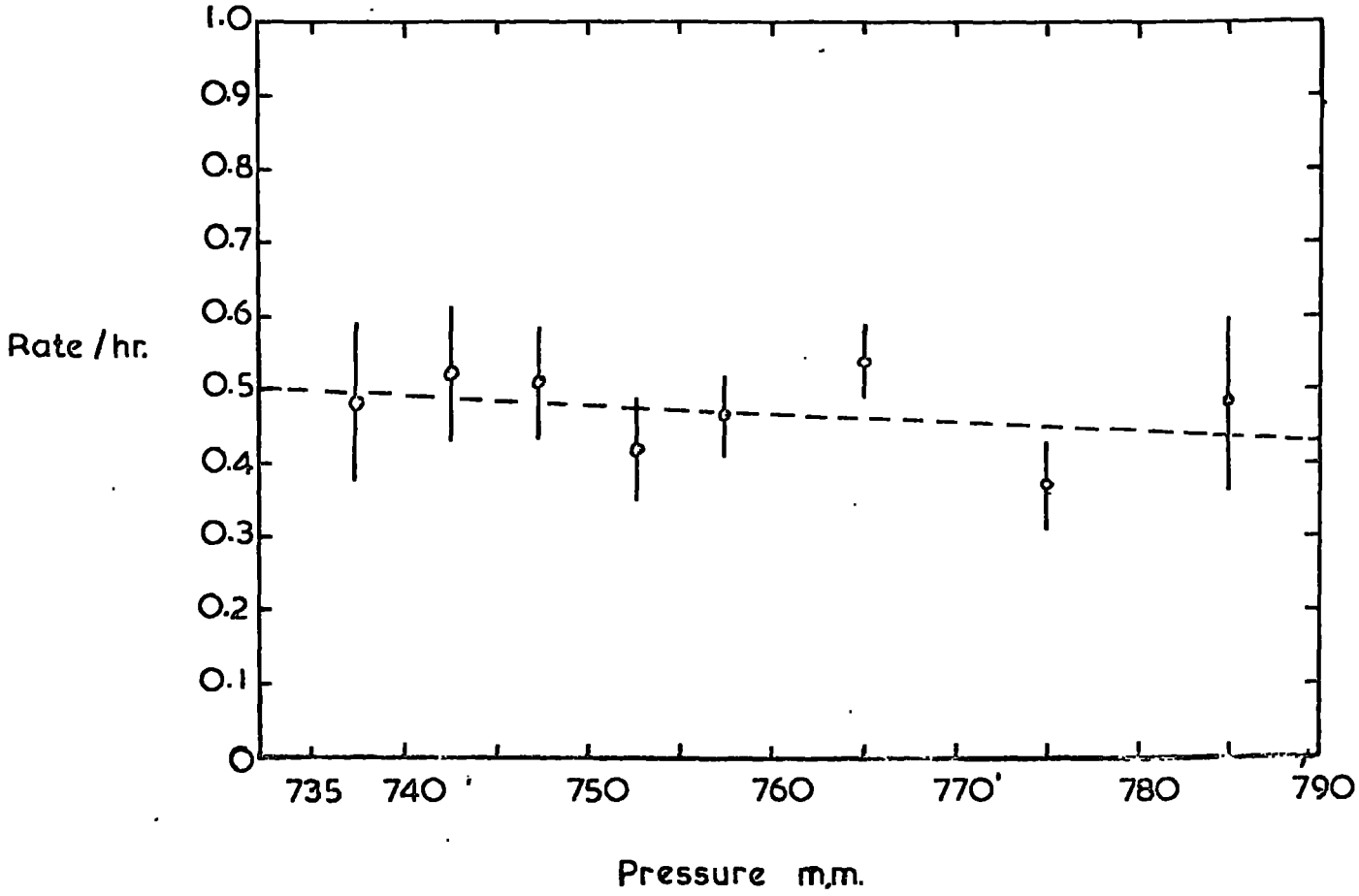

Fig 3. Pressure coefficient of muon showers.

consistent with the observed events being due to the muon component of E.A.S., as muons are attenuated slowly in the atmosphere.

4. The Distribution in Sidereal Time of the Observed Events.

Because there has been some interest in celestial anisotropies of muon triggered E.A.S. in the past (Sekido et al., 1966) a plot of the observed events in terms of sidereal time is of interest. The celestial coordinates of the events have also been determined but a meaningful result is difficult to obtain because the probability of detection for the showers is a complex function of angle.

The distribution in sidereal time is shown in figure 4, it is expressed in terms of observed rate/predicted rate. Equal time was not spent scanning equal intervals of sidereal time due to the uneven running time of the detector, so the distribution in sidereal time was first obtained. (The sidereal time being derived from the date and time of the event obtained from the film records). The predicted distribution in sidereal time was then obtained by folding in the mean rate with the total running time in each cell of sidereal time, and the ratio of the two found. No significant deviation of the ratio from unity is observed. This is to be expected since the median primary energy is less than 10^{15} eV.

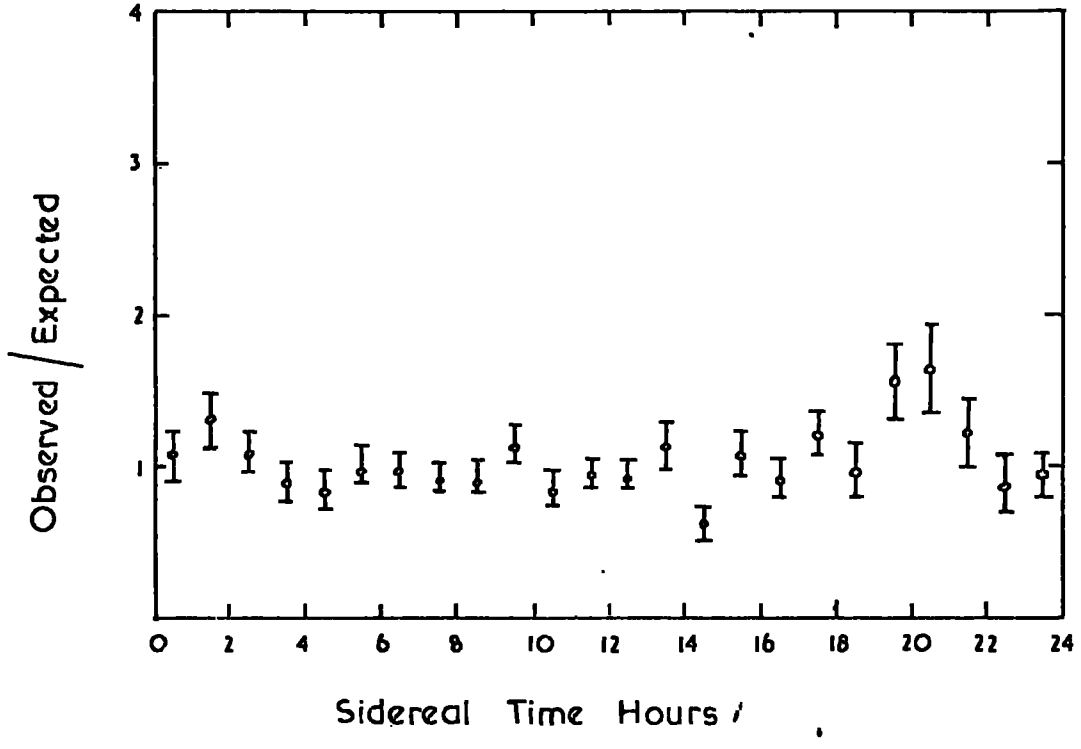

Fig 4. Distribution of events in Sidereal Ti

References for Appendix 1 and Appendix 2

Alexander, D., Thompson, M.G., Turner, M.J.L., Woldendale, A.W., Proc. 11th Int. Conf. Budapest.

Etim, E., and Picchi, P., 1969, Nuovo Cim., 1, 453

Greisen, K., 1956 Progress in Elementary Particles and Cosmic Ray Physics III. Ed. by Wilson and Wouthuysen, North Holland Publ. Co. Amsterdam.

Matano, T., et al. 1968. Can. J. Phys. 46, S369

Nishimura, J. and Kamata, K., Prog. Theor. Phys. Osaka 5, 899, 1950. Prog. Theor. Phys. Osaka 6, 628 1951 Prog. Theor. Phys. Osaka 7, 185 1952.

Osborne, J., 1966 Ph.D. Thesis. Univ. of Durham.

Said, S.S., 1966 Ph.D Thesis. Univ. of Durham.

References

Adcock, C., De Beer, J.F., Oda, H., Wdowczyk, J., Wolfendale, A.W., 1968 J. Phys. A. 1 82

Alexander, D., Holyoak, B., Thompson, M.G., Turner, M.J.L., 1968 Proc. 10th Int. Conf. on Cosmic Rays, Calgary, 1967 (Can. J. Phys., 46, S273)

Anand, K.C., Daniel, R.R., Stephens, S.A., Bhowmik, B., Krishna, C.S., Adita, P.K., Puri, R.K., 1968 Proc. 10th Int. Conf. on Cosmic Rays, Calgary, 1967 (Can. J. Phys., 46 S652)

Ashton, F., Coats, R.B., Holyoak, B., Simpson, D.A., Thompson, M.G., 1965, Nuc. Inst. and Methods 37 181

Baradzei, L.T., et al., 1962, Proc. Kyoto Con., 3 433
1963, Proc. Jaipur Con., Vol.5., 283

Barrett, P.H., Bollinger, L.M., Cocconi, G., Eisenberg, Y., Greisen, K., 1952, Rev. mod. Phys., 24 133

Barton, J.C., 1968, J. Phys. A 1, 43

De Beer, J.F., Holyoak, B., Wdowczyk, J., Wolfendale, A.W., 1966, Proc. Phys. Soc., 89, 567

De Beer, J.F., Holyoak, B., Oda, H., Wdowczyk, J., Wolfendale, A.W., 1968 J. Phys. A. 1 72

De Beer, J.F., Holyoak, B., Turner, M.J.L., Wdowczyk, J., Wolfendale, A.W., 1969 J. Phys. A. 2 354

Bergeson, H.E., et al., 1967, Phys. Rev. Lett., 19, 1487

Bingham, R.G., and Kellermann, E.W., 1965, Nuovo Cim., 38 1

Bohm, E., et al., 1968, Proc. 10th Int. Conf. on Cosmic Rays, Calgary, 1967 (Can. J. Phys., 46, S41)

Bowler, M., et al., 1962, Proc. Kyoto Conf. 3 424

Bray, A.D., et al., 1966, Proc. 9th Int. Conf. on Cosmic Rays, London, 1965, (London Inst. of Phys. and Phys. Soc.), 2 668

Brennan et al., 1958 Univ. Sydney Publication

Chatterjee, B.K., 1964 Ph.D. Thesis, University of Bombay

Clarke, G., et al., 1957 Nature, Lond. 180 353

Cocconi, G., Koester, L.G., Perkins, D.H., 1961 Lawrence Radiation Laboratory High Energy Physics Study Seminars, no. 28., part 2, UCID - 1444, p. 1-36.

Colgate, S.A. and White, R.H., 1966. Astrophys. J. 143 626

Conversi, M. and Gozzini, A., 1955, Nuovo Cim., 2, 189

Coxell, H. and Wolfendale, A.W., 1960, Proc. Phys. Soc. 75 378

Cranshaw, T.E., De Beer, J.F., Galbraith, W., Porter, N.A. 1958 Phil. Mag. 3 377

Earnshaw, J.C., Maslin, G.C., Turver, K.E., Can. J. Phys. 46, S115

Fan, C.Y., et al., 1968 Proc. 10th Int. Conf. Calgary, 1967 (Can. J. Phy.) 46 S498

Fowler, P.H. et al., 1967, Proc. Roy. Soc. (Lond.) A 39

Fowler, P.H., and Waddington, C.J., 1956, Phil. Mag. 1, 637

George, E.P., MacAnuff, J.W., Sturgess, J.W., 1953, Proc. Phys. Soc. A, 66, 346

Ginsburg, V.L. and Syrovatsky, S.I., 1964, The Origin of Cosmic Rays (Oxford: Pergamon Press)

Greisen, K., 1966, Proc. Int. Conf. Cosmic Rays, London 2 609

Griesen, K., 1966, Phys. Rev. Lett., 16 748

Grigorov, N.L., et al., 1967, Proc. 10th Int. Conf. Galgary, 1967 (University of Galgary)

Hillas, A.M., 1966, Proc. Int. Conf. on Cosmic Rays, London, 1965, 2 758

Hunter, H.W., and Trent, P.T., 1962, Proc. Phys. Soc. 79, 487

Jain, P.L., Lohrmann E., Teucher, M.W., 1959 Phys. Rev. 115, 653 and 643

Kaplon, M.F., and Ritson, D.M., 1952, Phys. Rev. 88, 386

Kessler, D., and Maze, R., 1957, Nuovo Cim., 5, 1540

Kidd, J.M., 1963, Nuovo Cim., 27, 57

Koshiba, M., Suda, E., Takasaki, F., 1968, Can. J. Phys. 46 S651

Kulikov, G.V., et al., 1960, Proc. Int. Conf. Moscow 2 85

Lal, D., 1953, Proc. Ind. Acad. Sci. A38, 93

Linsley, J., 1962, Phys. Rev. Lett. 9 126.

Linsley, J., and Scarsi, L., 1962, Phys. Rev. Lett. 9, 123

Malholtra, P.K. et al., 1966, Proc. 9th Int. Conf. on Cosmic Rays, London, 1965, (London: Inst. of Phys. and Phys. Soc.), 2 875

Matano, T., et al., 1968(a) Proc. 10th Int. Conf. Calgary 1967 (Can. J. Phys. 46 S56)

Matano, T., et al., 1968(b) Can. J. Phys. 46, S369 (also Institute for Nuclear Study, University of Tokyo, Annual Report, p.53, 1967)

McCaughan, J.B.T., et al., 1965(a) Nuovo Cim., 38 697

McCusker, C.B.A. 1968, Proc. 10th Int. Conf. Galgary, 1967 (University of Calgary.) A, 397

Morrison, P., 1961, Handbuch der Physik 46/1, 1

Norman, R.J., 1956, Proc. Phys. Soc. A 69, 804

Orford, K.J., and Turver, K.E., 1968 Nature, 219, 706

Ormes, J.F. and Webber, W.R., 1965, Proc. Int. Conf. London 1, 349

Ormes, J.F., Webber, W.R. and Von Rosenvinge, T., 1965, Proc. Int. Conf. London, 1, 407

Ormes, J.F., and Webber, W.R., 1968 Proc. Int. Conf. Calgary 1967 (Can. J. Phys. 46, S883)

Parker, J.L., 1967, Ph.D. Thesis, Univ. of Utah.

Peters, B., 1961, Nuovo Cim. 22, 800

Prescott, J.R., 1956. Proc. Phys. Soc. London, Ser. A. 69, 870.

Reid, R.J., et al., 1961. Proc. Phys. Soc., 103

Rogers, I.W., Thompson, M.G., Turner, M.J.L., Wolfendale, A.W., 1969 J. Phys. A 2, 365

Rossi, B., 1960, Proc. Int. Conf. Moscow, 1, 18

Samorski, M., et al. 1969 Zeit. fur Phys. (in the press)

Sekido, Y., et al., 1966, Proc. Int. Conf. London, 1965 (London Inst. of Phy. and Phys. Soc.) 2, 632

Swinson, D.B., and Prescott, J.R., 1965, Proc. Int. Conf. London, 2, 721

Thielheim, K.O., Schlegel, E.K., Beiersdorf, R., 1968 Proc. Int., Conf. Calgary 1967 (Can. J. Phy. 46 S.189)

Toyoda, Y., et al., 1965, Proc. Int. Conf. London 2 708

Vavilov, Yu. N., Pugachova, G.I., and Fedorov, V.M., 1963 Zh. Eksp. Teor. Fiz., 44, 487, (Sov. Phys. - JETP 17, 333).

Vernov, S.N., et al., 1967, Proc. Int. Conf. Calgary 1967 Part A 345 (Univ. of Calgary)

Waddington, C.J., 1960(a) Prog. Nuc. Phys. 8, 3.

Waddington, C.J., 1960(b) Phil. Mag. 5, 311

Yash Pal, and Tandon S.N. 1966, Phys. Rev. 151 4, 1071.

Zatsepin, G. T. and Kuzmin, V. A. 1968, 10th Int. Conf. Calgary 1967 (Can. J. Phys.) 46 S617

Kinsey, J. (quoted by A. G. W. Cameron, Colloq. on Cosmic Ray studies, Nov. 11 - 16, 1968, Tata Institute of Fundamental Research, 296, 1969).